Technological approaches to improve the engine efficiency and to reduce pollutant emissions of automotive diesel engines.

POLITECNICO DI TORINO

Doctor of Philosophy in Chemical Engineering

Department of Applied Science and Technology

XXVII Cycle (2012-2014)

PhD Thesis

Technological approaches to improve the engine efficiency and to reduce pollutant emissions of automotive diesel engines.

Academic Tutors:

Prof. Raffaele Pirone - Politecnico di Torino.
Prof. Debora Fino - Politecnico di Torino.
Prof. Michiel Makkee -TuDelft University.

PhD Student:

Sergio J. Castillo M.
(No. 189144)

2014

I dedicate this work who for many years has
been my spiritual and professional guide.
To you, that with humanity and human simplicity
have stolen my heart,
This thesis is for my wife,
You my only and great love.
Diana C. Hidalgo D.

CONTENTS

PREFACE

Particle matter (PM) and nitrogen oxides (NO_x) emitted directly into the air from diesel and gasoline engines are an origin of air pollution, and their presence have serious consequences for the human health. Diesel exhaust has been classified a potential human carcinogen by the U.S. Enviromental Protection Agency (EPA) and other international agencies for research on Cancer. The public-health problems associated with diesel emissions have intensified efforts to develop viable solutions for reducing these emissions, for this reason federal and state governments have adopting more stringent regulations to reduce diesel pollution.

The control of pollutants has a long history of regulatory work since the mid-1960s in both the United States and the European Union. In the US the first emission regulations were established in 1966 by California, where air pollution was a major public concern, forcing the control of hydrocarbons (HC) and carbon monoxide (CO) from passenger vehicles. In Europe, implementation of European emission regulations was delayed until the early 1990s (Walsh, 2010).

The introduction of particulate matter control by number (PN) and mass for the recent Euro 6 emissions regulations requires the use of wall-flow DPF for PM control. In-cylinder control measures require continuous research and development in combustion, including multimode fuel injection strategies at higher injection pressures and variable geometry turbocharger (VGT) to deliver tailored amounts of fuel and air at specific engine operational conditions. NO_x emission levels are reduced by 66% from Euro 5, requiring the use of NO_x after-treatment devices in addition to in-cylinder measures such as cooled EGR. LNTs have shown good NO_x reduction performance and durability. On the other hand, SCR, while offering also good NO_x reduction performance, offers more flexibility for fuel economy and reduction of CO_2 emissions. Manufacturers will likely choose the NO_x after-treatment technology based on a combination of cost, reliability, fuel economy, and consumer acceptance.

In order to satisfy the new Euro 6 emissions limits which took effect last September 2014, it is necessary to develop more efficient technologies by improving the strategies applicable to diesel engines, such as: engine efficiency or reduction of pollutant emissions, which are very often incompatible.

1. One of the strategies to improve the engine efficiency is the reduction of the mechanical losses: through the incorporation of nanomaterials in the lubricant formulation it is possible to reduce friction and to enhance the protection against wear in a stable way. In the case of the engine oil, these nanomaterials could help to increase the durability and

performance of exhaust treatments and reduce harmful emissions too. One major requirement for the application of nanomaterials as additives for lubricant oil, in substitution to the currently adopted ones, is their complete compatibility with the catalytic substrates present in the after-treatment line, whose lifetime operation should not be affected to in any extent. This analysis is crucial for the introduction of such nano-sized additives for lubricant oils on the market. The progressive poisoning of after-treatment catalysts is likely to be due to the presence of species that were originally present in the lubricant oil as additives, and which are then released into the flue gases after in-cylinder combustion.

2. The strategies to reduce pollutant emissions include:

   2.1. New fuels: There are two mainly reasons for the search of new fuels. The strategic interest lies in reducing the dependence on oil as energy source and in aiming to decrease the CO_2 emissions. In this sense, biofuels has attracted considerable attention by policy makers, researchers and industries as a renewable, biodegradable, and non-toxic fuel.

   2.2. After-treatment system: For diesel engines there is not a universally adopted technique to reduce pollutant emissions. One approach can be the mitigation of the production of particles matter or the production of NO_x and the removal of the other contaminants through a post-treatment system. Particulate traps or particulate filters (DPF Diesel Particulate Filter) are used to remove diesel exhaust particles and reduction catalysts are used for NO_x abatement. Often oxidation catalyst to remove small amounts of CO and hydrocarbons is also included.

Diesel exhaust particles consist mainly of highly agglomerated solid carbonaceous material, named ash, and volatile organic compounds, originated from different sources like trace metals in the fuel, metallic fuel additives used for enhancing regeneration of diesel particulate filters (Stratakis & Stamatelos, 2003), or from lube oil additives that enter into the combustion chamber via reverse blow-by of the piston rings. The structure of Particle matter is schematically illustrated in Fig. A.

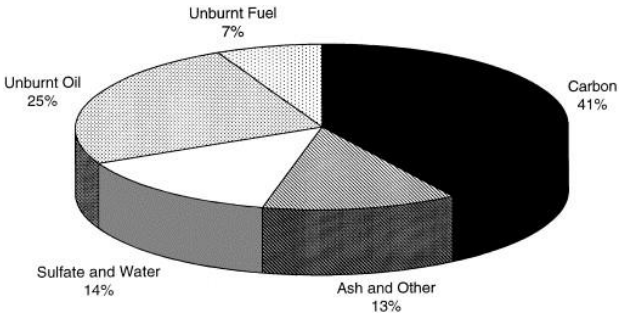

Figure A: Typical particle composition for a diesel engine (Kittelson et al., 1998)

The accumulation of ash in diesel particulate filters is an important factor limiting the filter's service life, increasing its pressure drop, having an adverse effect on fuel economy and poisoning the after-treatment catalysts.

The aims of the research work presented in this thesis were the improvement of the engine efficiency and the reduction of pollutant emissions of diesel engines by using different strategies: (1) a blend of biofuels and (2) a lubricant oil additivated with nanopowders to reduce friction and enhance protection against wear, with a particular focus on the compatibility of the nanolubricant with EURO 5 compliant catalysts for DOC, DPF and SCR systems usually employed in the after-treatment line, and finally (3) a multifunctional catalyst synthesized for an after-treatment system application, for NO_2-assisted soot abatement and NO_x storage.

In the current PhD thesis, Chapter I describe about the state of art of diesel engines, fuels, lubricants, emissions and future challenges, and Chapter II involves state of the art of after-treatment technologies and emerging technologies.

The Chapters III to VI relates to articles either published or in press during the PhD period. The sequence of these chapters corresponds to a tentatively order of the followed strategies applied to diesel engines to improve engine efficiency and reducing pollutant emissions in the engine, and a complementary study to evaluate the compatibility of nanoparticles additive to lubricants with the after-treatment EURO5 systems is presented.

In Chapter III is presented a description of the influence on the performance and emissions of an "automotive Euro 5 diesel engine" using a 30% by volume blend of a renewable diesel fuel (30% vol.), Farnasene, evaluated at full and partial load operating points of the New European Driving Cycles (NEDC).

Chapter IV deals with nanolubricant for diesel engines. MoS_2 nanoparticles were incorporated in engine lubricant oils and a further assessment was carried out about a possible interaction between the MoS_2 nanopowders and representative Euro-5 commercial catalyst. The study was developed monitoring and measuring the gas composition and particle size distribution at different operating points of the New European Driving Cycles (NEDC).

Chapter V describes a complementary study of compatibility of lubricants oil applied to EURO5 compliant catalysts for DOC, DPF, and SCR systems.

Chapter VI describes a multifunctional catalyst based on $BaO/Pt/CeO_2$ in order to perform NO_2-assisted soot abatement, where the combined catalytic effect of BaO, CeO_2 and Pt, was investigated: the Pt oxidize NO to NO_2, while the availability of NO_2 stored on BaO was functional for soot oxidation combining the effect of the redox cycle of the Ce.

Finally, in Chapter VII the present work will be evaluated.

Chapter I Diesel engines: State of the art, emissions and future challenges.

1.1 Introduction

Since the invention by Rudolf Diesel in 1892, diesel engines has been the workhorse of industry, and have been dominant in applications such as trucking, construction, farming, and mining, due to that provide important fuel economy and durability advantages for large heavy-duty trucks, buses, non-road equipment and passenger cars. While they have many advantages, they have the disadvantages of emitting amounts of particulate matter (PM), oxides of nitrogen (NO_x) and, to a lesser extend, hydrocarbon (HC), carbon monoxide and toxic air pollutants.

Particles emitted from diesel engines are small - in most cases less than 2.5 microns in diameter. The particles are complex, consisting of a carbon core, adsorbed hydrocarbons from engine oil and diesel fuel, adsorbed sulfates, water, and inorganic materials such as those produced by engine wear. Because of their extremely small size and composition, the particles emitted by diesel engines have raised many health concerns. Health experts have expressed concern that diesel PM may contribute to or aggravate chronic lung diseases such as asthma, bronchitis, and emphysema.

NO_x emissions from diesel engines also pose a number of health concerns. Once in the atmosphere, oxides of nitrogen react with volatile organic compounds (VOCs) in the presence of sunlight to form ozone. Ozone is a reactive and corrosive gas that contributes to many respiratory problems. Ozone is particularly harmful to children and the elderly.

Despite health and environmental concerns, the diesel engine remains a popular means of powering trucks, buses and other heavy equipment. Most buses and heavy-duty trucks are powered by diesel engines for good reasons. Diesel engines are reliable, fuel-efficient, easy to repair, and inexpensive to operate. One of the most impressive attributes of the diesel engine is its durability.

In response to public health concerns, a number of countries worldwide have demand significantly lower exhaust emission limits for new diesel engines. The pressures in diesel emissions control has grown considerably in recent years, and they are coming from the public and regulatory agencies to decrease criteria pollutants in developed and developing countries. Also, fuel efficiency is being aggressively regulated to reduce CO_2 emissions and decrease dependencies on petroleum fuels. And, although markets are growing rapidly in the developing countries, market and economic pressures are forcing vehicle manufacturers in the

established markets to strive the best competitive advantage. To address these forces, engine manufacturers are relying very heavily on technology developments. This Chapter focuses on a brief description of diesel engines, current technologies, and future trends, mainly oriented to the strategies applicable to improve engine efficiency and reducing pollutant emissions.

1.2 Basic Operation

A diesel engine or compression-ignition engine is an internal combustion engine that uses the heat of compression to initiate ignition to burn the fuel, which is injected into the combustion chamber during the final stage of compression. This is in contrast to spark-ignition engines such as a petrol engine (gasoline engine) or gas engine (using a gaseous fuel as opposed to gasoline), which uses a spark plug to ignite an air-fuel mixture. The diesel engine is modeled on the Diesel cycle. The engine and thermodynamic cycle were both developed by Rudolf Diesel in 1897.

The diesel engine has the highest thermal efficiency of any regular internal or external combustion engine due to its very high compression ratio. Low-speed diesel engines (as used in ships and other applications where overall engine weight is relatively unimportant) often have a thermal efficiency that exceeds 50 percent.

1.3 Present and Future Technological Challenges

Technological evolution of heat engines will be imposed by society through the various regulations and the price of fuel. Infact the environmental laws applied to “automotive” engines will be strictest.

1.3.1 Challenges

It can be expected that the interest keeps to further improves two basic aspects:

- Reduce emissions of pollutants: Especially those regulated substances like nitrogen oxides, particulate matter, carbon monoxide and unburned hydrocarbons.
- Increase engine efficiency: On the one hand, trying to reduce the consumption of fossil fuels, either to preserve the world's reserves, either political strategic or commercial

reasons. On the other hand, the efficiency improvement is possibly the most direct way to reduce CO_2 emissions, one of those responsible for the greenhouse effect.

Improve both aspects (increase engine efficiency and reduce pollutant emissions) are very often incompatible due to the fact they are in contrast without a NO_x abatement system.
In the case of automotive engines, a user requirement is that the car must be also fun to drive. Technical aspects to consider are the power delivery and torque, vibration, noise, etc. An additional objective is always reducing manufacturing and maintenance costs. However, in the current market situation these have a second role in comparison to the needs of increased performance and reduced emissions.

Strategies applicable to CI engines can be separated according to the main objective aimed at: improving engine efficiency or reducing pollutant emissions. This situation arises from the fact that the measures to improve efficiency and the ways to reduce emissions are very often incompatible.

Some strategies to improve efficiency are:

- Optimization of the thermodynamic cycle: The main way to achieve it in CI engines is by using new injection strategies. Thanks to electronic injection the number and duration of each pulse in an injection step is highly variable, and can help the mode of engine operation. Additionally, variable valve actuation systems allow changing the basic processes like shortening the compression stroke for approaching to a Miller cycle.
- Reduction in the mechanical losses: Focusing in reducing the friction between elements, e.g. with new lubricants and changing bearing by more sophisticated ones.
- Global energy management: In relation with automotive engines, whose operating conditions are fully variable, a strategy is to obtain always the optimum temperature of the engine by improving the cooling management. Also a very interesting strategy is to recover heat energy lost through the cooling system and the exhaust system. For this it is possible to install a turbine in the engine exhaust (turbocompound) or thermoelectric systems in order to obtain extra mechanical work or electric energy [1].
- Downsizing: This technique consists in reducing the size of the engine (displacement or number of cylinders) while maintaining the power. For this, higher boost pressure and duty cycle conditions are used. The main objective with a more compact engine is an increase in performance. To produce the same power, a miniaturized engine will work on operating points with better performance than a larger one.

Among the strategies to reduce emissions include:

- Using new fuels: There are two reasons for the search for new fuels, the strategic interest in reducing dependence on oil as energy source, and the aim to reduce CO_2 emissions. Among developing new fuels could be found biofuels, low-carbon fuels or gasoline-gasoil mixtures.
- Exhaust Gas Recirculation EGR: Recirculation of exhaust burned gases to admission gases aims at reducing emissions of nitrogen oxides (NO_x) due to a decrease in the combustion temperature. It is an essential technique in CI engines.
- After-treatment system: In CI engines there is not a universally adopted technique to reduce pollutant emissions. The differences are in mitigating the production of particles or the NO_x production and remove the other contaminant through a post-treatment system. Particulate traps or particulate filters (DPF Diesel Particulate Filter) are used to remove particles, and reduction catalysts are used for NO_x. It is also often includes an oxidation catalyst to remove small amounts of CO and hydrocarbons.
- New combustion modes: New combustion modes are an internal procedure to reduce particle and NO_x emissions avoiding their formation. The key to reducing NO_x emissions is to produce low-temperature combustion (lower than 2200 K), while to prevent the formation of soot is necessary that the combustion occurs with poor fuel ratios. However, the advantage of the simultaneous reduction of NO_x and soot, is opposed by the tendency to a higher emissions of CO and unburned hydrocarbons, and a tendency to produce more combustion noise. But the mean problem of these combustion modes is the low performance if the auto-ignition is not well controlled.

1.4. COMBUSTION

The characteristic combustion in compression ignition engines are based on the burning of a fuel spray in an oxidizing atmosphere, is a very complex process involving closely interrelated physical and chemical phenomena. However, nowadays the most relevant aspects of this combustion process are well known, and a detailed description is easily found in the classic Internal Combustion Engine literature [2].

In the conventional diesel combustion (CDC) concept the liquid diesel fuel spray is injected at high pressure into the previously compressed gas trapped inside the combustion chamber delimited by the cylinder head, liner and piston walls. From this moment a sequence of

processes develop including the atomization of the liquid vein, the evaporation of the fuel, the turbulent mixing between the fuel and the surrounding gas and finally the fuel oxidation.

1.4.1 New Combustion Modes

Looking at the combustion process from the local equivalence ratio and temperature conditions inside the combustion chamber as shown in Figure 1 [3], it is clear how different suitable options arise for avoiding both NO_x and soot formation processes. A comprehensive review of the advanced combustion concepts recently developed in the frame of compression ignition (CI) engines is already available in the literature [4].

Research work performed in the last two decades have confirmed how promoting a lean premixed combustion by detaching the fuel injection event from the combustion process is an interesting alternative for reducing these pollutant emissions. This combustion concept based on attaining sufficiently lean and homogeneous local equivalence ratios, well below the stoichiometric value, is widely known as Homogenous Charge Compression Ignition (HCCI). This lean combustion slows down or even avoids the chemical reactions leading to thermal NO_x formation due to the drastic reduction of the local temperatures inside the combustion chamber, while soot formation is also hindered by the absence of high local equivalence ratios during the combustion process.

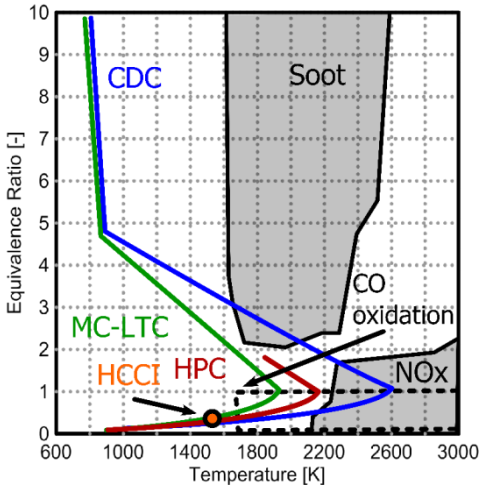

Figure 1: Schematic description of t new combustion modes in terms of local conditions plotted in the equivalence ratio vs. temperature map [3].

The injection strategies commonly reported in the literature as suitable for implementing a highly premixed combustion (HPC) concept, with different levels of local air/fuel mixture homogeneity, are the port-fuel injection, where the fuel is injected at the intake port and mixes

with the air before entering into the cylinder, and the direct injection characteristic of current CI engines. However, despite producing a perfectly homogeneous lean air/fuel mixture, port fuel injection of usual fuels for CI engines is not a realistic alternative due to its limited efficiency, high hydrocarbon and CO emissions, early onset of the combustion process, lack of combustion phasing control and high noise. Additionally, since diesel fuels have poor evaporation characteristics, they create a wall film which does not evaporate from the intake port walls because the temperatures there are not high enough.

The direct injection strategy comprises two different alternatives suitable to produce a highly premixed combustion, consisting of injecting the fuel early during the compression stroke or late during the expansion stoke. In the late direct injection alternative, as in the Modulated Kinetics (MK) or the Highly Premixed Late Injection (HPLI) concepts, the injection is placed just after the TDC and the fuel should ignite also relatively close to the TDC since displacing the combustion towards the expansion stroke produces combustion instability, high levels of CO and HC and the sharp decrease on engine efficiency caused by a delayed combustion phasing observed in Figure 2, [5]. Then, the practical application of the late direct injection alternative is limited by the available mixing time and the high sensitivity of the engine efficiency to combustion phasing, especially at high engine speed or loads, where it requires an extremely fine tuning and control of different engine parameters, such as the EGR rate and the swirl level.

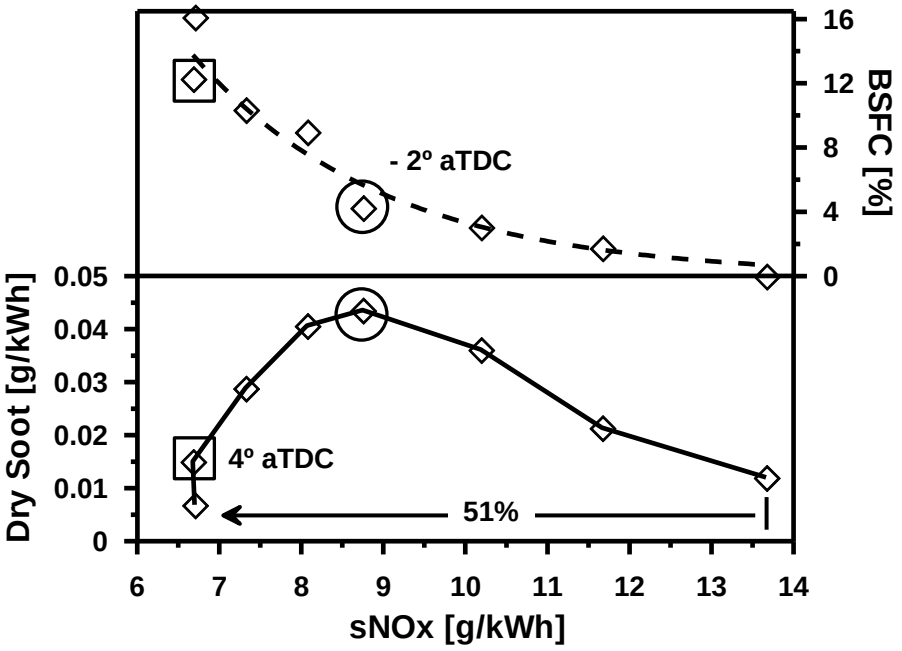

Figure 2. Pollutant emissions and fuel consumption trends observed while retarding the injection event for achieving a late injection HPC concept [5].

In the early injection alternative, the injection event can be arbitrarily advanced towards the compression stroke while combustion starts relatively close to the TDC, increasing the mixing time available for producing a suitable premixed combustion without intrinsically compromising the engine efficiency. However, injection timing is usually set close to the TDC as in the case of the Premixed Charge Compression Ignition (PCCI) concept, and the lack of homogeneity caused by a shortened mixing time is compensated by introducing EGR to reduce the temperatures in those zones of the mixture that reacts in locally stoichiometric combustion. This early direct injection represents the most promising alternative for implementing the HPC concept, as it is also confirmed by numerous investigations reported in the literature.

1.5. POLLUTANT EMISSIONS

The main contribution of pollutant emission from an engine is due to exhaust gases released to the atmosphere, especially in CI engines running on little volatile fuels. Health studies show that exposure to diesel exhaust primarily affects the respiratory system and worsens asthma, allergies, bronchitis, and lung function. There is some evidence that diesel exhaust exposure can increase the risk of heart problems, premature death, and lung cancer.

The combustion process produces many substances that find their way to the atmosphere, but during normal operation, the proportion of those considered as toxic is very small compared with the rest of products from the clean combustion. In addition to this, very few of these substances are considered legally as pollutants and regulated by the standards [8].

Non pollutants substances. Water (H_2O), carbon dioxide (CO_2) and oxygen appear in clean combustion. Considering CO_2 as a not polluting gas is questionable, since it is the main potential precursor of the so-called greenhouse effect. In the cases of incomplete combustion, hydrogen (H_2) is formed too.

Regulated pollutants. Their origin varies greatly. The incomplete combustion produces carbon monoxide (CO) and unburned hydrocarbons (HC). There may also be oxidation products of the intake air nitrogen (NO_x), and pollutants from fuel sulfur (SOx). Finally, there is particulate matter (PM), containing solid (ISF) and soluble organic fractions (SOF) of particles from elemental carbon formed during combustion.

Figure 3 shows the typical percentage of the more important pollutants in the exhaust gas of a light-duty diesel engine following one of the standard cycles.

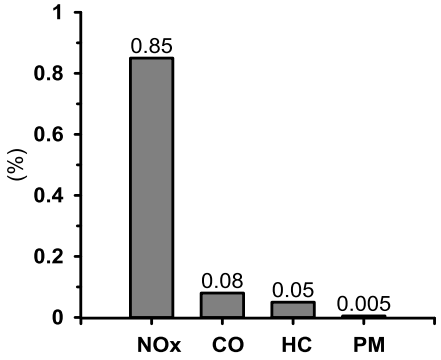

Figure 3. Typical composition of pollutant emissions in a Diesel engine

The increasing importance in reducing pollutants emission from CI engines has been stronger on automotive and heavy-duty transportation engines, due to their greater number and proximity to living beings.

1.5.1. Pollutants Formation

In the conventional diesel combustion carbon monoxide and unburned hydrocarbons are not very problematic due to the high efficiency of the DOC, nitrous oxides and soot or particulate matter present the main challenges

Nitrous Oxides (NO_x)

In CI engines, NO_x formation is due mainly to the so-called thermal mechanism, caused by the high local temperatures during combustion process and lean mixtures with excess of oxygen. It leads in the oxidation of the nitrogen of air. Since in the combustion chamber of the CI engine there are wide regions with lean mixture, NO_x formation is very sensible to the increase in combustion temperature. Hence all the measures that produce an increase in the gas temperatures (turbocharging) or in the rate of heat release (high injection pressure, advanced injection timing, etc), will probably produce an increase in NO_x emissions.

Soot and Particulate Matter

Soot is basically carbon particles of certain size and color that make them visible. Particulate matter is a more general term that includes soot (visible or not), but also other small particles (solid or liquid). The older emissions standards used the opacity of the exhaust gases as an indirect measurement of soot concentration, while current regulations focus on the mass, number and size of the particles collected by some filtering system.

Soot emission is the final result of a formation phase following by an oxidation process. The

formation is produced mainly by a very rich mixture entering the flame at the lift-off section of the diesel spray. The high temperature and default of oxygen leads to a dehydrogenation of the hydrocarbons. If the resulting soot particles are not burned later when they cross the flame around the spray envelop, they will exit the engine. In CI engines, soot is produced mainly when global mixture is very rich (excessive fuel injected), or when the mixing conditions are bad (low injection pressure, low in-cylinder gas density, injector malfunctioning, etc.).

Soot particles or particulate matter in general are the result of complex phenomena of agglomeration and nucleation, but also of adsorption of other substances in their surface. Figure 4 shows the typical composition of the particles emitted in CI engines.

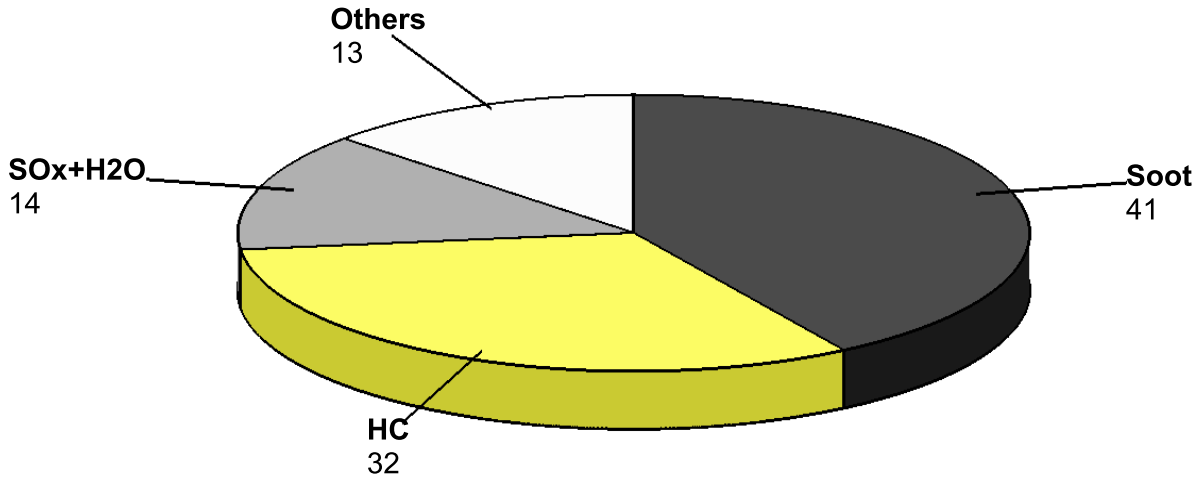

Figure 4. Typical composition of particulate matter

In general, those conditions that lead to a reduction in NO_x emissions produce an increase in soot and particulate matter, as it will be illustrated later.

Carbon monoxide, CO

The generated CO at the end of the diesel combustion depends on the balance between formation processes (fast reactions) and oxidation (slow reactions), being both very active at high temperatures. In general, if temperature is high enough, the main cause for high CO emissions is the excessively rich mixtures, i.e. the default of oxygen. This is not a common situation in CI engines that operate with lean mixtures, with excess of oxygen, but a small CO amount can be produced since the recombination process has some inertia that there is not enough time for the entire CO to oxidize to CO_2, as expansion and exhaust processes are relatively fast. In general, the CO emission in CI engines is smaller than that in SI engines. A different situation appears in the case of CI engines operating at any of the low-temperatures

combustion modes, especially in highly premixed combustion. In these circumstances, the excessively lean mixtures and the low combustion temperatures are responsible for high CO emissions.

Unburned Hydrocarbons (HC)

In diesel engines, the formation of HC takes place mainly by incomplete combustion in those inner spray regions with very rich mixture, and that cannot be oxidized later due to defective mixing or reduction in the chamber temperature during expansion stroke. Another eventual source of HC is the impingement of the spray on the piston, especially if the fuel wets the piston/cylinder walls. Aside from the gaseous emission of HC, some hydrocarbons can be adsorbed in the particle matter after condensation on the particles surface, adhering to them and being included in their structure.

One way of globally understanding the pollutant formation trends in CI engines is representing the emission concentration as a function of the global equivalence ratio, as represented in Figure 5. The plotted trends evidence that there is not an optimal range of equivalence ratio, where all the emission are low, except perhaps at very lean mixtures, that correspond with low-load operating conditions of the engine, being CO and HC relatively high in this zone.

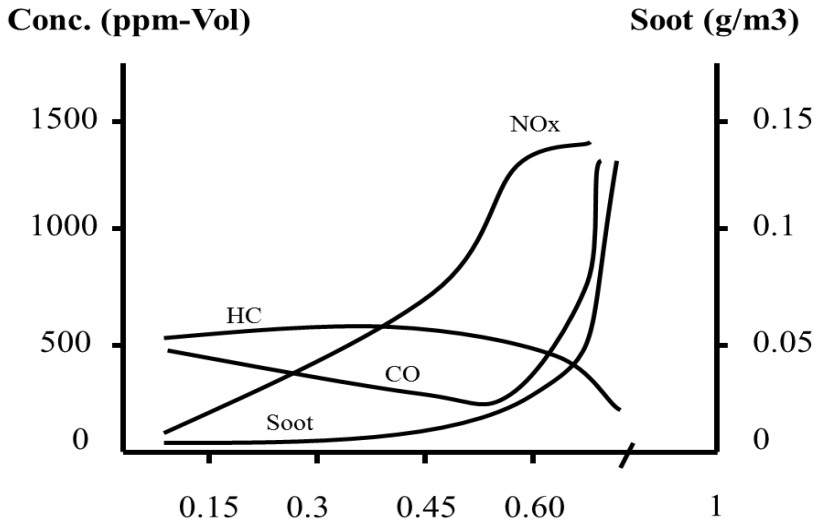

Figure 5. Typical trends in pollutant emissions as a function of the global equivalence ratio

As commented above, smoke opacity was substituted by particulate matter mass as the evaluating parameter for assessing the environmental impact of CI engines. However, the hazard on health is more linked to the particulate size than on the total mass. Smaller particles are more dangerous, since they stay longer suspended in the air, and after inhalation they

reach deeper in the airways. The typical size of the particles emitted from a diesel engine varies from a few nanometers to about 30 microns [9]. Figure 6 shows a typical size distribution of particles, and their contribution to total mass. It can be observed that the many small particulates have a small share in the total mass.

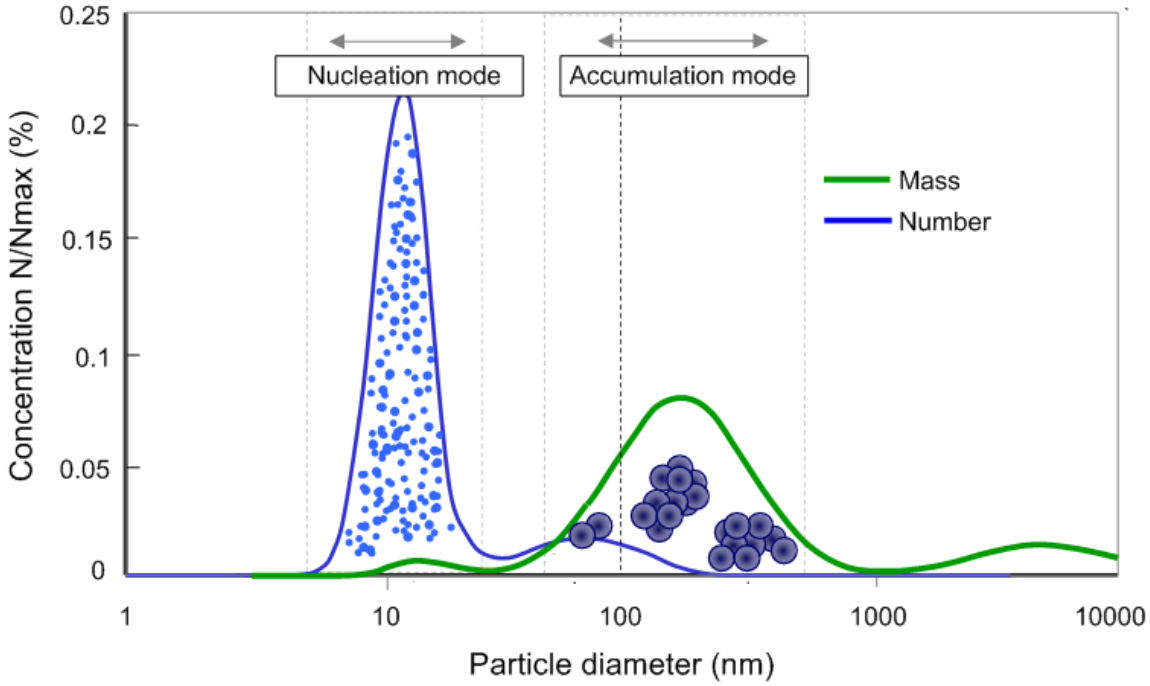

Figure 6. Typical distribution of exhaust particulate size and their contribution to total mass.

1.5.2 Present and Future Trends in Emissions Reduction

As already discussed, there is not an easy way of reducing simultaneously the generation of all the emission from CI engine by controlling the usual operating conditions: moreover, some of the actions that lead to the reduction of a particular pollutant may have a negative impact on fuel consumption or on engine noise and durability [10]. However, as it has been mentioned earlier, along the last decades, CI engines emissions have been greatly reduced, and so has been the fuel consumption. The success in this pursuit has been mainly due to two kinds of actions:

- **Internal measures:** based on the optimized design of the engine and the control of the air management and injection systems, aiming at preventing the production of the pollutants in the combustion chamber, i.e. limiting engine-out emissions.
- **External measures (after-treatment):** based on inserting devices that can extremely reduce pollutants leaving the cylinder, thus reducing the tailpipe emissions.

Internal measures, despite dealing with the source of the problem without requiring additional

equipment, are not able to fulfill the severe limits imposed by current and upcoming regulations. Hence, in automotive engines and heavy-duty vehicles, some kind of after-treatment device has been necessary since several years.

As previously discussed, it might be concluded that there is a conflict between the formation of different pollutants, mainly between NO_x and Soot. As explained above, NO_x own their origin mainly to high combustion temperatures and high oxygen content, favorable conditions to soot formation and CO and HC reduction.

The generators are reversible. Finally it should be noted that although CO_2 is not considered as a limiting pollutant emission, there is a growing pressure to reduce the emission of this gas, especially from the passenger car fleets. There are two basic strategies to achieve this goal: reducing fuel consumption and burning fuels that generate less CO_2 in his cycle life (from well to wheel). As far as the first strategy, there is a linear relation between fuel burnt and CO_2 emissions. Hence all the measures that allow reducing fuel consumption will be favorable. However, the expected results from applying engine design and control techniques may not be enough, and here a complete world of vehicle design and management strategies are being developed. On the other side, using low carbon fuels or biofuels can contribute to the reduction of the well-to-wheel emissions. In this sense, new generations of biodiesel fuel are being developed, as well as the combination of different fuels. It should be considered that some of these new fuels with typically higher contents in oxygen tend to produce a reduction in soot but an increase in NO_x emissions.

Internal techniques

These techniques are known as “active solutions” and basically are always limited the trade-off between NO_x and Soot, with the exception of the new combustion modes.

Combustion chamber design. In direct-injection diesel engines the combustion chamber is shaped as a bowl on the piston head. The smaller the diameter of the bowl, the faster the air motion will be when piston approaches top dead center and during the injection process. This increase in flow velocity is due to the squish of the gas into the cylinder and to the acceleration of the swirl motion produced during the intake process. In all, the mean velocity field and the turbulence improve the fuel-air mixture, which helps in shortening the combustion process, and can improve fuel consumption. This measure tends to reduce Soot formation and to increase NO_x emissions. Moreover, the high gas velocities increase heat transfer and this can counteract the benefits in terms of efficiency improvement combustion acceleration.

In large and slowly rotating CI engines (industrial and marine applications), where

combustion does not need to be extremely fast, the trend has been towards a quiescent chamber, leaving to the injection system the role of a good mixing, and so attaining a high fuel efficiency by reducing heat losses.

In automotive, high-speed engines the usual objective has been the opposite, but in the last decade, for a better fuel efficiency, the trend has been reducing the gas motion by open and shallow combustion bowl designs, exploiting the power o the new injection systems for the fuel-air mixture formation.

Injection system upgrade. *Increase in injection pressure*. The injection systems have been improved for higher injection pressures, and a better control of the fuel delivery, resulting in general in better fuel atomization. The increase in injection pressure enhances both fuel atomization and air entrainment into the spray, speeding up combustion. The immediate consequences are the reduction in Soot, CO and HC, and an increase in efficiency. However, the NO_x emissions tend to increase due to the higher combustion temperatures achieved. Figure 7 shows the commented effects of increasing injection pressure in a heavy-duty engine, at different EGR rates, that will be commented later.

These injection strategies, despite producing a smaller amount of soot mass, tend to produce a larger number of particulates with smaller size, with their worse impact for living beings. This is moving to establish new regulations that limit not only total particulate mass, but also the number of particulates.

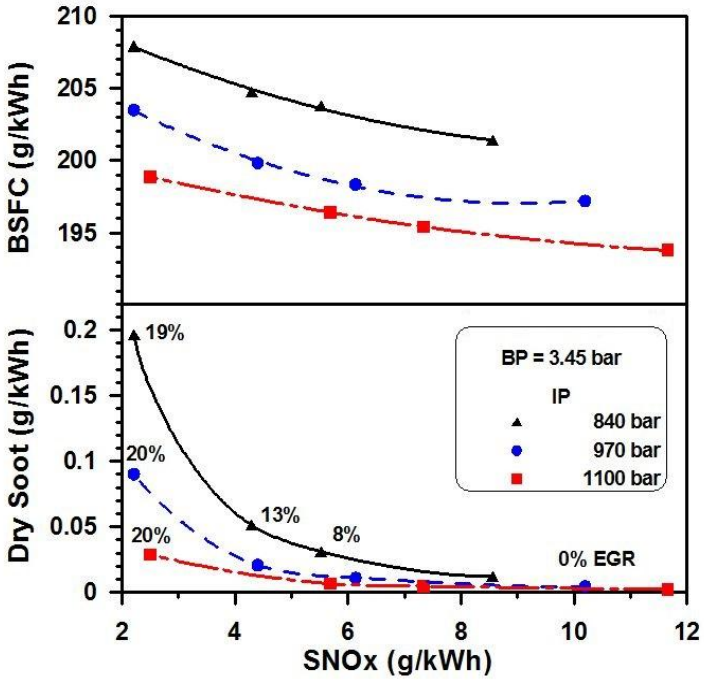

Figure 7. Effects of increasing EGR and boost pressure on the NO_x-soot trade-off in conventional diesel combustion.

Other improvements made in the injection process are the capability of modulating the injection rate, especially in the cases of common-rail systems and direct-acting injectors. A common application is the multiple injection event, that splits the injection process in several pulses, as illustrated in Figure 8.

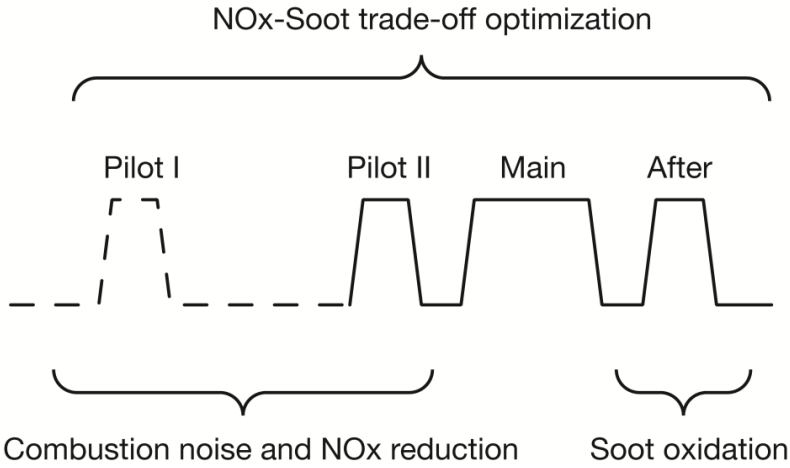

Figure 8. Multiple injections strategy for control of emissions and noise.

Pilot injection (or pre-injection). It is a technique commonly used in light-duty engines in order to reduce the combustion noise. It involves injecting a small quantity of fuel few degrees before the main injection. In this way, the amount of fuel burned is reduced the during premixed combustion phase. Its impact on exhaust emissions is scarce, but reduces the noise that is one of the classic problems of the diesel engine.

Post-injection. It involves injecting a small amount of fuel few degrees after the end of the main injection. This small amount of post-injected fuel will not burn under optimum conditions, thus fuel efficiency will decrease. However, if properly timed the last shot of fuel that has been detached from the trailing edge of the burning spray, can benefit from a better mixing with fresh air and it will burn at higher temperature, thus promoting to soot oxidation. The consequence is then a lower soot emission.

Exhaust gas recirculation. A general and widely used measure for the reduction in NO_x emissions is the exhaust gas recirculation (EGR) that introduces gases from the exhaust into the intake line, replacing and mixing with fresh air, and so reducing the oxygen concentration of the gas that later mixes with the fuel during the injection process. There are different effects affecting the NO_x formation, but the most important in usual combustion conditions is the lower oxygen concentration that reduces the flame temperature. As a counter effect, the less oxygen *contributes to higher soot emissions* by reducing the soot oxidation rate. Moreover the

slower reaction rates are responsible for a trend to increase fuel consumption, and a proportional increase in the production of CO_2 [11,12]. The EGR strategy is currently always combined with some degree of cooling of the recirculated gases, since this measure contributes further to the reduction in the flame temperature and NO_x formation.

Figure 7 shows some results of the clear effect of increasing EGR in a heavy-duty engine. In this case, introducing an EGR rate of about 20 % can reduce NO_x emissions by a factor of 4. In modern engines, EGR rates can range up to 40 and 50 % at low-load operation conditions. EGR is a necessary measure for controlling the alternative combustion modes based on a premixed charge auto-ignition.

EGR is the most significant technology for in-cylinder NO_x reduction in diesel-powered engines. The EGR fraction is tailored for each engine operating condition and may vary from zero up to 40% of the incoming air in the latest systems. The EGR system requires fuel sulfur level below 500 parts per million (ppm) to avoid pipe corrosion with sulfur compounds. The extra cost incurred to reach Euro 6 levels is stronger in larger LDVs. According to experts from emission control associations and manufacturers, solicited in personal communications with T. Johnson (2010) and J. Kubsh (2010), it is possible that small diesel engines would be able to achieve the emission levels with advanced combustion techniques, including advanced EGR and air-fuel management strategies, but many experts debate the fact that with the new and more stringent regulations EGR not be sufficient to achieve the new NO_x limits.

Increase in boost pressure. Increasing boost pressure is a desirable measure that has an already commented potential for largely increasing engine power if fuel mass is increased in proportion to the increase in intake air. However, if equivalence ratio is reduced, the general effect is a reduction in soot formation, due to the excess in air. The faster combustion with plenty of available oxygen produces a benefit in fuel efficiency and so in CO_2 reduction. The familiar repercussion is an increase in NO_x emissions.

New combustion modes. The trend in future active solutions focus mainly in new combustion modes. These combustion modes are focused on shifting the combustion curve illustrated above in figure 1 into areas where NO_x and Soot formation does not occur. On the one hand, systems known as Premixed Charge Compression ignition (PCCI), which perform the injection process at a lower temperature, thus increasing the delay period. This controls the combustion evolution below the NO_x -forming temperatures. In this sense, this type of combustion reduces NO_x emission but may produce a tendency to not to oxidize the CO and HC due to the decrease of temperatures.

External Measures

These techniques are also known as "passive solutions", and are mainly based on some after-treatment device. In Chapter II deals in detail with this subject, and only some comments are made here focusing on the effects on the engine operation and interrelation with other measures.

Despite being the most important pollutant emission similar to SI engines, the same type of after-treatment devices cannot be used, due to the excess of air in the exhaust gases of CI engines[13]. This conditions limits the use of any concept based on the reduction reactions (for instance for eliminating NO_x). On another hand, the lower exhaust gas temperature and the common use of turbocharging yields lower exhaust temperatures in the point where the after-treatment system is placed, compared with the equivalent SI engine.

The most common system used currently in CI diesel engines is the oxidation catalyst, which is able to abate simultaneously CO and HC emissions.

The catalytic reduction of NO_x is not easy in an ambient with excess of oxygen. The most common technique today is the Selective Catalytic Reduction (SCR), which need to introduce urea in the exhaust gas flow upstream of the device for generating ammonia (NH_3), that will reacts with the NO_2 to produce N_2 and H_2O. An alternative are the chemical filters, the latter being called NSR (NO_x Storage-Reduction) or LNT (Lean NO_x trap). These are characterized by their ability to hold NO_2 from the exhaust gas during lean operation conditions, and release it during rich operation conditions.

The current technology for reducing soot and particulate matter is the insertion of a particulate filter (DPF), that simply retain most of the particles in the exhaust flow. When the filter gets clogged, some regeneration strategy must be introduced to burn the particles.

As already commented, current engines are not able to meet the pollutant limits with only internal measures, and probably the same will happen in the future, hence some combination of after-treatment devices will be required. There are three ways of meeting lower pollutant limits:

- Accelerating combustion (high injection pressure and boost pressure, high turbulence, little or no EGR) which leads to low Soot and high efficiency and reduce the excessive NO_x emissions by after-treatment.
- The second alternative is the opposite: reducing injection pressure and especially introducing high rates of EGR. This leads to low NO_x emissions but to high soot. Soot is then reduced by a particulate filter. The aftermath of these systems is the trend to reduce the efficiency.

- The third way of improvement would be based on some technological breakthrough, like successfully implementing some new combustion concept that would lead to simultaneous reduction of NO_x and Soot ideally without the need of after-treatment device. However, current state of the art, allows applying these strategies only at low-load operation points.

In addition, it must be taken into account that the presence of some after-treatment equipment will interact with the engine operation, and with the other systems like the EGR circuits and the turbine, described in later sections. Negative effects on the engine operation are mainly due to the increased backpressure (that can be somehow mitigated by combining the design of the silencing devices), and to the requirement of some more or less frequent ineffective engine operation modes for the regeneration of the particulate filters or for the catalyst light-off in cold starting.

1.6. EXHAUST GAS RECIRCULATION

Soot (or particles) and NO_x are usually the most challenging pollutants to control in CI engines, and one effective way to reduce NO_x emission is the exhaust gases recirculation (EGR) into the combustion chamber. EGR has proven to be a cost-effective solution to fulfill NO_x emissions regulations, in spite of its trend to increase soot emissions and fuel consumption, in the conventional CI combustion mode. As a result, since several decades, EGR is a common technique in most CI engines, both in heavy and light-duty applications. In addition, the new combustion concepts exposed in Section 1.4, rely generally on a large amount of EGR for controlling the fuel-gas reactivity and extend the auto-ignition delay. Therefore, it is expected that EGR will continue playing a major role in CI engines.

There are basically two different ways of introducing burnt gases from previous cycles into the combustion chamber:

Internal EGR: Residual gases come from the backflows that exists in the intake and exhaust valves, together with the combustion gases that remain in the combustion chamber after the exhaust valve closing. These backflows are usually naturally produced without any specific design of the camshafts. In some cases, particular cam designs are manufactured in order to force back flows across the intake or exhaust valves, thus achieving relative amounts of internal EGR [14]. With these strategies, due to the short path of these burnt gases into the cylinder, it is not possible to cool down the internal EGR gases, being the consequence a lower effect on reducing NO_x emissions, and also some worsening of the volumetric efficiency of the intake process.

External EGR: This is the most used technique in IC engines for reducing NO_x emissions, and also the most effective. The main drawback is that a specific EGR circuit is necessary to be designed and installed on the engine. The EGR circuit connects the exhaust and intake manifolds, and enables the exhaust gases to be reintroduced on the engine, after being mixed with the fresh charge of air induced from the ambient. For this EGR circuit to force burnt gases in the intake manifold, it is mandatory to have higher pressure in the exhaust than in the intake.

External EGR is normally cooled down to exploit the additional benefits of low gas temperature on the NO_x emissions, and also to mitigate the reduction in the fresh air induced, due to the substitution by burnt gases. The cooling is normally achieved by using specific gas/liquid or gas/gas heat exchangers.

In the case of turbocharged engines, two different architectures for external EGR can be used:

High pressure EGR or short route EGR: The EGR pipe connects exhaust and intake manifolds from a point placed upstream of the turbine to another point placed downstream the turbo compressor.

Low pressure or Long route EGR: In this case the EGR circuit connects the exhaust manifold from a point downstream of the turbine to the intake manifold upstream of the compressor.

Figure 9 shows a scheme for a turbocharged diesel engine with the typical external high pressure EGR (HP EGR) and low pressure EGR (LP EGR) configurations.

The HP EGR approach is by far the most commonly employed EGR architecture in current engines. According to the system layout, the EGR rate is limited by the pressure difference between the intake and exhaust manifolds. In addition, since the turbocharger behavior also depends on the intake and exhaust conditions, a strong coupling between both systems appears. Other problems attached to the HP EGR systems are the difficulty to provide a homogeneous intake charge between cylinders or the important increment in intake temperature despite employing EGR coolers.

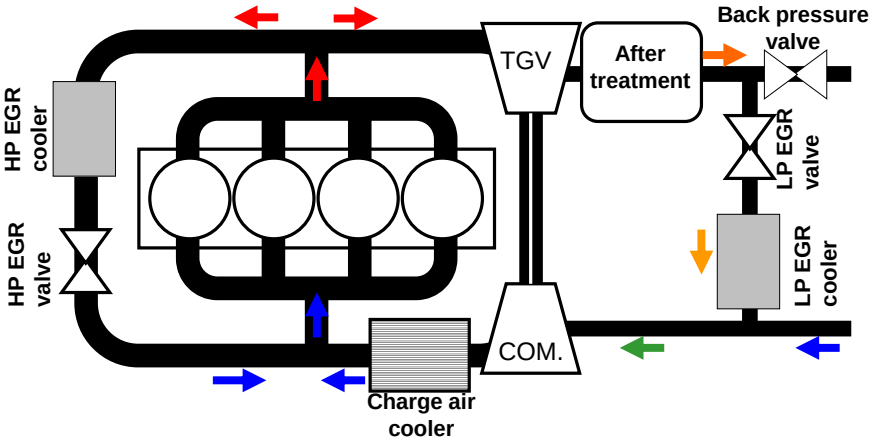

Figure 9. External EGR architecture: Low pressure and High pressure EGR circuits.

1.7. FUELS

1.7.1 Suitable fuels for CI engines

For the development of the conventional combustion process described in Section 4, involving the fast injection and mixing of the fuel, it is necessary that the used fuel accomplish a broad list of requirements involving thermo-physical and chemical properties closely related with volatility, injectability and combustibility in this particular application [15]. The usual values of these properties for a commercial gasoil and other fuels commented later, are given in Table 1

	Ultra-Low Sulfur gas-oil	**Bio-Diesel**	**Fischer Tropsch**
Specific Gravity	0.83 -0.87	0.87-0.89	0.77-0.79
Cetane Rating	40-55	45-70	>70
Viscosity at 40ºC (mm^2/s)	1.9-3.3	3.5-5.0	2.1-2.8
Sulfur (ppm)	7-15	0-24	<1
HFRR Lubricity (mm)	0.40-0.55	0.27-0.32	0.40-0.64
Lower Heating Value (MJ/kg)	42.7	39.0	42.7
H/C ratio	1.84	1.80	2.15

Table 1. Properties of several fuels for CI engines.

One of the first stages of injection is atomization, and in order to produce a huge amount of droplets, the fuel is injected through a narrow nozzle with a diameter of only a few hundreds of microns. A very important property for this condition is fuel viscosity, since a high viscosity is a common cause for a deficient atomization, leading to poor combustion. Moreover, the design of the injection system implies that some moving parts of diesel fuel pumps and injectors are protected from wear exclusively by the fuel. Hence, the fuel must be able to lubricate by itself the moving parts, and the determinant property is lubricity**.** The lubrication mechanism in the injection systems is a combination of hydrodynamic lubrication and boundary lubrication. These phenomena are closely related with the fuel viscosity, and here there is a compromise between adequate atomization, that requires low viscosity, and proper hydrodynamic lubrication, which means the opposite. On the other hand, boundary lubrication occurs when the liquid film is not continuous and small areas of the opposing surfaces get in contact. Although lubricity enhancing substances (mainly trace amounts of oxygenated, nitrogenated and aromatic compounds) are naturally present in diesel fuel derived from petroleum crude by distillation, the increase of the requirements of fuel regarding to contaminant emissions have led to severe distillate after-treatment systems, and to a loss of this property.

Once the fuel is atomized and droplets in vapor phase mixed with air, the starter of combustion is dependent on the ignition quality of the fuel. In the conventional combustion process, smoothness of operation, misfire, smoke emissions, noise, cold start performance and ease of starting can be improved using a fuel with good auto-ignition quality. The cetane number is a measure of how readily the fuel starts to burn, comparing the fuel to a scale made of two known chemical substances, in tests carried out in a special engine. Increasing the cetane number implies a shorter delay in combustion, this leads to an improvement of the process and performance on startup, and a reduction of NO_x and soot emissions. Cetane number varies systematically with the hydrocarbon structure and some fuel processing can reduce vary this parameter, so that a series of fuel additives have been developed to improve the cetane number

The energy released in the combustion of a certain amount of fuel is directly dependant on the chemical energy contained in the fuel, which is evaluated by the heating value. Since plain CI engine fuels are stored and used in liquid phase, the density is also an important parameter, since the injection systems operate on a volumetric basis. Fuel consumption is related to the heating value of the fuel, while the size of the relevant devices (pumps and injectors) are affected by fuel density.

Since the usual conventional fuels are distilled from crude oil, some relevant contents of sulfur present in fossil fuels will be found in the gasoil. Sulfur is a substance contributing to the lubricity of the fuel, but aside from producing pollutant oxides of sulfur, it can disturb the operation of the after-treatment devices in the exhaust. So, the increasingly stringent emissions standards in the world, have forced to reduce the amount of sulfur in the fuel to the level of several ppm.

An extensive use of additives has been applied to ensure the performance of the fuel and **to** broaden the range of distillation products that can be used in diesel combustion. Sometimes applied in ppm concentrations, these chemical compounds improve significantly the performance of the fuel used. Related to the performance of the fuel injection system, the main used additives are cetane number and lubricity improvers. Cetane number improvers are based on substances that decompose rapidly at high temperature in the combustion chamber. Starting from a conventional Ultra Low Sulfur Diesel, it is easily expected a benefit in cetane number from 40 up to 50 with less than 0.5% addition in mass of such cetane improvers.

In addition, lubricity additives are also used to compensate for the lower lubricity of diesel fuels that have undergone some sever physical or chemical post-processes. These additives are attracted to metal surfaces where they form a thin surface film that acts as a boundary lubricant. Usually, their concentration range varies from 50 to 250 ppm, in order to meet the specifications. Currently, because of the recent adoption of this specification in some countries, lubricity improver is the most widely used additive and some refining companies use a cetane improver when the additive cost is less than the cost of processing to increase the cetane number.

These basic requirements for CI engine fuels can vary depending on the engine type and application, so that different fuels are used in large and stationary engines like in electricity generation and marine applications. In these cases, it is common the use of heavier oil crude fractions, usually known as fuel-oils. These fractions share most of requirements mentioned above, but there's a strong difference in cleanliness, regarding specially to solid residues and sulfur, since the emission of SO2 originated from sulfur in the fuel are tightly restricted worldwide.

In the last decades, the use of the so called biodiesels has been introduced with the objective of reducing the dependence on the crude oil and the CO2 emissions. Biodiesel is a fuel comprised of long chain fatty acids derived from a diverse mix of feedstocks including recycled cooking oil, soybean oil, and animal fats through a process known as trans-esterification, that produces the so called fatty acid methyl esters (FAME), compounds

bonded with a glycerol group that contain oxygen, and have chemical and physical properties similar to those of conventional gas-oil (Sarin, 2012). Compared with a usual gas-oil, biodiesel fuel has less heating value, more viscosity, and higher cetane number (see Table 1). These and other more subtle differences, together with the limited mass production of this fuel make difficult the operation of CI engines with pure biodiesel. As far as technical fuel quality and engine performance specifications, biodiesel can be used in existing diesel engines without modification and is covered by all major engine manufacturers' warranties, most often in blends of up to 5 or 20 percent.

Currently, in almost all developed markets, gas-oil is blended with biodiesel in proportions that range from 5 to 10%, with a trend to increase. However, in some controlled transportation engines and transportation fleets biodiesel has been used in much higher proportions, even in pure state [16].

As far as the effects on combustion and pollutant emissions, in general biodiesel fuels reduce the overall exhaust emissions in current CI engines, number of particles, CO and HC emissions in a broad range of engine operation, but also promote NO_x formation [17]**.** In addition, the exhaust emissions of sulfur oxides and sulfates (major components of acid rain) from biodiesel are essentially eliminated compared to gas-oil.

In the pursue of reducing pollutant emissions, other fuels have been tested and are known to produce some benefits without important modifications in the engine design, even though their price and availability has curtailed their extensive applications [18]. One of them are the emulsions of water in gas-oil, that are known to reduce the combustion temperature and mitigate the production of NO_x. Another example is the synthetic fuels with tailored optimum properties, like those produce by the Fischer-Tropsch method, combining carbon monoxide and hydrogen into liquid fuel. Some properties of this synthetic fuel are given in Table 1.

1.7.2 Fuels for new combustion modes

Low-temperature compression ignition combustion processes can be an interesting way to achieve a cleaner and more efficient engine. This combustion mode is difficult to achieve with the usual fuels used in the conventional CI combustion mode, since they will auto-ignite very quickly after the start of injection into the cylinder. This effect of fast auto-ignition can be counteracted by applying complex and expensive technologies like high injection pressures and high swirl (to increase mixing rates) and high levels of cooled EGR (to delay auto-ignition) with higher boost pressures (to achieve the required power). Even then, with

conventional diesel fuels, low NO_x and low smoke with partially premixed CI combustion is possible only at low loads.

One way to overcome this shortcoming is to use a fuel with a lower reactivity, that leads to longer auto-ignition times, and so favor the mixing with air prior to start of combustion [19]. One convenient way to obtain this fuel in massive quantities is by mixing two existing fuels with different reactivity, like gas-oil and gasoline, in the convenient proportion and injecting it in the cylinder through the same fuel injection system [20].

Another even more flexible strategy that allows changing the fuel reactivity depending on the engine operating conditions, is by introducing the more volatile, less reactive fuel (like gasoline, ethanol or natural gas) in the intake manifold to produce a fully premixed charge, whereas the higher reactivity fuel (e.g. gas-oil) is injected directly in the cylinder to start the combustion process. [21]. A variation on this theme is to use some gasoline-like fuel and mix the required amount of some ignition improver to make the fuel more reactive and inject this reactive fuel directly into the cylinder [22].

On another hand, it has been also demonstrated that heavy-duty diesel engines can be run injecting gasoline or ethanol with very high efficiency and very low NO_x and smoke, if appropriate injection timing and strategies are used. Some of the problems associated with premixed CI combustion such as high pressure rise rates caused by high heat release rates can be alleviated by using multiple injections. Gasoline also might not need the small injector holes and the high injection pressures required by diesel fuels to increase mixing rates, and consequently the complexity and cost of the fuel injection system can be significantly reduced.

1.8. LUBRICANTS

The lubricant must protect the automotive component that it lubricates. In some cases this protection is in the form of a fluid film that keeps opposing surfaces separated. In other cases, the lubricant provides wear protection by forming a chemical film on a surface, to generate boundary lubrication protection. Automotive lubricants protect against corrosion by virtue of alkaline agents to neutralize acids that form in hot spots. The lubricant transports protective chemicals to the sites where they are needed and transports waste products away from the sites where they are generated. This diversity of function strongly influences the choice of chemical composition and physical properties for a given type of lubricant and dictates that a variety of lubricants are required to perform the various lubrication functions in a vehicle.

That is, different engine components require substantially different kinds of protection. Transmission fluid must withstand high temperatures and loads. Engine oil must remain effective despite the fact that fuel and combustion products can enter the oil under all driving conditions. In particular, during short-trip cold-start conditions, fuel and water may be present in oil at concentrations greater than 5%. During high temperature operation engine oil must not evaporate or degrade excessively. Various types of bearings require the presence of a fluid film that separates a rotating shaft from its opposing bearing surface. Brake fluid must remain in place and continue to function, even if the vehicle drives through pouring rain or encounters puddles of slush on the road.

The continuing pursuit for better fuel efficiency stands behind many recent advancements in engine technology. "Downsize and charge" has become the major development trend alongside broad acceptance of fuel stratified injection [23]. The introduction of higher power densities (around 65 kW/L and 150 Nm/L in modern diesel engines) raises performance requirements for engine oil. Engine lubricants will have to be reformulated to meet the increased severity resulting from the modifications. Nanoadditives open new ways to maximizing lubricant performance [24–26].

Future Trends

Stringent federal legislation calling for better fuel economy and reduced emissions is the driving force for improved fuel efficiency and development of new engine technology. The use of energy conserving engine oil is the most economic way in the automotive industry to acquire the necessary gains, compared to complicated hardware changes[27]. In addition, design and legislative pressures for cleaner, more efficient engines with higher specific power outputs is forcing tribological engine components to be operated with generally thinner oil films in an effort to improve fuel economy.[28]

The engine tribologist is required to achieve effective lubrication of all moving engine components. In order to reduce friction and wear, with a minimum adverse impact on the environment. This task is particularly tough given the wide range of operating conditions of speed, load, and temperature in an engine.

Improvements in the tribological performance of engines can generate the following benefits: Reduced fuel consumption, increased engine power output, reduced oil consumption, a reduction in harmful exhaust emissions, improved durability, reliability and engine life, reduced maintenance requirements and longer service intervals.

Under highly loaded, high temperature conditions, fluid film lubrication may not be sufficient to provide complete wear protection such as those experienced by piston rings at the top of the cylinder under the influence of the burning fuel. In such cases, the lubricant must contain additives that interact with rubbing surfaces to form anti-wear films. These chemical films form on hot iron surfaces during vehicle operation as long as the lubricant has not degraded excessively. However, these chemical films may be partially scraped away during severe engine service. Once the additives that provide this chemical film (typically, zinc dialkyl dithiophosphate, ZDP, and other antioxidant/antiwear agents) are sufficiently degraded, the engine oil needs to be changed, otherwise engine wear will accelerate during use.

Zinc dialkyl dithiophosphate (ZDDP) and molybdenum dithiocarbamate (moDTC) are two advanced nanomaterials that have shown some promise for their contribution to reducing friction and enhancing protection against wear by the formation of a molybdenum disulfide layer on the rubbing surfaces. In the case of engine oil applications, these nanomaterials can help increase the durability and performance of exhaust -treatments and reduce harmful emissions – in fact, exhaust catalysts might become poisoned by sulfur and phosphorus that are present in conventional lubricant additives.

The next innovation of lubrication technology incorporates nanotechnology. The inspiration for nanolubricants is the spherical carbon molecule, the fullerene. Fullerenes are hollow spheres formed by a network of at least 60 carbon atoms. Different researchers have experimented with different nanomaterials. Friction is reduced by multiple mechanism one whereby the nanoparticles behave like ball bearings in the interface between the two surfaces. The small size allows the particles to penetrate into smaller surfaces, creating a more complete coverage. Van der Waals forces ensure that the particles adhere to the surfaces and tribochemical reactions can also occur modifying the metal into a low friction surface.

These particles are non reactive so they can be added to existing lubricants. Furthermore, these particles are non toxic and are environmentally friendly. Nanotechnology can be the innovation that will allow lubricant products to meet environmental regulations, mitigating costs for the company as stricter regulations regarding release of lubricants to environment can result in fines.

1.9. REFERENCES

[1] Challen, B. and Baranescu R. (1999) *Diesel engine reference book.* 2nd edn, Butterworth-Heinemann

[2] Heywood J. E. (1988), *Internal Combustion Engine Fundamentals,* 1st edn, MCGraw-Hill.

[3] Kamimoto T and Bae M. (1988), High combustion temperature for the reduction of particulate in diesel engines. *SAE paper* 880423.

[4] Musculus M.P.B., Miles P.C. and Pickett L.M. (2013), Conceptual models for partially premixed low-temperature diesel combustion. *Progress in Energy and Combustion Science* 39 (2-3)246-283,.

[5] Benajes J, Molina S, Riesco JM and Novella R. (2004) Enhancement of the Premixed Combustion in a HD Diesel Engine by Adjusting Injection Conditions. *THIESEL Conference on Thermo- and Fluid Dynamics Processes in Diesel Engine*, Valencia, Spain.

[6] Pickett L. and Siebers D. (2004), Non-Sooting, Low Flame Temperature Mixing-Controlled DI Diesel Combustion. SAE Paper 2004-01-1399.

[7] Benajes J., Molina S., Novella R. and Amorim R. (2010), Study on Low Temperature Combustion for Light-Duty Diesel Engines, *Energy & Fuels* 24, 355-364,.

[8] Turns, S. R. (1996) *An introduction to combustion. Concepts and applications*. 3th edn. McGrawHill Book Co, New York.

[9] Giechaskiel, B., Maricq, M., Ntziachristosc, L., Dardiotisd, C., Wange, X., Axmannf, H., Bergmanna, A., Schindlerg, W. (2014), Review of motor vehicle particulate emissions sampling and measurement: From smoke and filter mass to particle number. *Journal of Aerosol Science*, 67(1), 48-86

[10] Heck R. M., Farrauto R. J., Suresh T. G. (2009), *Catalytic air pollution control. Commercial technology*, 3th edn., Wiley.

[11] Ladommatos N., Balian R. Horrocks R. and Cooper L. (1996a) The effect of exhaust gas recirculation on combustión and NO_x emissions in a high-speed direct-injection diesel engine, *SAE Paper* 960840

[12] Ladommatos N., Balian R. Horrocks R. and Cooper L. (1996b), The effect of exhaust gas recirculation on soot formation in a high-speed direct-injection diesel engine. *SAE Paper* 960841.

[13] Eastwood, P. G. (2000), *Critical topics in exhaust gas after-treatment*. Research Studies Press Limited.

[14] Benajes, J., Reyes, E. and Luján, J.M. (1996), Modelling Study of the Scavenging Process in a Turbocharged Diesel Engine with Modified Valve Operation, *Proceedings of the Institution of Mechanical Engineers, Part C: Journal of Mechanical Engineering Science*, 210(4), 383-393

[15] Chevron Corporation (2007), Diesel Fuels Technical Review. Accessed online.

[16] Agarwal, A. K. and Das L. M., (2000), Biodiesel Development and Characterization for Use as a Fuel in Compression Ignition Engines, *J. Eng. Gas Turbines Power* 123(2), 440-447

[17] Lapuerta, M., Armas, O. and, Rodríguez-Fernández, J. (2008). Effect of biodiesel fuels on diesel engine emissions, *Progress in Energy and Combustion Science* 34, 198–223

[18] Desantes, J.M.; Benajes, J.; Arrègle, J.; Delage, A. (2000) Effect of the properties of several fuels on the injection and combustion process in HDSI Diesel engines, *Proceedings of the THIESEL 2000 conference*, p.269-285 .

[19] Kalghatgi, G.T. (2014). The outlook for fuels for internal combustion engines. *International Journal of Engine Research* 1–17

[20]Lu, X., Han, D. and Huang, Z. (2011) Fuel design and management for the control of advanced compression-ignition combustion modes, *Progress in Energy and Combustion Science* 37, 741-783

[21] Kokjohn SL, Hanson RM, Splitter DA and Reitz RD. (2011) Fuel reactivity controlled compression ignition (RCCI): a pathway to controlled high-efficiency clean combustion. *Int J Engine Res*; 12, 209–226.

[22] Splitter D., Reitz R. and Hanson R. (2010), High efficiency, low emissions RCCI combustion by use of a fuel additive. *SAE Int J Fuels Lubr*; 3(2), 742–756.

[23] Zhmud, B. Pursuit for better fuel economy: Reducing engine friction helps maxing out miles per gallon. Veh. Compon. 2012, 5, 18–21

[24] Kolesnikov, V.I.; Myasnikova, N.A.; Volnyanko, E.N.; Ermakov, S.F.; Sychev, A.P.; Sychev, A.A. Lubricants with ceramic nanoadditives and wear-resistant surface structures of heavy-duty frictional joints. Russ. Eng. Res. 2011, 31, 454–457.

[25] Gitis, N.V. Tribology Testing of Lubricating Oils with Nano-Additives. In Proceedings of 16th International Colloquium Tribology, TAE, Stuttgart, Germany, 15–17 January 2008; p. 78.

[26] Zak, Z.; Fleischer, N.; Zarbuv, M.; Drangai, L.; Genut, M. Nanomaterials for gear lubrication solutions. Available online: http://www.gearsolutions.com/media//uploads/assets//PDF/Articles/Dec_09/1209_Nano.pdf (accessed on 18 November 2013).

[27] S.C. Tung, S. Hartfield-Wünsch Advanced engine materials: current development and future trends, NIST (National Institute of Science and Technology), Engine Materials and Tribology Workshop, Gaithersberg, Maryland, April 4–7 (1995)

[28] Simon C Tung, Michael L McMillan, Automotive tribology overview of current advances and challenges for the future, Tribology International, Volume 37, Issue 7, July 2004, Pages 517-536

CHAPTER II AFTER-TREATMENT TECHNOLOGIES: STATE OF THE ART AND EMERGING TECHNOLOGIES

2.1 Introduction

Engines are devices that convert chemical energy into mechanical energy. When hydrocarbon fuels burn, the complete oxidation leads to CO_2 and H_2O. In the case of diesel engines, the typical lean-burn conditions occurring in the combustion chamber lead to an average composition of the flue gases being the following: CO_2 2-12%, H_2O 2-12%, O_2 3-17%, N_2 balance. None of these species has adverse effects on the environment or on human health, with the exception of the CO_2 greenhouse effect. The characteristics of the diesel fuel itself, and of the diesel engine operating conditions, are responsible for the formation of other species, generally in rather small concentrations. However, these low emissions have serious noxious effects both on humans and on the environment. These species may originate from incomplete combustion (i.e. CO, HC, PM), from temperature and pressure conditions prone to the formation of particular compounds (i.e. **NO_x**), or from the oxidation of species present in the fuel which are not hydrocarbons (i.e. SO_2). Some of them are regulated by the legislation related to diesel engine emissions, while others are still unregulated.

2.2 Diesel Oxidation Catalysts

2.2.1 DOC principle of operation

The diesel oxidation catalyst (DOC) promotes the oxidation of several species present in the diesel engines exhaust gases. The oxidation occurs by means of the oxygen already present in the gases, which is abundant due to the fact that diesel engines work under lean conditions. This oxidation is tailored to the formation of harmless substances, such as carbon dioxide and water. The species oxidized within the DOC are mainly carbon monoxide (CO), unburned hydrocarbons in gas phase (HC) and the organic fraction of diesel particulates (SOF). The latter is commonly adsorbed onto the carbonaceous particles present in the exhaust. Other pollutants affected by the DOC are aldehydes and PAH.

The oxidation process through which the above mentioned pollutant emissions are mitigated is the following:

$$CO + ½\ O_2 \leftrightarrow CO_2 \qquad (1)$$

$$C_xH_y + (x + y)\, O_2 \leftrightarrow x\, CO_2 + \tfrac{1}{2}y\, H_2O \qquad (2)$$

where Eq. 2 is representative for both HC and SOF compounds.

Other oxidative reactions can occur in the DOC, whose effect could be undesirable and could lead to noxious products: one of these is the oxidation of sulphur dioxide to sulphur trioxide, which is the precursor of acid rains through sulphuric acid formation in the atmosphere. In some other cases, the DOC effect on the species present in the gases could become favourable, even if the product is not a harmless compound. This is the case of NO to NO_2 oxidation, the latter being more toxic than NO; however the strong oxidative capacity of nitrogen dioxide can be effectively used to facilitate the regeneration of trapped soot in diesel particulate filters [1]. It is evident that the whole after-treatment device must be compliant with the NO_x emission regulations, and avoid excessive NO_2 slip.

The most common DOC catalytic converter design is a ceramic honeycomb monolith, characterized by many parallel channels, open at the front and at the back (from which derives the appellation "flow-through" monolith), running in the axial direction. The material of the honeycomb monolith can be metallic as well, made of a thin foil appropriately bent to form a honeycomb structure. Both metallic and ceramic commercial DOC monoliths for automotive applications have cell densities of hundreds of cells per square inch (cpsi). The ceramic or metallic substrate of the monolithic catalytic converter is only the structured support for the active species with a specific catalytic activity. Hence, the function of the monolith substrate is to ensure a high geometric surface for catalytic deposition, and a satisfactory structural stability to the high temperature gradients along space and time. The catalyst can be directly deposited onto the support or, more frequently, the channel walls of the monolithic support are coated with porous, high surface area inorganic oxides such as Al_2O_3, CeO_2, and ZrO_2, characterized by high specific surface (hundreds of m^2/g) and good material contact compatibility with the support itself [2]. That coating is called the washcoat. The active catalyst (in most cases noble metals, such as Platinum-Pt, Palladium-Pd and Rhodium–Rh [3]) is then deposited within the pores of the washcoat, with a procedure that maximizes the active species dispersion. The exhaust gases flowing into the DOC channels diffuse from the bulk of the gas to the washcoat pore structure, and down to the catalytic sites, where the heterogeneous catalytic reactions occur.

2.2.2 DOC performance

The CO and HC diesel engine emissions control via the DOC is very effective, however the oxidation catalyst may suffer of low temperature low activity, and show light-off limitations. Conversely, at mild and high temperatures, the catalyst activity increases rapidly until the plateau of almost complete conversion is reached.

The CO conversion is reached at a temperatures which are the lowest among hydrocarbons. Generally, the DOC conversion efficiency depends upon several factors related to catalysis and fluid-dynamics: hence crucial elements, beside the intrinsic catalytic activity of the catalyst, are the specific surface of the catalytic layer and the mass transfer coefficient in the gas phase, which depends on the geometry of the converter (i.e. cell density). On the other hands, the light-off temperature depends mainly on the chemical reaction kinetics in the catalyst. Therefore, it is influenced primarily by the catalyst noble metal/washcoat system. The overall performance of a catalyst system is therefore a combination of the applied catalyst technology and the substrate geometry.

The total NO_x emissions are almost not affected by the DOC, in terms of total concentration [4]. Hence, other catalytic converters than DOC undertake the duty to achieve NO_x abatement in the exhaust line, such as SCR catalysts or NO_x adsorbers (treated later in this chapter). In some cases a small reduction in the NO_x concentration is detected, mainly due to three factors: the lean NO_x performance of the DOC catalyst, the storage of nitrates in catalyst washcoat, and the reactions with diesel PM or HCs. The former can occur over the common Pt/Al_2O_3 system, at high HC/NO_x concentrations. The conversion of NO_x over Pt, occurring at low temperatures of approximately 200-250°C, leads essentially to the partially reduced N_2O [5]. Although its concentration in the exhausts is not regulated at the moment, N_2O is a strong greenhouse gas, and therefore it is an undesirable product. Storage of NO_x on the washcoat may occur as well, leading to the formation of adsorbed nitrates on materials such as Barium, a common alumina washcoat stabilizer in oxidation catalysts [6]. However, the Barium sites are quickly saturated, and nitrates do not decompose as it happens in tailored NO_x adsorbers that are periodically regenerated.

Reduction of the NO_x concentration after the DOC may also involve the reaction between the NO_2 present in the exhaust gases, or the one formed inside the DOC itself due to NO oxidation, and diesel particulates or HC (including HC stored in the washcoat) [7]. However, these reactions occur only partially inside the DOC: hence, they need a longer PM residence

time in the catalytic zone, which is a condition encountered in the DPF where soot is physically trapped on the porous surface of the flow-through monolith.

Although the total NO_x concentration remains almost unchanged across the DOC (due to the mentioned NO_x to N_2 kinetic pathways which are not favoured), the NO/NO_2 proportion may vary considerably due to NO to NO_2 oxidation over DOC oxidizing catalysts. The most favourable temperature range for NO to NO_2 oxidation is above 250-300°C [8]: NO_2 concentration can increase from about 10 ppm in the raw exhaust to a maximum of 120 ppm downstream the DOC [8]. Above 400°C the NO_2 formation is inhibited by the thermo-dynamic equilibrium.

As far as diesel particulate matter emissions are concerned, it has to be taken into account that the total PM is composed of three major fractions (solid particles, SOF and sulphates), and that each fraction is differently affected by the DOC catalytic activity. Generally, the carbonaceous fraction remains practically unchanged since the residence time inside the DOC is too small to produce any relevant oxidation effect [9]. Conversely, the SOF fraction, composed of heavy hydrocarbons, can be efficiently oxidized within the DOC, thus leading to a reduction in the total PM mass [10]. Finally, sulphates increase due to the oxidation of SO_2 [11] with subsequent formation of sulphuric acid. Hence, in the case of high sulphur containing fuels, the DOC is likely to increase the total PM emissions due to sulphate formation. Only ultra-low sulphur diesel fuels eliminate the sulphate problem, allowing for more flexibility in diesel oxidation catalyst formulation.

2.2.3 *DOC catalysts*

The most important DOC catalytic components and functionality are:

1) Noble metals: Oxidation of CO, HC and SOF;
2) Base metals: Cracking and/or oxidation of SOF;
3) Zeolites: Washcoat storage of HC;

Noble metals (Pt, Pt/Pd) are devoted to the catalytic oxidation of the gaseous species (CO and HC) and of SOF. The most common formulation is constituted by Platinum over an Al_2O_3-based washcoat [3]. The amount of Pt loading is quite high in order to achieve satisfactory CO and HC emission reduction (50 g/ft^3 and higher) [12]; the loading is even higher if good

performances are required at low temperatures (which is a typical trend of current diesel engines, resorting to high EGR).

Base metals (Ce, Fe, V, Cu, and others) can be employed for PM emissions reduction, by promoting cracking and oxidation of the long chain hydrocarbons which constitute the SOF fraction of diesel particulates [10]. As far as CO and HC oxidation is concerned, base metals are not as performing as required by the emission regulations, which entails that nowadays the presence of Platinum in the DOC catalytic formulation is mandatory.

An important role in the DOC performance is played by the washcoat chemical activity, apart from its enhanced surface area promotion for homogeneous catalyst dispersion. Hence, the washcoat has a storage capacity towards the gaseous species, which can be adsorbed and released back to the gas within appropriate temperature ranges. The most important washcoat storage capacity is directed to the adsorption of hydrocarbons in cold start conditions, when the catalyst is still inactive [13]. The successive release is optimized to occur above the catalyst light-off temperature. As a result, this approach reduces the diesel exhaust HC emissions and odour immediately after engine start-up. In this context, Zeolite-based HC traps have become a common component of the DOC washcoat in both light and heavy duty applications. HC storage in the washcoat also plays a role in SOF and NO/NO_2 conversion, even with a washcoat that does not contain HC traps.

2.3 Catalytic Diesel Particulate Filter Systems

2.3.1 DPF principle of operation

Diesel particulate filters (DPF) are the most common devices for the collection of particulate matter for on-board diesel exhaust after-treatment. The filter cannot accumulate particles indefinitely and needs to be thermally regenerated: this operation can be continuous or periodical, and in both cases involves the in-situ combustion of the trapped PM.

The capture of the solid fraction present in the diesel engine emissions is carried out through a physical entrapment, thus preventing its release into the atmosphere. The filtration is carried out in monolith-shaped reactors, which differ from the DOC flow-through structure described before. Hence, DPFs have a wall-flow structure: the channels of the monolith are alternatively plugged, thus forcing the gas to flow through the porous walls which separate neighbouring channels. The DPF manufacturing materials are generally ceramics, in most cases cordierite or silicon carbide. The material selection is tailored to the optimization between thermo-

mechanical properties and cost. Thermal resistance is needed since regeneration involves considerable temperatures for soot combustion, as detailed later. PM filtration is the combination of two phenomena: depth filtration, namely particle collection in the porous network inside the wall material, and cake filtration, characterized by the formation of a soot cake layer on the top of the porous wall due to the occlusion of the pores of the ceramic material [14,15]. The overall filtration can exceed 90% over a cycle of filtration/regeneration [15]. On the other hand, due to the intrinsic DPF mechanism, the reduction of the non-solid fractions of PM, like SOF or sulphate particulates, must be addressed by other means since for these species DPFs are clearly ineffective.

PM filtration is associated with an increase of the pressure drop across the filter itself. Therefore, DPFs need to provide a way of removing particulates from the filter, to restore its soot collection capacity, and reduce the pressure loss across it. Particle removal can be continuous, during the normal DPF filtration activity (passive regeneration) or periodical, through a temperature increase at the front of the DPF until the trapped soot starts to ignite and is converted to oxidized gaseous products (active regeneration). Active regeneration is mandatory if gas thermal levels are not sufficient to ensure a passive regeneration. Both regeneration strategies are invisible to the driver and are performed without his/her intervention.

Usually filters are coated with catalysts on the surface of the porous ceramic walls in order to reduce the temperature at which soot ignites: in the case of passive regeneration, this could be crucial to allow a soot oxidation rate equal to the deposition one; instead, for active regeneration this reduces the temperature to be reached by the gases at the DPF inlet to start the process. Hence, such temperature increase is obtained by injecting some additional fuel that burns in a specific upstream DOC catalyst, thus increasing the exhaust gases temperature. The frequency at which active regeneration is carried out is a matter of fuel economy. From one side the injection of fuel to increase the temperature of the exhaust gases is clearly associated with a fuel penalty, which tends to delay the filter regeneration. On the other hand, the increased engine backpressure due to soot accumulation involves a certain energy loss, which requires to clean the filter and to reduce the pressure drop. The optimization between the two phenomena has to be performed to select the most suitable regeneration frequency. There is another factor involved in the regeneration timing: soot accumulation must be below a certain limit, otherwise excessive temperatures are reached during regeneration due to the

high amount of burning soot. This in fact could irreparably damage the material and cause cracks that invalidate its filtration capacity [16].

2.3.2 DPF characteristics and materials

Cordierite and Silicon Carbide (SiC) are the most commonly employed materials for DPF manufacturing [4]. Cordierite dates back to the 80s, while SiC is more recent and was first introduced in a large commercial scale in the 90s. At present, SiC is the most employed on-board diesel engine passenger cars [4]. A third, and less exploited, material is the Aluminum Titanate.

Cordierite ($2MgO\text{-}2Al_2O_3\text{-}5SiO_2$) has been originally developed for flow-through monoliths, constituting the three-way catalytic converters for gasoline engine cars. Its main advantages are a very low thermal expansion coefficient and a low E-modulus. As a result, Cordierite can withstand high thermal shocks and thermal cycles: these characteristics are crucial for DPFs that are meant to work shifting from loading to regeneration periodically. Cordierite is an oxide that can be easily coated with platinum or other noble metal catalysts. This operation can be carried out by direct dipping of the monolith into a solution of noble metal precursors. Alternatively, Cordierite could be wash-coated in order to exhibit a higher specific surface for metals dispersion. The maximum diameters for Cordierite extrusion are around 300 mm, since greater dimensions could lead to cracks during regeneration. In fact the sudden increase of temperature is localized in some parts of the filter, due to soot ignition unevenness along the filter itself [17]. Consequently, if higher diameters of the full scale filter have to be reached, smaller segments are glued together using a ceramic cement. This obviously reduces the filtration area since the channel sides adjacent to the glue are not permeable [18].

SiC monoliths are manufactured through the extrusion of Silicon Carbide powder. The extrusion process generates the porous network of the filter walls, as a result of the sintering of the initial particles. The compatibility of SiC with catalysts is not high, and a washcoat is preferred for metal deposition. The main advantage of SiC over Cordierite is its high thermal resistance: this feature is extremely important since uncontrolled regeneration occasionally occurs, leading to temperatures exceeding 1200°C, which may cause the filter melting [19]. Compared to Cordierite, SiC is more resistant to temperature peaks, since its upper temperature limit is above 2000°C. In any case high temperatures must be avoided, otherwise the filter could undergo massive melting; therefore the soot loading seldom exceeds 7-10 grams per litre of filter. Another characteristic of SiC is its high thermal conductivity, which

facilitates the temperature homogenization during regeneration. However, it facilitates cracks formation in the case of high temperature gradients. Finally, SiC has a pore network that increases the permeability with respect to cordierite and reduces the bare filter pressure drop. DPF monoliths are then packaged into stainless steel housings in the exhaust line. The stability of the filter position is ensured by a vermiculite bed surrounding the DPF. This bed is rolled up around the DPF which is then positioned inside the steel housing; afterwards, the housing is heated at a certain temperature until vermiculite expands and irreversibly blocks the DPF in its position, thus protecting it from vibrations and external shocks.

2.3.3 *DPF filtration*

The filtration activity of the DPF is associated to a certain pressure drop. Initially, this pressure drop is caused by the clean filter itself, namely by the resistance given by the filter to the gas flow. The total pressure drop of a clean filter is the combination of three factors: the pressure drop due to the sudden contraction and expansion at the inlet and outlet of the filter, the pressure drop due to channel wall friction induced by the gas flow, and the pressure drop due to wall permeability [14]. The last contribution to the total pressure drop increases linearly with respect to the velocity if the flow is laminar.

As the particulate starts to deposit into the filter channels, the pressure drop increases with time following a non-linear profile (Fig. 7). This phase is called depth filtration, during which pore properties like permeability and filter porosity continuously change due to the increasing soot deposit inside the pore network [20]. The occlusion of the pores of the ceramic filter due to particle deposition shifts the filtration regime from depth to cake filtration: in this phase the pressure drop increases linearly with time and soot loading (Fig.7).

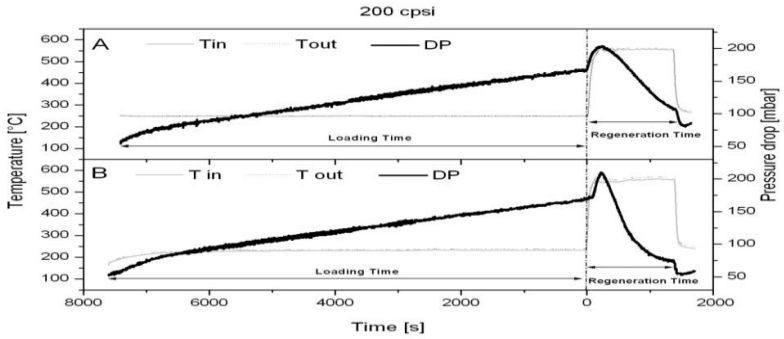

Fig. 7 Comparison between a non-catalyzed filter (top) and a $La_{0.8}K_{0.2}Fe_{0.9}Cu_{0.1}O_3$+2%Au catalytically coated filter (bottom) in terms of pressure drop (right axis) and temperature (left axis) [21].

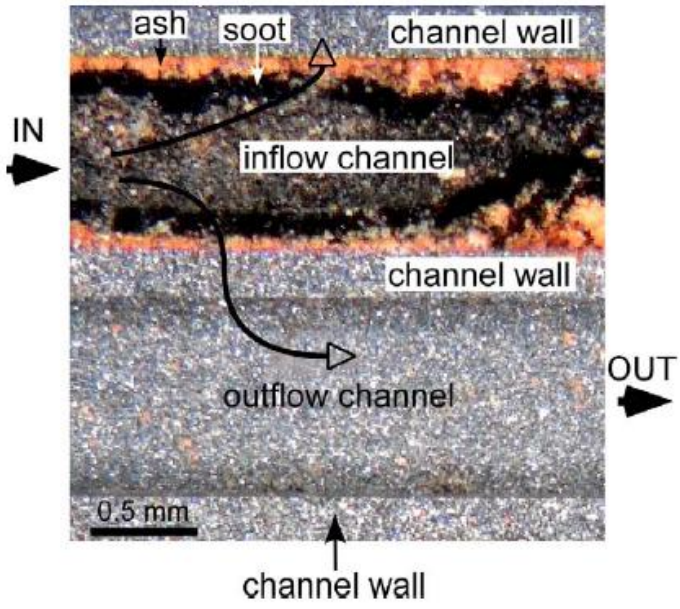

Fig. 8 Representative microphotograph of two neighboring (inflow–outflow) channels (section parallel to the flow) showing the distribution of ash (reddish) and soot (black) at the outlet-mid part of DPF1. (Reproduced from [22]).

The cake filtration is characterized by higher filtration efficiencies than during depth filtration, since the deposited cake acts as the real filtration device. In addition, cake filtration involves a relatively high pressure drop due to high packing density of the deposited soot Fig. 8 : the total pressure drop is now caused mainly by the deposited soot, and only a small fraction accounts for the DPF bare material [14]. On the grounds of the described filtration mechanism, it arises that DPFs are prone to solid particulate filtration, while they are less effective towards liquid particles, or ineffective in the case of gases or vapours. PM is mainly constituted by a solid fraction of carbonaceous particles and ashes, which are effectively filtered [23]. However, the remaining part of PM accounts for liquid particulates, namely SOF and sulphates. At the exhaust gas temperatures inside the filter, SOF and sulphates can be at a vapour state, thus being ineffectively trapped by the DPF. SOF, which mostly derives from lube oil, is somewhat oxidized by the DPF catalytic activity at high temperatures (abatement efficiency 80%) [24]. Sulphate emissions can even increase due to the DPF oxidizing activity during regeneration; therefore, ultra-low sulphur diesel fuel be adopted to control sulphate emissions.

Downstream the DPF, the exhaust gases are cooled down and the formation of liquid particles (through nucleation and condensation) occurs. As a result, a decrease of the particle filtration efficiency at low diameters can be detected, if volatile nanoparticles are not removed before particle number sampling [25].

2.3.4 DPF regeneration

DPF filters are designed to hold a certain quantity of soot. When the filter becomes overloaded, the deposited particulate generates an excessive obstacle to the gas flow in terms of pressure drop, which may also lead to the clogging of the filter. Since the filter PM trapping capacity is sufficient only for few hours of continuous operation, the filter must be regenerated. The regeneration consists of the combustion of the deposited soot particles, thanks to the temperature increase of the exhaust gases at the filter inlet: their temperature promotes the auto-ignition of soot particles. When the filter regeneration is performed, the initial filter properties are recovered. This recovery is not complete, since regeneration does not eliminate all the formerly deposited soot; moreover, ashes tend to accumulate into the filter channels without being eliminated since they are incombustible [26]. Even though the contribution of ashes in the total PM is much less than carbon, the accumulation of ash causes a gradual and irreversible increase in the pressure drop across the filter over its lifespan [27].

During active regeneration, the above mentioned exhaust gases temperature increase is obtained through the addition of a certain quantity of fuel, either in the engine cylinder [28], or in the exhaust after-treatment system, upstream the filter. Generally, the in-cylinder strategy involves higher fuel penalties but a lower system complexity. No matter which fuelling strategy is adopted, the added fuel is burnt in a converter before the DPF, such as the DOC itself or a specific oxidation catalytic converter close to the DPF. This catalytic converter reduces the light-off temperature of the fuel to be burnt [29]. Clearly, the regeneration might not be carried out at idle or at light engine load conditions, when the exhaust gas temperature is very low and the light-off temperature is difficult to be reached. In addition, low exhausts temperature involves the consumption of a big amount of fuel to reach high thermal levels in the DPF, at which the trapped soot starts to ignite. Generally, light-off temperatures for fuel combustion are around 250°C, while temperatures for inside-DPF soot oxidation are around 500-550°C if the DPF is catalytically coated, or around 600°C and above if not [29]. One important issue is the good atomization of the liquid fuel, which allows a fast

evaporation, and the good mixing with the exhaust gases, which facilitates a complete combustion. A static mixer can be provided to improve mixing.

The evolution of the temperatures across the DOC and the DPF during regeneration, coupled to the behaviour of the pressure drop due to soot combustion, are presented in Fig. 7: the DOC inlet temperature is around 300°C, which increases up to roughly 550°C under the effect of a constant fuel injection flow rate. At these conditions, the pressure drop inside the filter begins to decay, and its evolution is nearly linear with time, indicating an overall constant soot combustion reaction rate. The temperature increase across the DPF ascribable to PM combustion is moderate, namely around 30°C in the figure. The pressure drop across the DPF experiences a peak at the beginning of the regeneration phase, and this is due to the increased gas viscosity and velocity, and the decreased gas density, caused by the temperatures involved in the regeneration, which are higher than those during filtration.

Since the soot combustion rate follows an Arrhenius type relationship, a moderate increase in the DPF inlet temperatures is strongly beneficial to the efficiency of the regeneration phase. This can be appreciated by comparing Fig. 7 (DPF inlet temperature: 550°C) with Fig. 7 (DPF inlet temperature: 600°C): the latter exhibits a faster regeneration, as reflected by the steeper slope of the pressure drop curve. However, temperatures must be kept somewhat low not to damage the catalytic coating of the DPF, which is responsible for the soot combustion efficiency at lower temperature, and therefore reduces the regeneration fuel requirement.

2.3.5 DPF catalysts

Most DPFs perform a catalytically assisted regeneration: the catalytic coating is located in the porous walls of the filter, and is normally constituted by a washcoat on the top of which noble metals are deposited. Alternative catalysts, such as mixed oxides of non noble metals are also object of investigation [29]. The scope of the catalyst is to lower the active regeneration temperature, and to allow a certain degree of passive regeneration at suitable engine points characterized by high exhaust gas temperature, thus delaying the regeneration phase. The drawback of DPF catalytic coating is the increased pressure drop given by the filter due to the washcoat layer.
Several soot oxidation mechanisms are involved, either thermally driven or catalytically assisted, the latter depending on the catalyst formulation:

1) Thermal oxidation by O_2: oxygen is present in the exhaust gases since diesel

engines work under lean conditions, and the post-injected fuel for regeneration purposes do not consume all the residual oxygen in the gases [30,31]. The combustion of CO, HC and other gaseous species, in combination with the ignition of the deposited soot, releases a certain amount of heat that increases the temperature inside the filter. These phenomena can be appreciated by measuring the temperature before and after the filter during a non catalytic regeneration. Generally the temperature increase is not very high as shown in Fig. 7.

2) Catalytic oxidation by O_2: this mechanism involves the soot deposited on the catalytically coated porous wall [32,33], and therefore depends on the contact conditions between the soot particle and the catalyst. Good contact conditions are very difficult to be reached due to the different orders of magnitude of the soot particle and the catalyst cluster sizes. Clearly, this hinders the overall activity of the catalyst, and the established concepts of tight and loose contact conditions were introduced to reproduce these features in laboratory tests [32,33].

3) Catalytic oxidation by NO_2: nitrogen dioxide can be produced in the upstream DOC or in the DPF if specific catalysts are synthesized. Starting from the NO in the flue gases, NO_2 is a strong oxidizer which is very effective in promoting soot combustion [34]. NO_2 acts as an oxygen carrier in the gas phase, and it reduces the inefficacity of solid-solid contact interface between the soot particles and the catalyst. The NO_x emissions downstream the DPF are almost equal to the ones at the DOC inlet, since the reaction of NO_2 with carbon generates NO and CO. The CO slip should be reduced through its catalytic oxidation to CO_2 inside the DPF. The NO_2 regeneration has been fully utilized in the "CRT filter" by Johnson Matthey, which involves NO_2 generation through a catalyst positioned upstream the non-catalyzed filter [35].

The mechanisms of soot catalytic oxidation are complex, and not entirely understood. It is clear that a number of processes occur in parallel, which can be promoted by different types of catalysts. These catalysts can be regrouped into two categories: noble metals and base metals, which both enhance regeneration in the presence of NO_2. The commonest noble metal based catalysts are: Pt, Pd, Rh, Ru; base metals include V, Ce, Mg, Ca, Sr, Ba, Mn, Cu, Ag, and often the catalyst formula is a crystalline mixed oxide, like Perovskites [36], Delafossites [37] and Spinels [38]. Noble metals, usually Pt, show a greater activity towards soot combustion

and CO/HC oxidation. Their high oxidizing activity is however detrimental towards sulphates production and NO_2 slip [39]. On the other hands, base metals are less active and thus require a higher fuel penalty to carry out the regeneration. Their lower cost is practically offset by the increased fuel consumption. Higher CO and HC emissions are produced with a catalytic system based on base metals, while no sulphate particulates and/or nitrogen dioxide emissions are detected. A combined system with both functionalities of noble and base metals is commonly employed [4].

2.4 Selective catalytic NO_x -reduction by ammonia

The legislation regulating NO_x from diesel engines has become more and more stringent through the years; therefore, engine design and calibration techniques have been introduced to reduce their emissions. The implementation of catalytic converters on-board heavy duty class vehicles, and in the near future also on light duty ones, has become essential. Hence, NO_x reducing catalysts are tailored to allow a more efficient calibration of diesel engines, which at the moment is limited by the requirement to reduce NO_x emissions by means of EGR to avoid the presence of NO_x converters in the exhaust line.

The following technologies have been investigated and/or implemented for the reduction of NO_x in the exhaust gases of diesel engines:

1) Selective catalytic reduction with ammonia (NH_3-SCR);
2) Selective catalytic reduction with hydrocarbons (HC-SCR or $DeNO_x$ or lean NO_x catalyst);
3) NO_x adsorber systems (Lean NO_x Traps).

The direct decomposition of NO has been investigated as well [40], even if its implementation has been proven to be difficult [3]. The decomposition of nitric oxide to nitrogen and oxygen is favoured by the thermo-dynamics at the exhaust gases pressure and temperature, but the reaction rate without catalytic promotion is negligible. Catalysts based on copper exchanged zeolite, such as Cu/ZSM-5, showed interesting results, although they suffer from the inhibiting effect of water, the poisoning effect of SO_2, and the low reaction rate [41-43].

2.4.1 NH_3-SCR principle of operation

Selective catalytic reduction of NO_x based on ammonia is realized through the injection of an ammonia source, like urea, upstream a catalytic converter which favours the urea decomposition and the reduction of NO_x to N_2.

The NH_3-SCR global reaction is:

$$4\ NO + 4\ NH_3 + O_2 \leftrightarrow 4\ N_2 + 6\ H_2O \quad (3)$$

High NO_x to N_2 conversions can be achieved with this technology, up to 90% [44]. The main disadvantages include the associated capital and operating cost, the space requirements for the catalytic converter and for the urea tank, and the possible generation of unreacted ammonia emissions, called ammonia slip [45].

The main issues related to the ammonia based SCR are the following:

1) Catalyst formulation: diesel engines operate under wide ranges of mass flow rates, temperatures and pollutant concentrations, according to the different duty cycles. In particular, the low temperature condition is severe both in terms of NO_x activity and catalyst durability (deactivation by ammonium nitrate and/or sulphate formation) [44], also considering the limited availability of catalysts due to possible health impact associated to their emissions, as for the case of vanadium;

2) Control strategy: the transient operations introduce the challenges of reducing the undesired ammonia slip and other secondary emissions, such as N_2O and NH_4NO_3 [46,47]. The retrofit through NO_x measurement downstream the SCR is therefore required for the system improvement efficiency;

3) Reducing agent: urea has been primarily selected as the best ammonia source, due to its low toxicity, safety, availability and low cost. However, 32.5% urea solutions have freezing temperatures of -11°C, which is not acceptable for winter conditions in cold climates. The use of ammonium formate has been proposed for SCR applications in cold climates (40% solution of ammonium formate in water has a freezing point of -35°C), but it has a lower NH_3 content than urea. An alternative reductant supply method is to use solid urea rather than water solutions, but systems proposed for dosing solid urea appear to be more complex than those utilizing urea water solutions, which is now the most common application.

4) Infrastructure: the urea distribution infrastructure needs further development, in order to allow regular urea tank replenishment.

Selective Catalytic Reduction (SCR) is a method to reduce the level of nitrogen oxides (NO_x) with the help of a catalyst. SCR technology can achieve more than 95% NO_x reduction in combustion processes and can meet stricter incoming legislation. It is the absolute NO_x control system but the investment cost of the technology is high.

The competition of SCR with the other NO_x reduction technologies, such as NO_x adsorbers, is a balance of fixed and operating costs: the former entails high costs of the system as well as of urea, which is consumed at about 3-5% of the fuel volume [4], while the latter brings an associated fuel penalty during adsorber regeneration, as explained later.

2.4.2 NH_3-SCR reactions

The typical layout of a NH_3-SCR for mobile diesel engines and fuelled with urea is generally configured as an open loop control, namely the amount of injected urea follows a pre-determined map of the NO_x emissions as a function of engine speed and load. Under transient test conditions, open loop systems can provide NO_x reduction of up to about 80% [4]. The urea solution is injected in the exhaust line upstream the SCR catalyst. The atomization allows a fast evaporation of the solution tailored to reach a good mixing with the exhaust gases, which can be assisted by the use of static mixers. Hence, a homogeneous distribution of the flow into the catalytic converter is crucial to reach good conversion efficiencies [48].

After mixing, the vaporized urea enters the whole NO_x catalytic converter, which is composed by three parts with different functionalities. The first one is devoted to urea decomposition into ammonia, also called hydrolysis. The different blocks have not to be physically independent, but only zones with different catalytic coatings within a unique monolith. The catalytic converter is usually a structured monolith, as the ones described in the section related to the DOC, having cell densities as high as 300 cpsi, and typically working at space velocities ranging between 20000 and 30000 hr^{-1}. An increase in the cell density allows reaching lower space occupancies of the monolith.

Straight after urea decomposition, ammonia reacts with the NO_x and oxygen present in the exhaust gases, through the following chemical reactions, to produce nitrogen:

$$4\ NO + 4\ NH_3 + O_2 \leftrightarrow 4\ N_2 + 6\ H_2O \qquad (4)$$

$$2\ NO_2 + 4\ NH_3 + O_2 \leftrightarrow 3\ N_2 + 6\ H_2O \quad (5)$$

$$6\ NO + 4\ NH_3 \leftrightarrow 5\ N_2 + 6\ H_2O \quad (6)$$

$$6\ NO_2 + 8\ NH_3 \leftrightarrow 7\ N_2 + 12\ H_2O \quad (7)$$

$$NO + NO_2 + 2\ NH_3 \leftrightarrow 2\ N_2 + 3\ H_2O \quad (8)$$

These reactions are inhibited by water, which is always present in the exhaust gases from the diesel engine. In addition, other possible reaction paths can occur, leading to undesired products. These reaction paths may include a partial reduction of NO_x leading to N_2O, or the direct oxidation of NH_3 causing a NO_x concentration increase instead of an expected decrease:

$$8\ NO_2 + 6\ NH_3 \leftrightarrow 7\ N_2O + 9\ H_2O \quad (9)$$

$$4\ NO_2 + 4\ NH_3 + O_2 \leftrightarrow 4\ N_2O + 6\ H_2O \quad (10)$$

$$2\ NH_3 + 2\ O_2 \leftrightarrow N_2O + 3\ H_2O \quad (11)$$

$$4\ NH_3 + 3\ O_2 \leftrightarrow 2\ N_2 + 6\ H_2O \quad (12)$$

$$4\ NH_3 + 5\ O_2 \leftrightarrow 4\ NO + 6\ H_2O \quad (13)$$

Among the reactions involving NH_3 and NO_x, particular temperature conditions (100-200°C) could lead to the formation of NH_4NO_3, which is explosive and deposits in solid or liquid form in the pores of the catalyst, causing temporary deactivation [49]. The strategy to reduce ammonium nitrate or other secondary emissions is to tailor the urea injection at different amounts rather than stoichiometric with respect of NO_x.

$$2\ NH_3 + 2\ NO_2 + H_2O \leftrightarrow NH_4NO_3 + NH_4NO_2 \quad (14)$$

Low amounts of ammonia result in insufficient NO_x conversions, while excessive amounts cause a dispersion of ammonia in the environment. In practice, ratios between 0.9 and 1 are used [44]. In any case, the ammonia slip is minimized through the use of a specific oxidation catalyst downstream the SCR which prevents unreacted ammonia from leaving the system. An additional advantage to have the ammonia slip catalyst is to provide a guard for CO and HC emissions [50]. A disadvantage is the increase of N_2O and NO in the exhaust gases from the oxidation of ammonia [51].

Finally, the SCR catalyst can be fouled and deactivated by the deposition of ammonium

sulphate and disulphate, resulting from the oxidation SO_2 to SO_3 with the following formation of H_2SO_4 in the DOC, and the reaction with NH_3 in the SCR. The SCR deactivation occurs at temperatures below 250°C; hence, at low temperatures (between 150 and 300°C depending on the catalyst [52]), the urea injection can be shut to prevent SCR catalyst deactivation.

$$NH_3 + SO_3 + H_2O \leftrightarrow NH_4HSO_4 \quad (15)$$

$$NH_3 + SO_3 + H_2O \leftrightarrow (NH_4)_2SO_4 \quad (16)$$

NO_x reduction based on the engine map pollutants production is not sufficient to achieve NO_x conversions above 90% [53]. Hence, a closed loop control of the urea injection via NO_x and NH_3 measurement is under development. The hardest hindrance to the implementation of this kind of retrofit is the accuracy and the fast response of the on-line sensors. The most common in-situ NO_x measurement technology relies on ZrO_2-based electrochemical sensors [53], which are similar in construction and operating principle to the oxygen sensors used in gasoline three-way catalyst systems. The measurement can be operated downstream the ammonia slip catalyst, through a feed-back strategy, or upstream the SCR catalyst through a feed-forward one. The latter presents some advantages since higher NO_x concentrations are measured, thus decreasing the required sensitivity limits and so making possible the use of the available NO_x sensor technology (i.e., NO_x sensors that were introduced in 2002 for gasoline passenger cars with NO_x adsorbers) [54].

2.4.3 NH_3-SCR catalysts

The main NH_3-SCR catalyst families are based on Platinum, Vanadium oxide and zeolites (Fig. 9). The first technology that has been developed is the one resorting to Pt. Practically, NO_x reduction over Pt is somewhat efficient only at temperatures below 250°C [55]. Hence, at temperatures between 225°C and 250°C, the oxidation of NH_3 to NO_x and H_2O becomes dominant: a poor selectivity towards N_2 is thus reached, and the conversion begins to fall with increasing temperature. It has to be mentioned that low temperatures (around 150-200°C) lead to the above mentioned NH_4NO_3 formation, which entails a very narrow range of available working conditions [55]. Vanadium oxide based catalysts (V_2O_5) operate efficiently in a wider and upper temperature range, from 260°C up to 450°C, reaching a maximum conversion plateau between 300°C and 400°C [34]. This range is optimal both for light duty (lower limit) and high duty (upper limit) applications. To maximize its efficiency, thermal losses need to be minimized in the case of low engine points in light duty applications, especially for the most

modern vehicles that resort to EGR at a great extent. The Vanadium oxide catalyst is the active species that promotes the redox reactions through which NO_x reduction is accomplished, due to the several oxidation states that V can assume [56]. TiO_2 is also present in the catalyst formulation because it is a high surface area carrier [57,58]. The thermal stability of the catalyst at the high temperatures is finally promoted through the addition of WO_3 [59], since the TiO_2 degrades above 500°C from the form of anatase, having a high surface area, to the one of rutile [57,58]. In the last years, reports on the health issues concerning vanadium emissions from SCR catalysts in mobile applications [60], being V_2O_5 classified as possibly carcinogenic in some countries [61], are bound to limit its further exploitation for mobile applications. Zeolites have a very wide temperature range of application, and the most extensively studied is the Cu-exchanged ZSM-5 zeolite [62,63]. This catalyst does not oxidize ammonia to NO_x at high temperatures, and the upper temperature limit for zeolite catalysts may be determined by catalyst durability rather than selectivity [64]. Low-temperature zeolites have been synthesized as well, aiming at widen the temperature range at which they are operative, reaching moderate NO_x to N_2 conversion efficiencies between 200-400°C [65]. Better conversions can be reached in the presence of NO_2.

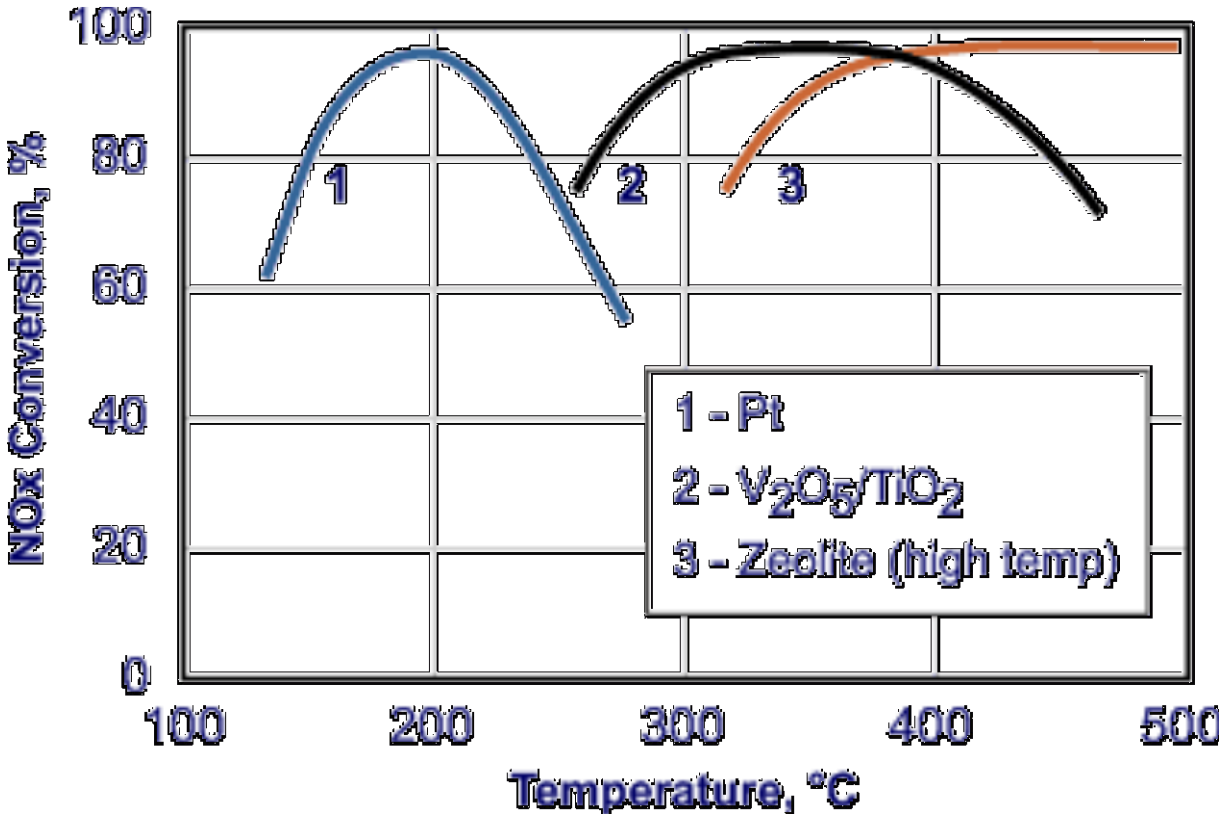

Fig. 9 Operating temperature windows for different NH_3-SCR catalysts (Reprinted from [4]).

The most recent investigations shows a novel Cu-SSZ-13 exhibited NO_x conversions of near 100% over a wide temperature range (160–550 °C). Besides, its activity exceeded 80% even after extensive high-temperature hydrothermal aging and HC fouling. Moreover, Cu-SSZ-13 was more selective toward the formation of N_2, producing lower amounts of undesirable by-products such as N_2O. The enhanced performance of Cu-SSZ-13 has been attributed to the location of Cu ions within the cage; i.e., just outside the six-membered rings of the zeolite framework [66]. Obviously, the enhanced Cu-SSZ-13 demonstrates superior activity and N_2 formation selectivity as well as robust durability in comparison with the conventional Cu-beta and Cu-ZSM-5 SCR catalysts, leading to widespread SCR application.

2.5 Selective catalytic NO_x -reduction by hydrocarbons

2.5.1 HC-SCR principle of operation

The alternative to the use of ammonia as the NO_x reductant is the employment of hydrocarbons. The HC promoted SCR reaction of NO_x reduction, and the parasitic one of HC combustion, are the following:

$$C_xH_y + (2x + ½y)\ NO \leftrightarrow (x + ¼y)\ N_2 + x\ CO_2 + ½y\ H_2O \quad (17)$$

$$C_xH_y + (x + ¼y)\ O_2 \leftrightarrow x\ CO_2 + ½y\ H_2O \quad (18)$$

Catalysts promoting HC-SCR are also known as $DeNO_x$ catalysts or lean NO_x catalysts. Practically, the reaction of Eq. 17 leading to N_2 is not the only path involving NO_x reduction, since also undesired products can be obtained, such as N_2O [36]. As a result, the catalyst selectivity is the key parameter to be optimized in terms of catalyst loading, HC/NO_x ratio and temperature range.

The hydrocarbons operating as reducing agent are either already present in the exhaust gases or injected on purpose, with a tailored timing. In the former case we call this operation "passive $DeNO_x$", while in the latter it is called "active $DeNO_x$".

In passive $DeNO_x$ the hydrocarbons source is the diesel exhaust itself, which makes the system simpler and cheaper. However, since the HC concentration in the exhausts is dependent on the engine points and it is somewhat limited, low conversion efficiencies can be reached.

In active $DeNO_x$ systems, the increase of the HC amount, and the control of their concentration to optimize the SCR catalyst, can be practically realized by two means: the injection of hydrocarbons, preferably diesel fuel, into the exhaust system upstream of the catalyst, or the late in-cylinder injection in a common rail fuel system. Clearly, active $DeNO_x$ systems have higher NO_x conversion efficiency at a cost of increased system complexity and a fuel economy penalty.

The DOC, which has its classical function of CO/HC emission reduction, can be conveniently positioned downstream the $DeNO_x$ system, in order undertake also the duty to avoid HC emissions during active $DeNO_x$.

2.5.2 HC-SCR catalysts

The two main groups of catalysts investigated for HC-SCR purposes are metal-exchanged zeolites (primarily Cu/ZSM-5 [67]), and Alumina supported Pt [68]. The two families exhibit maximum efficiencies at different temperature ranges, which are quite similar to the ones mentioned in the NH_3-SCR section. Hence, Pt/Al_2O_3 shows a good NO_x conversion efficiency in the low temperature window of application, between 200°C and 300°C [68]. On the contrary, the conversion peak for Cu/ZSM-5 is at higher temperatures, above 350°C [67]. It has to be stressed that zeolites are generally more demanding in terms of HC, which implies higher fuel penalties. Hence, HC/NO_x ratios between 3 and 12 are necessary to achieve NO_x to N_2 conversions of 60% [4] (for comparison, the ratio in diesel exhaust is typically below 1). In any case, engine points with low oxygen concentrations allow better NO_x conversions, since a low amount of HC is consumed in the parasitic reaction of direct hydrocarbons oxidation.

2.6 NO_x -adsorbers

2.6.1 NO_x adsorber principle of operation

The technology of NO_x adsorbers is based on the incorporation of NO_x trapping materials in the catalyst washcoat, having the ability to adsorb NO_x and to convert them into solid species (i.e. metal bonded nitrates). The accumulation is carried out under lean conditions, and it

proceeds until the adsorber needs to be regenerated, through windows of rich air-to-fuel mixture, in order to reduce NO_x to N_2.

The amount of fuel and the periodicity of this regeneration, as well as the improvement of the storage capacity of the materials, are the parameters to be optimized to reduce the fuel penalty associated with this operation Among the main drawbacks of this technology, one has to consider that the supply of additional fuel, either into the cylinder, or directly in the exhausts' pipe, generates PM, CO, and HC emissions, whose concentration must comply with the legislation limits. In addition, the regeneration must be carried out as efficiently as possible in order not to be excessively impacting on the fuel economy of the vehicle. Finally, as many other catalysts, NO_x adsorbers are sensible to sulphur [69], which entails both the use of ultra-low sulphur diesel fuels and the development of efficient desulphation strategies.

NO_x adsorbers demonstrated to reach NO_x to N_2 conversions around 70%-90% [4]; due to a number of reasons, this technology is generally considered more suitable for light duty applications, as discussed later in this section. It has to be pointed out that NO_x adsorbers are also referred using different denominations: NO_x adsorber catalysts (NAC), Lean NO_x traps (LNT), $DeNO_x$ traps (DNT), NO_x storage catalysts (NSC), NO_x storage/reduction (NSR) catalysts.

2.6.2 NO_x adsorber reactions

The reaction mechanism in a NO_x adsorber is depicted in Fig. 10, and is the combined effect of an oxidation catalyst (for example Pt), an adsorbent material (such as barium oxide BaO), and a reduction catalyst (for example Rh).

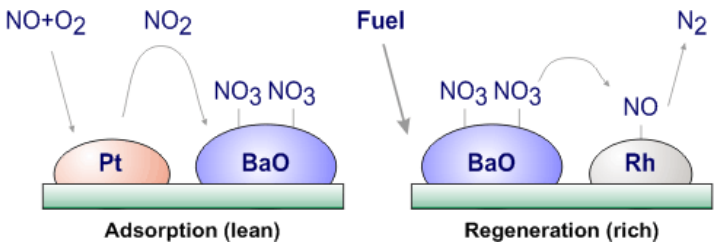

Fig. 10 NO_x storage(Adsorption)/reduction(Regeneration) mechanisms (Reprinted from [4]).

As a premise, most of the NO_x emissions are constituted by NO, but adsorbents are more effective towards NO_2 entrapment. Therefore, the step immediately before NO_x adsorption

should be the NO oxidation to NO_2. This operation is carried out by an oxidation catalyst, able to operate at the peculiar low temperatures of the exhausts of light duty diesel engines, which are the focus of this thesis. The best catalyst to carry out NO oxidation is Pt [70].

$$NO + ½\ O_2 \leftrightarrow NO_2 \quad (19)$$

The NO_2 produced at the catalytic surface is stored thanks to the BaO specific capacity to adsorb NO_2 and to form Barium nitrate (Eq. 20), which is chemically stable at the working operating conditions. The total NO_x adsorptive capacity of NO_x trap obviously depends on the availability of free sites of BaO, which must be recovered when a certain NO_x concentration is attained at the exit of the converter.

$$BaO + NO_2 + ½\ O_2 \leftrightarrow Ba(NO_3)_2 \quad (20)$$

When the regeneration is started, the oxygen concentration decays to almost zero, and suitable conditions for the NO reduction are achieved. The reducing agents can be several, such as CO, HC, or even hydrogen. The most common species devoted to NO reduction are hydrocarbons, which can be directly fed to the system, without further fuel reforming.

The first step of the regeneration is the decomposition of the nitrate, and the recovery of the BaO site (Eqs. 21-22). In this step, NO is released, therefore the proper amount of fuel has to be dosed in order to promptly reduce the NO released.

$$Ba(NO_3)_2 \leftrightarrow BaO + 2NO + 1½\ O_2 \quad (21)$$

$$Ba(NO_3)_2 \leftrightarrow BaO + 2NO_2 + ½\ O_2 \quad (22)$$

NO reduction is carried out by a reducing catalyst such as Rh, incorporated in the overall catalyst formulation [71]. This step is very similar to what occurs in a conventional three-way converter for the treatment of the exhausts from gasoline fuelled engines.

$$NO + CO \leftrightarrow ½\ N_2 + CO_2 \quad (23)$$

As a result of this overall mechanism, the operating temperature window has a lower limit determined by the Pt catalyst activity regarding the oxidation of NO to NO_2, as well as the NO_x release and reduction in the regeneration phase; the upper limit is related to the stability of nitrates, which undergo thermal decomposition at higher exhaust temperatures, even under lean conditions [72].

The above description of a step-wise process is a simplification of what really occurs on the catalyst surface. For instance, barium carbonate and barium hydroxide coexist with barium oxide on the catalyst surface [73,74]. In addition, the NO_x release and reduction does not occur as a sequence of two separate and consecutive steps, but it could evolve also following a direct nitrate reduction without thermal decomposition of the adsorbed NO_x species as a preliminary step [75]. Another source of discussion is the determination of the exact characteristics the NO_x storage on the catalytic surface, both in terms of chemical composition (nitrates or nitrites) and of physical adsorption mode (surface or bulk adsorption).

NO_x adsorption catalysts are sensitive to sulphur: apart from the poisoning of noble metals, sulphur (in the form of SO_3) is competitive with NO_2 in the formation of Barium salts. Hence, BaO sites tend to form $BaSO_4$ in presence of SO_3, which causes a loss of activity towards the adsorption of NO_2. The decomposition of $BaSO_4$ follows the same mechanism as the one shown for $Ba(NO_3)_2$, however it occurs at higher temperature since $BaSO_4$ is more stable than the corresponding nitrate [72].

Another issue of major concern is the possibility of having parasitic reactions that do not lead to N_2, but to undesired reduced products, such as ammonia (NH_3), nitrous oxide (N_2O), and hydrogen sulphide (H_2S), which reduce the NO_x adsorber efficiency and require a careful control of such secondary emissions.

2.6.3 NO_x adsorber catalysts

As stated before, three types of catalysts are present in a NO_x adsorber, namely an adsorbent, an oxidation catalysts and a reduction catalysts, the last two being commonly noble metals. As far as the adsorbent catalyst is concerned, it belongs to one of the three following metals groups: Alkaline earths (Ba, Ca, Sr, Mg), Alkali metals (K, Na, Li, Cs) and Rare earth metals (La and Y) [76]. These metals could be in the form of single metal oxides (the commonest of which is the BaO), or in the form of oxides like Perovskites or metal substituted zeolites [76]. The different oxides are ranked regarding to their NO_x storage capacity, nitrate thermal stability and desorption temperature, of the nitrate, susceptibility to sulphur poisoning and/or sulphate desorption temperature. In this context, alkali metals like K show the greatest NO_x conversion activity among the mentioned metal groups: hence, the inclusion of K, Na, Cs based oxides in the adsorbent catalyst formulation increases the NO_x reduction between 350°C and 600°C [77]. However, the associated nitrates have a lower thermal stability than the ones based on alkali metals, entailing that a direct reduction mechanism rather than a two steps NO_x release + reduction is likely to occur [78]. Another advantage of Alkali based

adsorbents is the good resistance to sulphur poisoning: their inclusion in a Ba based sorbent gives a better performance in this context rather that Ba-only adsorbers; however this leads to a lower NO conversion promoted by hydrocarbons, which makes the adsorbent more fuel demanding [79]. Finally, Alkali based adsorbents have poor performance as far as water induced leaching is concerned [80]. As a result, a trade off between the good NO_x reduction activity at high temperatures of Alkali metal oxides and their excessive mobility has to be found if one wants to include them in a Ba based adsorbent formulation. Adsorbers for light-duty diesel engines, which operate at lower temperatures, may avoid the necessity of using Alkali metals, while high-duty ones have to resort to them.

The washcoat is typically based on γ-alumina, Al_2O_3, which is often employed due to its high surface that allows good dispersion of the active catalyst. Ba and Alumina mixed oxides are designed to minimize BaO sintering at temperatures around 700-800°C [81]. Another washcoat component could be TiO_2 since its acidity gives a lower sulphur affinity, but at the same time it reduces the stability of the nitrate [82]. On the other hand, the more basic oxide ZrO_2 has opposite peculiarities with respect to TiO_2 [82]. Finally, CeO_2 can be included due to its Pt sintering prevention, but its oxygen storage capacity under lean conditions can cause a higher fuel penalty during rich ones since part of the hydrocarbons react with the released oxygen [83]. As for the adsorbent composition, a trade-off among all the materials functionalities has to be found. The effect of BaO loading on the NO_2 trapping capacity and on the overall NO_x conversion performance are shown in Figs. 11 and 12, respectively [84].

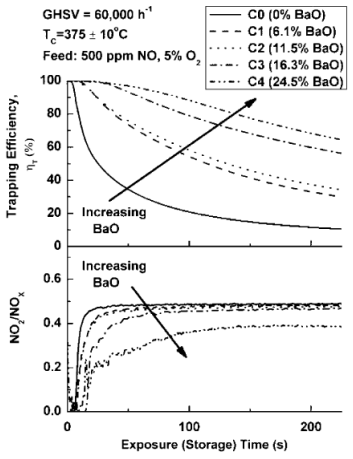

Fig. 11 Dependence of trapping efficiency and NO_2/NO_x effluent concentration ratio as a function of exposure time for several catalysts. The flow rate is 1 Nl/min and the catalyst temperature is 375±10 °C. Feed gas composition is 500 ppm NO, 5% O_2, and balance N_2 (Reprinted from [84]).

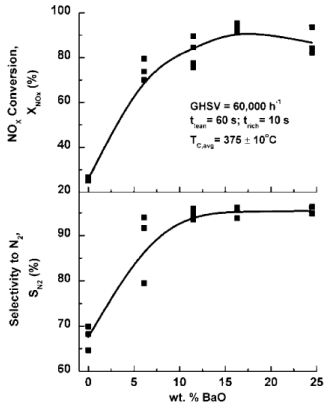

Fig. 12 Dependence of the time-averaged NO_x conversion and selectivity to N_2 on BaO loading. The flow rate is 1 Nl/min, the total cycle time is 70s (Reprinted from [84]).

In this work, the reference catalyst had a Pt loading 2.20 wt% and BaO 16.3 wt% over alumina, reaching a mean NO conversion of 85% over cycles lasting 60s, with injection C_3H_6 every 10s. The inlet concentrations were: NO = 500 ppm, O_2 = 5% (with C_3H_6 = 0.7% during regeneration), temperature = 375 °C and GHSV = 60000 h^{-1}. The complete cycle involves a fuel penalty which can be kept under 4% with an overall NO conversion above 80%.

The kind of regeneration strategy and of reductant species are strictly linked, and are optimized in combination with the catalyst development. The regeneration is constituted by a short pulse of a reducing agent such as hydrogen (H_2), carbon monoxide (CO) and hydrocarbons (HC) to convert the stored nitrates. The performance towards NO_x reduction of a catalyst formulation characterized by the materials and functionalities discussed above is present in the work of [85]: the catalyst consisted of an Alumina based washcoat of Ceria-Zirconia oxygen storage materials, Ba and K oxides as the NO_x storage compounds and the supported noble metals of Pt and Rh. Fig. 13 shows the adsorption capacity of the fresh catalyst and of the regenerated catalyst: by these means, the capacity of the reductant species to regenerate the BaO sites is assessed. “Lean 1” is the inlet composition of the gas, fed at 250°C, and represents a gas model for the exhausts of a diesel engine; “RS1” is the composition of the gas during a 3s lasting regeneration, enriched with CO, HC and H_2. The latter is investigated due to its high reducing potential, which could be exploited in the case of the embodiment of WGS and reforming catalysts in the NO_x adsorber.

	NO (ppm)	O_2 (%)	H_2 (%)	CO (%)	C_3H_6 (ppm)	CO_2 (%)	H_2O (%)	N_2
Lean 1	400	7	0	0.01	200	11	5	Balance
RS1	400	0	1.6	6	1070	11	5	Balance

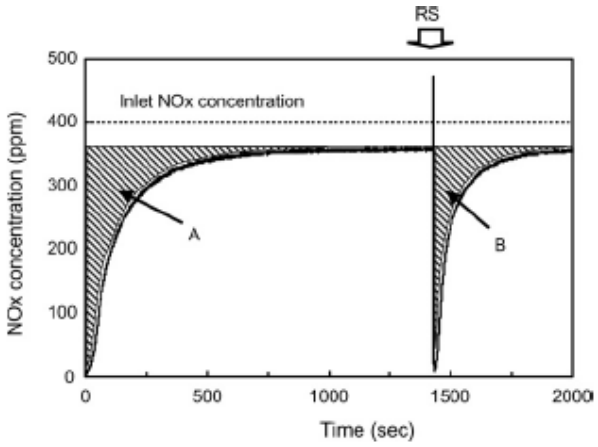

Fig. 13 NO_x concentrations in the inlet and outlet using Lean 1 and RS1 gases at 250 °C (Reprinted from [85]).

When the lean atmosphere is switched on, the outlet NO_x concentration gradually increases with time and then reaches an approximately constant level around 1400s. The shadow area A is related to the NO_x amount stored on the catalyst, while the shadow area B relates to the amount of the regenerated NO_x storage sites on the catalyst. In [85] it is elucidated that the effectiveness of the different reducing agents is in the following increasing order: C_3H_6 < CO < H_2.

2.7 After-treatment technologies

2.7.1 Light duty applications

The current strategy of Euro5 compliant after-treatment line of light-duty diesel engine vehicles is based on a combination of in-cylinder control and active after-treatment. The former is tailored to be compliant with NOx emissions, while low PM tailpipe concentrations are achieved through a DOC+DPF system with active regeneration. This configuration is installed in close-coupled position (i.e. directly attached to the engine) (Fig. 14), in order to improve the thermal management during warm-up and active regeneration. Such a system can be possibly installed in the whole light duty diesel engines range (from the 1.3l up to the 2.4l).

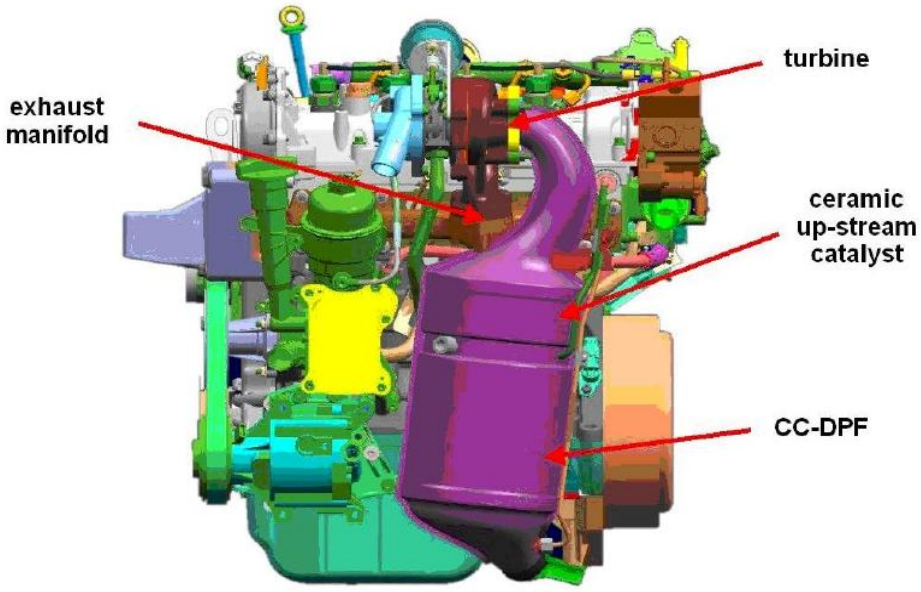

Fig. 14 Fiat Powertrain Technologies architecture: close-coupled DOC+DPF (Courtesy of Fiat Powertrain Technologies).

Euro 6 standards are to about be enforced : the further 10% reduction in PM emissions, coupled to a 66% reduction in NO_x ones, with respect to Euro 5, will require an aggressive strategy of in-cylinder combustion management, cooled EGR and engine compression ratio reduction [86-88] in order to meet these specifications without any NO_x-tailored catalytic converter. This approach penalizes the overall fuel efficiency of the vehicle; therefore, it is likely that either NO_x adsorbers or SCR technology will be also implemented [89,90]. A schematic of the architectures of the after-treatment line to meet the near future Euro 6 and beyond emission can be seen in Fig. 15.

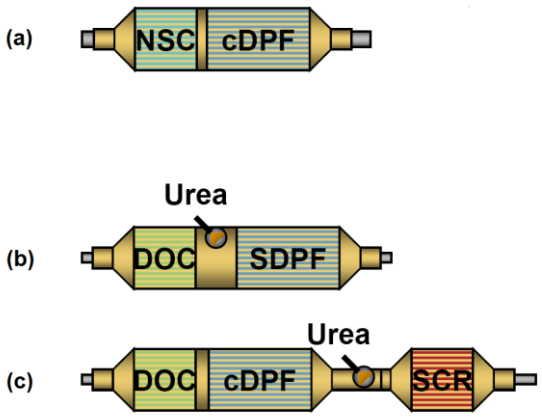

Fig. 15 (a) Coupled NO_x absorbers (NO_x storage Catalyst) + DPF; (b) Coupled DOC + DPF with NH_3-SCR functionality; Coupled DOC + DPF with dedicated NH_3-SCR converter (Courtesy of Umicore [91]).

Manufacturers will likely choose the NO_x after-treatment technology based on a combination of cost, expertise, reliability, fuel economy, and consumer acceptance.

The solution Fig. 15-(a) involves the use of NO_x absorbers (or NSC, NO_x storage catalysts, or LNT, lean NO_x traps), and is suited to light duty engines with relatively low displacement, since it avoids the complex architecture of the SCR technology as well as the periodic refilling of urea. However, the overall efficiency of NO_x absorbers is nominally 70-80%, much lower than that of the next generation SCR system at 95+%, and the precious metal usage is still high [88]. One extremely interesting attempt to improve the NO_x absorbers activity is the one from Toyota [92], who investigated the effect of an oscillating air : fuel ratio for the regeneration of the trap (Fig. 16). The fundamental finding of this phenomenon is that a high frequency injection of hydrocarbons might considerably improve the NO_x regeneration phase, at high temperatures, with a very moderate fuel penalty (<2%).

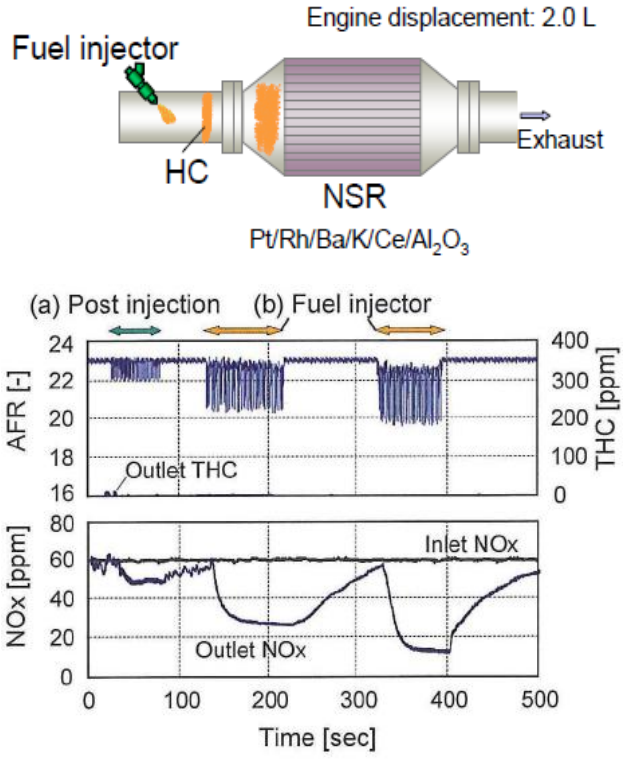

Fig. 16 (top) Engine exhaust layout (catalyst volume: 0.8 L); bottom: Changes in outlet NO_x concentration as function of HC oscillation amplitude (SV = 75,000 h-1, NSR temperature = 550°C, a = post injection, b = fuel injector, injection frequency f = 0.5 Hz)Coupled DOC + DPF with dedicated NH_3-SCR converter (Reprinted from [92]).

The solution depicted in Fig. 15-(b) is the combination of the DPF and the catalysts of SCR in one single monolith. This solution has the advantage of saving a relevant space on-board the

vehicle, which is extremely important for light duty vehicles. Clearly, this coupling involves the combination of a oxidizing functionality with a reducing one, and this might not be always an easy compromise: for example, a 1:1 NO:NO_2 ratio favours the fast SCR reaction, while the consumption of NO_2 due to soot combustion could hinder NO_x reduction. One major advantage of the SDPF is that is positioned close to the engine outlet, therefore helping the activity of the catalyst in its most favourable range of temperatures. Several successful examples of SDPF are being report in the last years, among them the work of Rohe, et al. [93] show that the new acidic zirconia mixed-oxide catalyst, who also reported a reduction the soot oxidation temperature by 50°C as compared to a Cu-zeolite catalyst. As reported by [94], Stiebels, et al. [95] showed that during DPF regeneration the SCR catalyst on the DPF can remove 70-90% NO_x at inlet temperatures of 560-630°C if NH_3 is injected.

The last solution in Fig. 15, namely (c), involves single converters for the soot and NO_x, the former in close coupled position with the DOC, and the latter down-floor. This configuration pushes the optimization of low temperature SCR catalysts (as described in the section dedicated to SCR catalysts). A refined control of the NH_3 injected is mandatory to avoid excessive ammonia slip, which is released in the form of oxidized NO_x or N_2O. A solution based on two Fe-zeolites beds, with intermediate NH_3 monitoring to control its consumption, was devised in [96] and illustrated in Fig. 17. This solution allows a full functionality of the first bed, and a finely tuned injection of ammonia to avoid its slip or over-consumption.

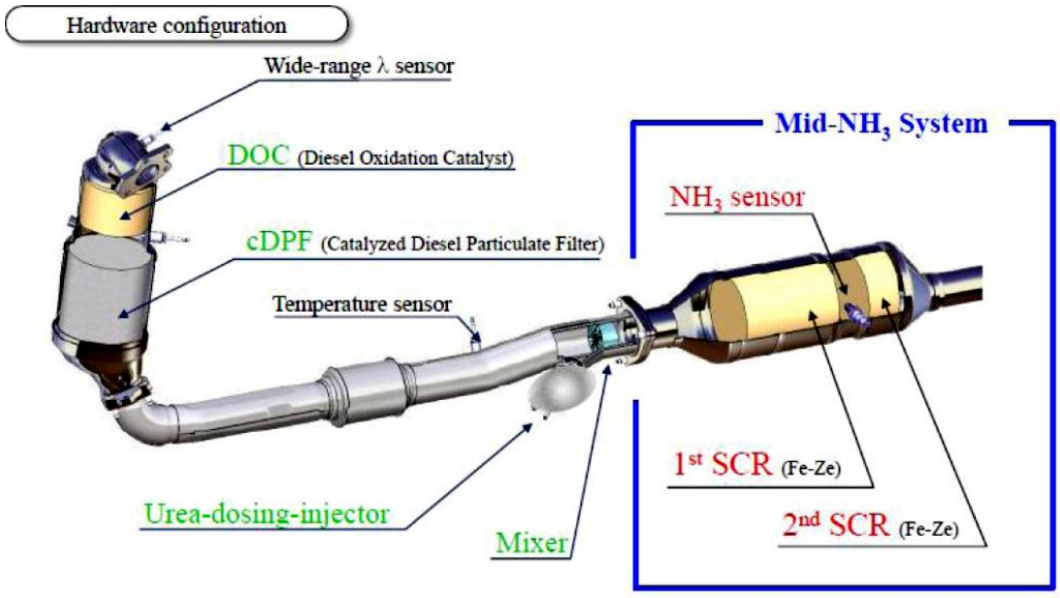

Fig. 17. Layout of a new LD SCR system incorporating two SCR catalysts with an ammonia sensor in-between (Reprinted from [96]).

A summary for the cost of emission reduction technology for a different displacement engines was performed in [88], which includes equipment cost, manufacturing cost and labor cost (Fig. 18). It can be seen that these calculations place the cost competitiveness transition from LNT (NO_x adsorbers) to NH3-SCR after-treatment technology is slightly above 2 l. This estimation is sensitive to the final market and the enforced emission limits based on the testing cycle.

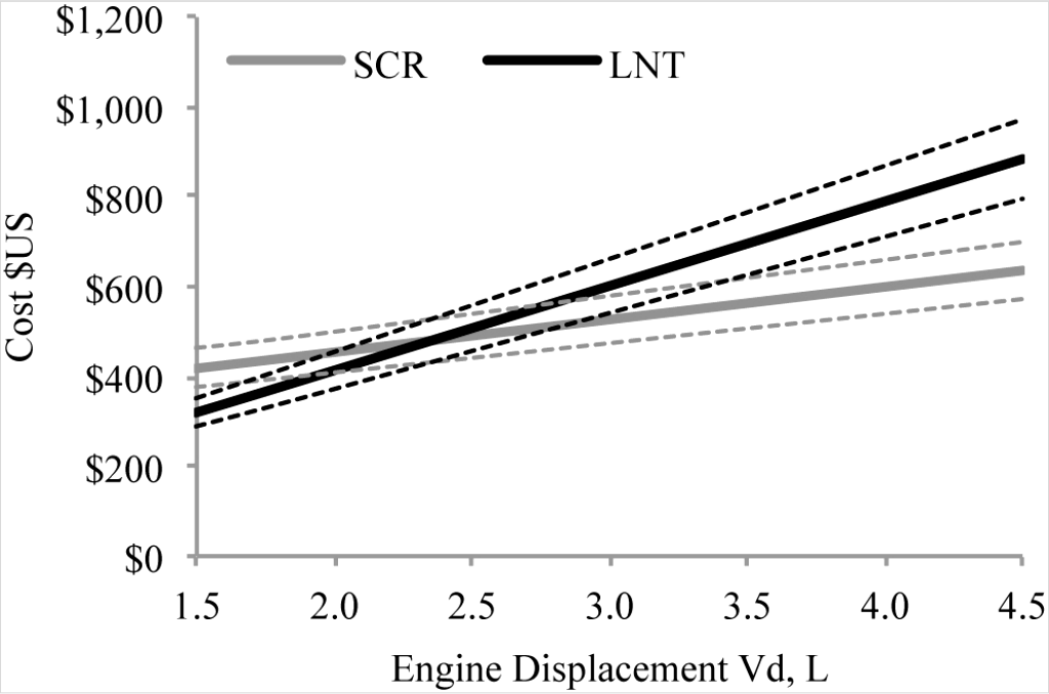

Fig. 18. Cost comparisons between LNT and SCR for LDVs. Dotted lines represent cost uncertainties of ± 10% (Reprinted from [88]).

2.7.2 Heavy duty applications

In heavy duty applications, the availability of space, and the lower relative cost of the after-treatment line, with respect to the whole vehicle, than in light-duty vehicles, directed the implementation of the SCR technology as depicted in Fig. 15.(c). As a matter of fact, the management of the EGR to reduce NO_x is accompanied by a decrease in the combustion efficiency that is not counterbalanced by the advantage of hardware and running cost savings. As a result, in the high-NO_x regimes, about 1% fuel can be saved for every 1.2-1.5% urea solution consumed (relative to fuel) to drop the NO_x [94]. In order to achieve these benefits, at

least an NO_x removal efficiency of 85% should be targeted, although up to 98% are desirable to allow the engine to work in the high- NO_x low-fuel consumotion window [94].

A picture of Scania's Euro 6 technological solution to achieve these targets is the one depicted in Fig. 19 (the figure refers to a 12.7 l, 6 cylinder, engine). This unit is extremely integrated and compact, with a DOC, a DPF, with two parallel NH_3-SCR converters with ammonia slip catalysts. Downstream the ammonia slip catalyst, there is a NO_x sensor to monitor the effectiveness of the whole system. The EGR and SCR processes are continuously balanced to optimize the emission performance. Typically, around 50% of NO_x emissions are eliminated at source by the EGR system, and another 95% in the SCR catalysts. The DPF eliminates 99% of particulate emissions. Overall, this signifies that the emissions of nitrogen oxides and particulates are cut by around 80 percent compared with the Euro 5 standards [97].

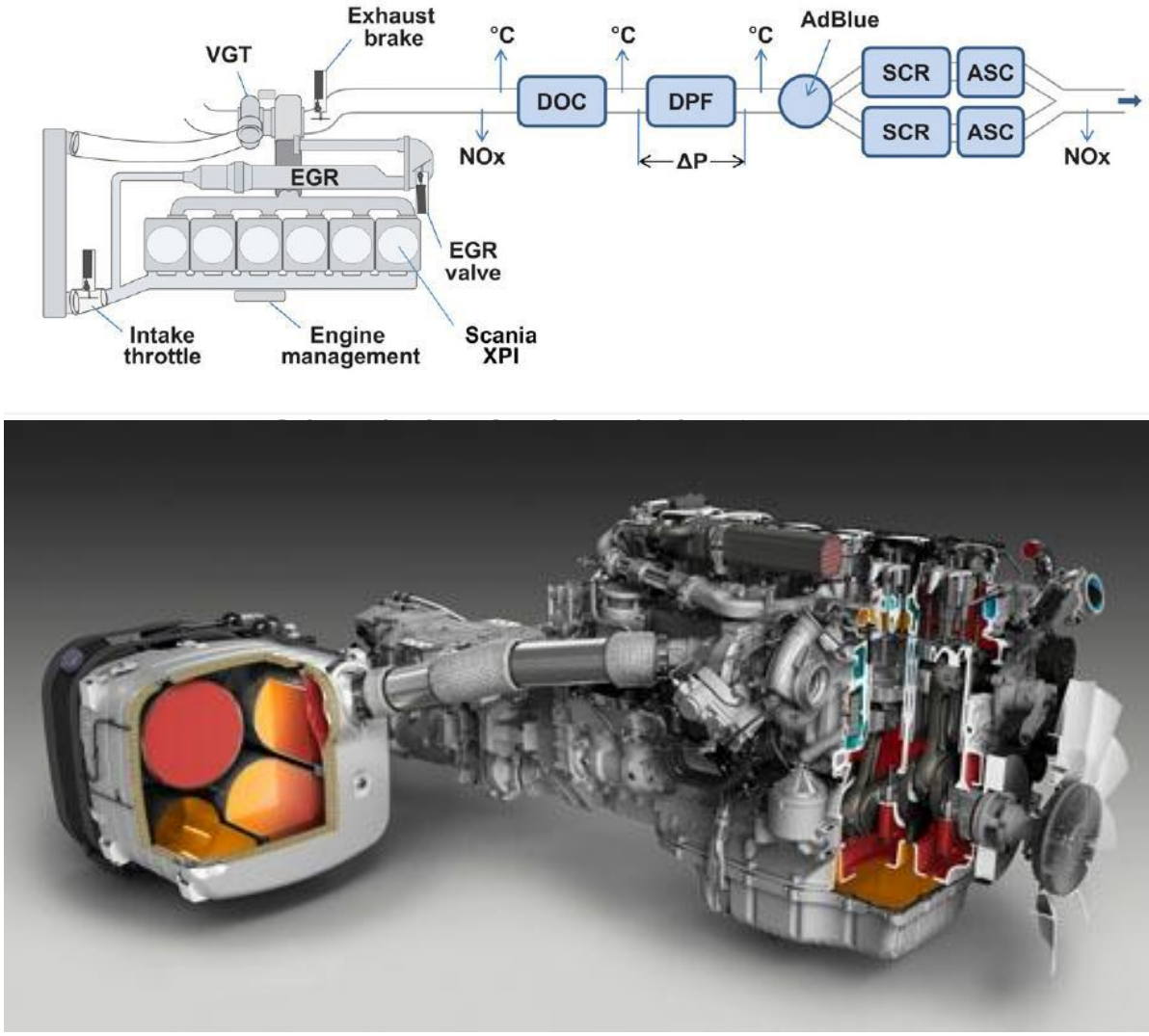

Fig. 19. Schematic and picture of the after-treatment unit of Scania, mounted on vehicle equipped with a 12.7 l, 6 cylinder, diesel engine (Reprinted from [4]-top and [97]-bottom).

2.8 References

[1] Allanssonn, R., Blakeman, P.G., Cooper, B.J., Hess, H., Silkock, P.G., Walker, A.P., Optimizing the low temperature performance and regeneration efficiency of the continuously regenerating diesel particulate filter (CR-DPF) system, SAE 2002-01-0428 (2002).

[2] Jiang, P., Lu, G., Guo, Y., Zhang, S., Wang, X., Preparation and properties of a γ- Al_2O_3 washcoat deposited on a ceramic honeycomb, Surface and Coating Technology, 190:2-3, (2005), 314-320.

[3] Twigg M.V., Progress and future challenges in controlling automotive exhaust gas emissions, Applied Catalysis B: Environmental, 70:1-4 (2007) 2-15.

[4] www.dieselnet.com

[5] Burch, R., Breen, J.P., Meunier, F.C., A review of selective reduction of NO_x with hydrocarbons under lean-burn conditions with non-zeolitic oxide and platinum group metal catalysts, Applied Catalysis B: Environmental, 39:4 (2002), 283-303.

[6] Kolli, T., Lassi, U., Rahkamaa-Tolonen, K., Kinnunen, T.-J.J., Leiski, R.L., The effect of barium on the catalytic behaviour of fresh and aged Pd-Ba-OSC/Al_2O_3 catalysts, Applied Catalysis A: General, 298, (2006), 65-72.

[7] Irani, K., Epling, W.S., Blint, R., Effect of hydrocarbon species on NO oxidation over diesel oxidation catalysts, Applied Catalysis B: Environmental, 92:3-4, (2009), 422-428.

[8] Ambs, J.L. and McClure, B.T., The influence of oxidation catalysts on NO_2 in diesel exhaust, SAE Technical Paper 932494 (1993).

[9] Eastwood, P., Critical Topics in Exhaust gas after-treatment, Research Studies Press Ed., Baldock-Hertfordshire UK, (2000).

[10] Farrauto, R.J. and Voss, K.E., Monolithic diesel oxidation catalysts, Applied Catalysis B: Environmental, 10:1-3 (1996), 29-51.

[11] Diesel emission control - Sulphur effects program: Diesel fuel sulphur effects on particulate matter emissions, The U.S. Department of energy – Engine Manufacturers Association – Manufacturers of Emission Controls Association, (1999).

[12] Stein, H.J., Diesel oxidation catalysts for commercial vehicle engines: strategies on their application for controlling particulate emissions, Applied Catalysis B: Environmental, 10:1-3 (1996), 69-82.

[13] Klein, H., Van Den, T.H., Lox, E., Kreuzer, T., Eckhoff, S., Oxidation Catalyst for Internal Combustion Engines, US Patent 6,077,489, (2000).

[14] Konstandopoulos, A.G., Skaperdas, E., Papaioannou, E., Zarvalis, D., Kladopoulou, E., Fundamental studies of diesel particulate filters: transient loading, regeneration and aging, SAE 2000-01-1016, (2000).

[15] Wirojsakunchai, E., Schroeder, E., Kolodziej, C., Foster, D.E., Schmidt, N., Root, T., Kawai, T., Suga, T., Nevius, T., Kusaka, T., Detailed diesel exhaust particulate characterization and real-time DPF filtration efficiency measurements during PM filling process, SAE 2007-01-0320 (2007).

[16] Martirosyan, K.S., Chen, K., Luss, D., Behavior features of soot combustion in diesel particulate filter, Chemical Engineering Science, 65:1, (2010), 42-46.

[17] Konstandopoulos, A.G., Kostoglou, M., Housiada, P., Vlachos N., Zarvalis, D., Multichannel Simulation of Soot Oxidation in Diesel Particulate Filters, SAE 2003-01-0839, (2003).

[18] Masoudi, M., Pressure drop of segmented diesel particulate filters, SAE 2005-01-0971, (2005).

[19] Pattas, K.N., Stamatelos, A.M., Kougianos, K.N., Koltsakis, G.C., Pistikopoulos, P.K., Trap protection by limiting A/F ratio during regeneration, SAE Paper 950366, (1995).

[20] Ohara, E., Mizuno, Y., Miyairi, Y., Mizutani, T., Yuuki, K., Naguchi, Y., Hiramatsu, T., Makino, M., Takahashi, A., Sakai, H., Tanaka, M., Martin, A., Fujii, S., Busch, P., Toyoshima, T., Ito, T., Lappas, I., Vogt, C.D., Filtration behaviour of diesel particulate filters (1), SAE 2007-01-0921 (2007).

[21] Caroca, J.C., Villata, G., Fino, D., Russo, N., Comparison of different diesel particulate filters, Topics in Catalysis, 52:13-20, (2009), 2076-2082.

[22] Liati A., Eggenschwiler P.D., Characterization of particulate matter deposited in diesel particulate filters: Visual and analytical approach in macro-, micro- and nano-scales, Combustion and Flame 157:9 (2010) 1658–1670.

[23] Mayer, A., Particulate traps for heavy duty vehicles, Swiss Agency for the Environment, Forests and Landscape (SAEFL), Environmental Documentation No. 130, (2000).

[24] Osada, H., Aoyagi, Y., Shimada, K., Akiyama, K., Goto, Y., Suzuki, H., SOF component of lubricant oil on diesel PM in a high boosted and cooled EGR engine, 2007-01-0123, (2007).

[25] Burtscher, H., Literature study on tailpipe particulate emission measurement for diesel engines, Report for Particle Measurement Programme, BUWAL/GRPE, (2001).

[26] Sappok, A.G. and Wong, V.W., detailed chemical and physical characterization of ash species in diesel exhaust entering after-treatment systems, SAE 2007-01-0318, (2007).

[27] Johnson, T.V., Diesel emission control in review, SAE 2007-01-0233, (2007).

[28] Belloir, M., Sakushima, N., Lahjaily, H., A CFD Study to optimize the injection strategy for diesel particulate filter regeneration, SAE 2007-01-0164, (2007).

[29] Labhsetwar, N.K., Watanabe, A., Mitsuhashi, T., New improved syntheses of $LaRuO_3$ perovskites and their applications in environmental catalysis, Applied Catalysis B: Environmental, 40, 1, (2003) 21-30.

[30] Cauda, E., Fino, D., Saracco. G., Specchia, V., Preparation and regeneration of a diesel particulate filter, Chemical Engineering Science, 62, (2007) 5182-5185.

[31] Cauda, E., Fino, D., Saracco. G., Specchia, V., Catalytic wall-flow filters for abatement of diesel particulate: regeneration parameters study, Topics in catalysis, 1-4, (2007) 125-129.

[32] Neeft, J.P.A., Makkee, M., Moulijn, J.A., Catalysts for the oxidation of soot from diesel exhaust gases. I. An exploratory study, Applied Catalysis B: Environmental, 8, (1996), 57-78.

[33] Setiabudi, A., Allaart, N.K., Makkee, M., Moulijn, J.A., In situ visible microscopic study of molten Cs_2SO_4_V_2O_5–soot system: Physical interaction, oxidation rate, and data evaluation Applied Catalysis B: Environmental, 60, (2005), 233–243.

[34] Cooper, B.J., Roth, S.A., Flow-through catalysts for diesel engine emissions control, Platinum Metals Reviews**,** 35, (1991), 178-187.

[35] Cooper, B.J., Jung H.J., Thoss, J.E., Treatment of Diesel Exhaust Gases, US Patent 4902487 Johnson Matthey, (1990).

[36] Fino, D., Russo, N., Cauda, E., Saracco, G., Specchia, V., La–Li–Cr perovskite catalysts for diesel particulate combustion, Catalysis Today, 114, (2006), 31–39.

[37] Fino, D., Cauda, E., Mescia, D., Russo, N., Saracco, G., Specchia, V., $LiCoO_2$ catalyst for diesel particulate abatement, Catalysis Today, 119, (2007), 257–261.

[38] Fino, D., Russo, N., Saracco, G., Specchia, V., Removal of NO_x and diesel soot over catalytic traps based on spinel-type oxides, Powder Technology, 180:1-2, (2008), 74-78.

[39] Krishna K. and Makkee M., Pt–Ce-soot generated from fuel-borne catalysts: soot oxidation mechanism, Topics in Catalysis, 42-43:1-4, (2007), 229-236.

[40] Williams, F.J., Palermo, A., Tikhov, M.S., Lambert, R.M., Electrochemical promotion by sodium of the rhodium-catalyzed NO + CO Reaction, The Journal of Physical Chemistry B, 104:50, (2000), 11883-11890.

[41] Pirone, R., Ciambelli, P., Palella, B., Russo, G., Simultaneous NO and N2O decomposition on Cu-ZSM5, Studies in Surface Science and Catalysis, 30 A, (2000), 911-916.

[42] Nakatsuji, T. and Komppa, V., A catalytic NO_x reduction system using periodic two steps: an operation in oxidizing conditions and a relatively short operation in reducing conditions, Applied Catalysis B: Environmental, 30:1-2, (2001), 209-223.

[43] Nakatsuji, T., Ruotoistenmäki, J., Komppa, V., Tanaka Y., Uekusa, T., A catalytic NO reduction in periodic lean and rich excursions over Rh supported on oxygen storage capacity materials, Applied Catalysis B: Environmental, 38:2, (2002), 101-116.

[44] Forzatti, P., Present status and perspectives in de-NO_x SCR catalysis, Applied Catalysis A: General, 222, (2001), 221-236.

[45] Ito, E., Hultermans, R.J., Lugt, P.M., Burgers, M.H.W., van Bekkum, H., van den Bleek, C.M., Selective reduction of NO_x with ammonia over cerium exchanged zeolite catalysts:

Towards a solution for an ammonia slip problem, Studies in Surface Science and Catalysis, 96 (1995), 661-673.

[46] Ansell, G.P., Diwell, A.F., Golunski, S.E., Hayes, J.W., Rajaram, R.R., Truex, T.J., Walker, A.P., Mechanism of the lean NO_x reaction over Cu/ZSM-5, Applied Catalysis B: Environmental, 2:1, (1993), 81-100.

[47] Nova, I., Beretta, A., Groppi, G., Lietti, L., Tronconi, E., Forzatti, P., in: Cybulski, A. and Moulijn, J.A. Ed., Structured Catalysts and Reactors, Dekker, New York, (2006), 171-214.

[48] Mathes, W., Witzel, F., Schnapp, S., Exhaust gas control system for diesel engine exhaust gases, International Patent Application, WO 99/05402, 1999.

[49] Raja, A., Lea, T.H.N., Kaliaguine, S., Auroux, A., Involvement of nitrate species in the SCR of NO by NH_3 at ambient conditions over TS-1 catalysts, Applied Catalysis B: Environmental, 15:3-4, (1998), 259-267.

[50] Koebel, M., Elsener, M., Madia, G., Recent advances in the development of urea-SCR for automotive applications, SAE 2001-01-3625, (2001).

[51] Gekas, I., Nyengaard, L., Lund, T., Urea-SCR catalyst system selection for fuel and PM optimised engines and a demonstration of a novel urea injection system", SAE 2002-01-0289, (2002).

[52] Orsenigo, C. Beretta, A., Forzatti, P., Svachula, J., Tronconi, E., Bregani, F., Baldacci, A., Theoretical and experimental study of the interaction between NO_x reduction and SO_2 oxidation over $DeNO_x$-SCR catalysts, Catalysis Today, 27:1-2 (1996), 15-21.

[53] Kato, N., Karachi, H., Hamada, Y., Thick film ZrO_2 NO_x sensor for the measurement of low NO_x concentration, SAE Technical Paper 980170, (1998).

[54] Hofmann, L., Rusch, K., Fischer, S., Lemire, B., Onboard emissions monitoring on a HD truck with an SCR system using NO_x sensors, SAE 2004-01-1290, (2004).

[55] Heck, R.M., Farrauto, R.J., Catalytic Air Pollution Control: Commercial Technology, Van Nostrand Reinhold Ed., New York, (1995).

[56] Kartte, K. and Nonnenmaker, H., Selective Removal of Oxides of Nitrogen from Gas Mixtures Containing Oxygen, US Patent 3,279,884 (1966).

[57] Nakajima, F., Tacheuci, M., Matsuda, S., Uno, S., Mori, T., Watanabe, Y., Inamuri, M., Catalytic process for reducing nitrogen oxides to nitrogen, US Patent 4,085,193 (1978).

[58] Went, G.T., Leu, L.J., Bell, A.T., Quantitative structural analysis of dispersed vanadia species in TiO_2 (anatase)-supported V_2O_5, Journal of Catalysis, 134, (1992), 479–91.

[59] Cristiani, C., Bellotto, M., Forzatti, P., Bregani, F., On the morphological properties of tungsten–titania de-NOxing catalysts, Journal of Material Research, 8, (1993), 2019-2026.

[60] Advanced Clean-Energy Vehicles (ACEVs), Project Summary, Japan Automobile Research Institute JARI, (2004).

[61] Chemicals Known To The State To Cause Cancer Or Reproductive Toxicity, California Environmental Protection Agency, Office of Environmental Health Hazard Assessment (OEHHA), Safe Drinking Water and Toxic Enforcement Act of 1986 (Proposition 65), Updated 27/05/2005, (2005).

[62] Iwamoto, M. and Hamada, H., Removal of nitrogen monoxide from exhaust gases through novel catalytic processes. Catalysis Today, 10, (1991), 57–61.

[63] Iwamoto, M., Yahiro, H., Tanda, K., Mizuno, N., Mine, Y., Kagawa, S., Removal of nitrogen monoxide through a novel catalytic process. 1. Decomposition on excessively copper–ion-exchanged ZSM-5 zeolites. The Journal of Physical Chemistry, 95, (1991), 3727–3730.

[64] Kröcher, O., Devadas, M., Elsener, M., Wokaun, A., Söger, N., Pfeifer, M., Demel, Y., Mussmann, L., Investigation of the selective catalytic reduction of NO by NH_3 on Fe-ZSM5 monolith catalysts, Applied Catalysis B: Environmental, 66:3-4, (2006), 208-216.

[65] Gieshoff, J., Pfeifer, M., Schafer-Sindlinger, A., Spurk, P., Garr, G., Leprince, T., Advanced urea SCR catalysts for automotive applications, SAE 2001-01-0514, (2001).

[66] Ja Hun Kwak, Russell G. Tonkyn, Do Heui Kim, János Szanyi, Charles H.F. Peden, Excellent activity and selectivity of Cu-SSZ-13 in the selective catalytic reduction of NO_x with NH3, Journal of Catalysis, Volume 275, Issue 2, 22 (2010), Pages 187-190.

[67] Engler, B.H., Leyrer, J., Lox, E.S., Ostgathe, K., Catalytic reduction of NO_x with hydrocarbons under lean diesel exhaust gas conditions, SAE Technical Paper 930735, (1993).

[68] Burch, R., Millington, P.J., Walker, A.P., Applied Catalysis B: Environmental, 4:1 (1994), 65-94.

[69] Epling, W.S., Campbell, L.E., Yezerets, A., Currier, N.W., Parks II, J.E., Overview of the fundamental reactions and degradation mechanisms of NO_x storage/reduction catalysts, Catalysis Reviews, 46:2, (2004), 163-245.

[70] Lindholm, A., Currier, N.W, Fridell, E., Yezerets, A., Olsson, L., NO_x storage and reduction over Pt based catalysts with hydrogen as the reducing agent influence of H_2O and CO_2, Applied Catalysis B: Environmental 75, (2007), 78–87.

[71] Gill, L.J., Blakeman, P.G., Twigg, M.V., Walker, A.P., The use of NO_x adsorber catalysts on diesel engines, Topics in Catalysis, 28, (2004), 157-164.

[72] Milt, V.G., Querini, A., Mirò, E.E., Ulla, M.A., Abatement of diesel exhaust pollutants: NO_x adsorption on Co, Ba, K/CeO_2 catalysts, Journal of Catalysis, 220:2, (2003), 424-432.

[73] Kobayashi, T., Yamada, T., Kayano, K, Study of NO_x trap reaction by thermodynamic calculation, SAE Technical Paper 970745, (1997).

[74] Lietti, L., Forzatti, P., Nova I., Tronconi, E., NO_x Storage Reduction over Pt-Ba/γ- Al_2O_3 Catalyst, Journal of Catalysis, 204:1, (2001), 175-191.

[75] Nova, I., Lietti, L., Castoldi, L., Tronconi E., Forzatti, P., New insights in the NO_x reduction mechanism with H_2 over Pt-Ba/γ-Al_2O_3 lean NO_x trap catalysts under near-isothermal conditions, Journal of Catalysis, 239:1, (2006), 244-254.

[76] Krutzsch, B., Webster, D., Chaize, E., Hodjati, S., Petit, C., Pitchon, V., Kiennemann, A., Loenders, R., Monticelli, O., Jacobs, P.A., Martens, J.A., Kasemo, B., Weibel, M., Wenninger, G., Reduction of NO_x in Lean Exhaust by Selective NO_x-Recirculation (SNR-Technique). Part II: NO_x Storage Materials, SAE Technical Paper 982593.

[77] Hepburn J.S., Watkins, W., Sulphur resistant lean-burn NO_x catalyst for treating diesel emissions, European Patent Application, EP 0 857 510 A1, (1998).

[78] Lide, D.R., CRC Handbook of Chemistry and Physics, CRC Press, Boston, (2006).

[79] Dou, D. and Balland, J., Impact of alkali metals on the performance and mechanical properties of NO_x adsorber catalysts, SAE 2002-01-0734, (2002).

[80] Cutler, W.A. and Day, J.P., Mechanical durability of cordierite-based NO_x adsorber/catalyst systems for lean burn gasoline applications, SAE 1999-01-3500, (1999).

[81] Belliere-Baca, V., Harle, V., Pitois, C., Rohart, E., Ceria doped Ba-Alumina oxides for durable NO_x-storage catalysts efficient at low temperature, SAE 2007-01-1241, (2007).

[82] Hachisuka, I., Yoshida, T., Ueno, H., Takahashi, N., Suda, A., Sugiura, M., Improvement of NO_x storage-reduction catalyst, SAE 2002-01-0732, (2002).

[83] Shoji, A., An Improvement of Diesel PM and NO_x rduction system", US DOE, 13th Diesel Engine-Efficiency and Emissions Research (DEER) Conference, Detroit MI, (2007).

[84] Kabin, K.S., Muncrief, R.L., Harold, M.P., Li, Y., Dynamics of storage and reaction in a monolith reactor: lean NO_x reduction, Chemical Engineering Science, 59, (2004), 5319-5327.

[85] Takahashi, N., Yamazaki, K., Sobukawa, H., Shinjoh, H., The low-temperature performance of NO_x storage and reduction, Applied Catalysis B: Environmental, 70, (2007) 198-204.

[86] Winkler, M., Particle Number Emissions of Direct Injected Gasoline Engines", presentation at IQPC Advanced Emission Control Concepts for Gasoline Engines 2012, May 2012, Stuttgart

[87] Herold, R., Wahl, M., Regner, G., Lemke, J. et al., Thermodynamic Benefits of Opposed-Piston Two-Stroke Engines, SAE Technical Paper 2011-01-2216.

[88] Posada, F., Bandivadekar, A., German, G., Estimated Cost of Emission Control Technologies for Light-Duty Vehicles Part 2 - Diesel, SAE 2013-01-0539

[89] European Commission (EC), Commission Staff Working Document. Proposal for a Regulation of the European Parliament and the Council on type approval of motor vehicles with respect to emissions and on access to vehicle repair information - Impact Assesement, 2005, Commission of the European Communities: Brussels.

[90] TNO, Euro 5 Technologies and Costs for Light Duty Vehicles - The Expert panels Summary of Stakeholders Responses. Prepared for the European Commisson DG Environment, 2005: Brussels.

[91] K. Ruth, I. Grisstede, W. Müller, S. Franoschek, M. Seyler, R. Hoyer, H. Noack, S. Basso, Diesel NO_x -After-treatment Systems for Upcoming LDV-Emission Legislations, Umicore AG & Co. KG, Hanau-Wolfgang, Germany.

[92] Bisaiji, Y., Yoshida, K., Inoue, M., Umemoto, K., Fukuma, T., Development of Di-Air - A New Diesel de NO_xSystem by Adsorbed Intermediate Reductants, JSAE 20119272, SAE 2011-01-2089.

[93] Rohe, R., Marques, R., Harris, D., Jones, C., New Acidic Zirconia Mixed Oxides for NH3-SCR Catalysts for Better Passenger Cars Integration", presentation at the IAV Min NO_x Conference, June 2012, Berlin.

[94] Timothy Johnson, Vehicular Emissions in Review, SAE 2013-01-0538.

[95] Stiebels, S., Wendt, C., Neubauer, T., Müller-Stach, T., "Smart Catalyst Technologies for Future Automotive Emission Control", presentation at the IAV Min NO_x Conference, June 2012, Berlin.

[96] Yasui, Y., Matsunaga, H., Hashimoto, E., Satoh, N., Hardam, H., Balland, J., Yamada, M., Takahashi, T., "A New Clean Diesel Concept for US LEV-III SULEV - First Report - A New Emission Strategy and After-treatment Management Control, presentation at the IAV Min NO_x Conference, June 2012, Berlin.

[97] http://www.volkswagenag.com/

CHAPTER III Influence on performance and emissions of an automotive Euro 5 diesel engine fuelled with Blended 30% from Farnasene

ABSTRACT

The effects of using a 30% by volume blend of renewable diesel fuel (30% vol.), Farnasene, in a Euro 5 small displacement passenger car diesel engine have been evaluated in this paper.

Farnesane is a 15-carbon long molecule and can be obtained from fermentation of biomass-derived sugars (such as sugar cane, amidaceous and cellulosic crops) which are first fermented to Farnesane and then hydrogenated to Farnesane. Farnesane shows chemical and physical properties similar to diesel fuel as far as its viscosity and density are concerned. The higher Lower Heating Value and cetane number indicate better combustion properties of the biofuel and the lack of aromatics and sulphur could contribute to a decrease of smoke and Particulate Matter emissions.

Tests were carried out on a last generation Euro5 small displacement diesel engine for passenger cars applications. The impact that Farnesane blend may have on engine performance was first evaluated at full load. Afterwards, the effects of the usage of the Farnesane blend on engine emissions and fuel consumption were evaluated at 7 different part load operating points selected after a preliminary numerical simulation of different driving cycles as representative of the New European Driving Cycle. Further experimental investigations were carried out to fully exploit the benefits that could be obtained by adjusting the Exhaust Gas Recirculation (EGR) EGR rates in order to take into account the different biofuel blend Soot-NO_x and CO- NO_xtrade-off.

At full load operating conditions, without any modifications to the ECU calibration, when fuelling the engine with B30 blend, levels of torque output comparable with reference diesel could be observed over almost the entire speed.

At part load operating conditions, representative of the New European Driving Cycle, no significant variations for fuel consumption, on a mass basis, at same fuel conversion efficiency and CO_2 emissions were found for Farnesane blend compared to diesel. CO and HC specific emissions were significantly reduced with the biofuel blend at low and medium

loads, while only modest or even insignificant variations were registered at higher loads. NO_x emissions with the biofuel blend were generally comparable with those of the reference diesel fuel, while a noticeable reduction of smoke levels could generally be observed for medium and high load operating conditions.

Finally, soot- NO_x and CO- NO_x trade-off obtained by means of EGR sweeps highlighted the potential for gathering some further emissions benefits through a better exploitation of the biofuels characteristics thank to a more extensive ECU recalibration.

1. Introduction

Biofuels have attracted considerable attention by policy makers, researchers and industries as renewable, biodegradable, and non-toxic means to increase energy sources diversification and to reduce carbon dioxide emissions from internal combustion engines. At international stage, United States Environmental Protection Agency's (US EPA) Energy Independence and Security Act of 2007 (EISA) established the annual renewable fuel volume targets, setting an overall target of 36 billion gallons in 2022. On the same path, European directive 2009/28/EC introduced a target for the European Union (EU) member states concerning the share of energy from renewable sources in all forms of transport; in particular a target of at least 10% of the final energy consumption in transport should be achieved by 2020.

Nevertheless, the real environmental benefits of first generation biofuels have been quite often overestimated, without a full lifecycle analysis, including Indirect Land Use Change (ILUC) effects such as the expansion of agriculture onto non-agricultural land. First generation biofuels industry still faces challenges regarding the competition with food crops, the high water demand for cultivation and the "energy sprawl" due to very low power density of fuel crops. In view of these and other biofuel issues, international regulations are under review by legislators with the purpose of increasing the share of biofuels of second generation, sourced by e.g. cellulosic material and food industry wastes. Recently, the US EPA proposed 2014 standards for cellulosic biofuel, biomass-based diesel and agricultural biofuels proposing a total production of 18.5 billion gallons. Compared to the 2013 quotas, the volumes of first generation biofuels would be reduced for the first time, the volume of biomass-based diesel would remain unchanged, while the production of cellulosic biofuels will be doubled. On the other side, European Parliament too is adopting changes to the biofuel legislation. In more

detail the use of biofuels sourced from agricultural feedstocks would be limited at 6%, compared to a 10% target that is currently required by 2020 and the gap would be filled by second generation biofuels. In this context the development and study of new biodiesel typologies is of crucial importance.

Among potentially available biofuels for diesel engines, the following categories are worth mentioning: biodiesel from alkyl-esters of fatty acids (most commonly Fatty Acid Methyl Esters, called FAME, or Ethyl Esters, called FAEE); alkanes and olefin mixtures (also called green diesel or renewable diesel); Farnesane (belonging to the family of isoprenoids).

Biodiesel has several advantages over petroleum-derived diesel: it is biodegradable, non-toxic, sulfur-free, aromatic-free and can be produced from a number of renewable feedstock, such as fresh [1-5] or waste [6,7] vegetable oils and animal fats [8,9]. The blend of diesel with biodiesel, from 5% till its full substitution, to be used as fuel in compression ignition engines, has been carried out in several comparative studies [10-13], focused on both performances and emissions. In terms of engine power output, no difference is observed at biodiesel volumetric concentrations below 5%; instead, around 10% power reduction is recorded with pure biodiesel, especially at high engine loads, due to its slightly lower calorific value as compared to conventional diesel [10]. As far as the emissions are concerned, biodiesel produces substantially lower amounts of carbon monoxide (CO), hydrocarbons(HC) and soot: -50%, -70% and -50% with pure biodiesel, respectively, which slightly decreases to -12%, -20% and -12% for a diesel with just a 20% biodiesel content [13]. These are average values, but more than 80% particulate matter emission reduction was recorded in tests with pure biodiesel [14]. These emission reductions are reached at the price of a modest 10% oxides of nitrogen (NO_x) emission increase for pure biodiesel, which becomes close to zero at 20% biodiesel content [13].
However, although a plethora of studies concerning the effects of FAME can be found in literature (see for instance [15, 16]), only few studies have been carried out on last generation automotive engines, as the one which was adopted for the present work.
Experimental activities reported in literature are usually carried out running the engine with the original, diesel oriented, electronic control unit (ECU) calibration; a specifically adjusted ECU calibration optimized for alternative fuels is rarely used [17] and the possible decrease of engine torque output is often recovered by increasing the torque demand through an increase of the accelerator pedal position, thus simulating a switch of the supplied fuel.

An extension of the investigations to modern engines, which may include advanced combustion technologies and closed loop combustion controls [18], [19] seems therefore to be necessary, as well as to different biofuels..

A de-oxygenation of triglycerides and free fatty acids can be achieved through hydro-treatment, leading to a mixture of alkanes and alkenes, which is called green diesel or renewable diesel. This treatment generally leads to chains of hydrocarbons with 12 to 24 carbon atoms, characterized by a full compatibility with fossil diesel, high cetane number, and great stability [20]. Green diesel outperforms conventional diesel in terms of particulate emissions, due to the absence of aromatics (which are precursors of soot), and of CO and HC emissions; moreover, it produces no emissions of oxides of sulfur (SO_X) due to the absence of sulfur in the original feedstock. Furthermore, no NO_x emission increase is detected as happens in the case of biodiesel, due to the absence of oxygen after hydrogenation [21]. Despite these advantages, virgin oil cost coupled to hydrogen's one limits the commercial use of this fuel, unless low cost waste oils are used [22]: due to their high content of impurities, these feedstock cannot be used for conventional transesterification processes, and may require non-catalytic supercritical conditions [23].

The most recent class of diesel surrogates are isoprenoids, among which Farnesane has attracted major attention. Farnesane is a 15-carbon single molecule (Fig. 1), and has therefore pure component properties instead of the ones of a mixture as occurs in the case of biodiesel and green diesel. Farnesane can be obtained from fermentation of biomass-derived sugars: these sugars can be either readily available like from sugar cane, or from amidaceous and cellulosic crops which require a complex pretreatment and hydrolysis steps to obtain the fermentable sugars. By means of genetically modified micro-organisms, the sugars can be fermented to Farnesane, which is then hydrogenated to Farnesane. Several industrial players have addressed Farnesane production and are on the way of commercializing it. For instance, Amyris Biotechnologies Inc. [24], which ferments Farnesane via the mevalonate or deoxyxulose phosphate pathways carried out with E. coli or yeast [25,26], has a pilot plant in USA (Emeryville, Ca) and a demo-plant in Brazil (Campinas, SP) [24,25]. Amyrisreports that presently this fuel, blended in a concentration of 10% with conventional diesel, is used daily by approximately 300 public transit buses in Sao Paulo and Rio de Janeiro [24].

The combustion properties of Farnesane as a pure component or in blends with diesel were retrieved by the activation energies of thermo-gravimetric oxidation experiments [27]: from the oxidation activation energies, it was found that pure Farnesane had higher values than fossil diesel, therefore its use in blends with diesel is more advisable than in pure form. This can be explained by the lower molecular weight of some diesel components, which are more reactive than Farnesane especially in the initial part of the combustion. Compared to biodiesel, Farnesane has lower activation energies, and thus it should be more suitable than the former to be blended with diesel as its surrogate.

In terms of emissions, Farnesaneis claimed to lead to a reduction of the NO_x and particulates [24], although the literature lacks of systematic studies. Conversely, the use of Farnesane, i.e. the fermented product without further hydrogenation, leads to almost equivalent emissions of CO, NO_x and particulates as compared to fossil diesel, and to their increase if Farnesane is present in blends with diesel [28]. It is worth mentioning that, beyond the mass or number of particulates, the structure and reactivity of the produced soot might significantly change depending on the aliphatic or aromatic nature of a fuel, which should also be a matter of comparison [29].

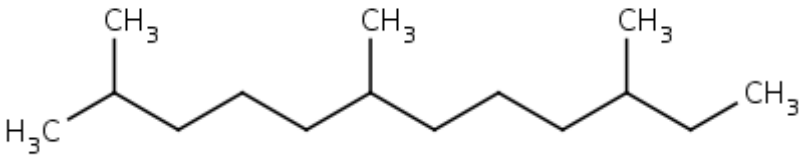

Fig. 1:Farnesane

The objective of this study is to investigate systematically the performance of 30% volume blends of Farnesane with standard Ultra Low Sulphur Diesel (ULSD) by running it in an Euro 5 small displacement passenger car diesel engine, featuring a close loop combustion control. The results obtained by running the engine with the fuel blend are compared with baseline diesel data. The impact that Farnesane blend may have on engine performance was first evaluated at full load. Afterwards, the effects of the usage of the Farnesane blend on engine emissions and fuel consumption were evaluated at 7 different part load operating points selected after a preliminary numerical simulation of different driving cycles as representative of the New European Driving Cycle. Further experimental investigations were carried out to fully exploit the benefits that could be obtained by adjusting the Exhaust Gas Recirculation

(EGR) EGR rates in order to take into account the different biofuel blend Soot- NO_x and CO-NO_x trade-off.

2. Experimental Methodology

2.1. Fuels

Experimental investigation was performed using the two following fuels:
•Diesel: standard Ultra Low Sulphur Diesel (ULSD) fuel compliant with Directive 2003/17/EC (sulphur < 10 mg/kg);
• Farnesane-B30: 30% vol. blend of Farnesane with 70% vol. diesel;

The main properties of reference diesel, neat and blended biofuel are listed in Table 1, while distillation curves and viscosity vs. temperature trends are shown in Figs.2 and 3, respectively.
Farnesane-B30 presents physical and chemical characteristics similar to diesel fuel. In more detail, biofuel blend shows a net heating value (LHV) which is slightly higher than that of diesel fuel. On the other hand Farnesane blend is characterized by a lower total aromatics content and fuel density respect to diesel fuel.

The slight increase of LHV (43.3 MJ/kg instead of 42.8 MJ/kg of diesel, with a 1% difference) does not fully compensate for density decreasing (density of Farnesane is about 2% lower respect to diesel), thus leading to an energy content introduced into the cylinder roughly 1.5% lower, assuming on first approximation that, for the same injection pressure and duration, the injected quantity depends on fuel density only. As far as fuel properties impacting on combustion and emissions are concerned, the lower aromatic contents of Farnesane blend highlights the potential of reducing smoke and particulate matter (PM) emissions. The significantly higher cetane number of the Farnesane blend should lead to a decrease of unburned HC and CO emissions, although the closed loop combustion control implemented in the ECU is expected to minimize combustion phasing shifts due to different fuel ignition qualities, and therefore to minimize fuel conversion efficiency changes as well.
As far as distillation curves are concerned, neat biofuel exhibits the typical behavior of a pure substance, characterized by an almost flat trend [26, 27]. On the contrary, a 30% in volume of Farnesane blend shows distillation characteristics closer to those of the diesel fuel, especially

for temperatures below 250°C (Fig.2). Both diesel and biofuel blend show similar viscosities characteristics, while an overall increase of viscosity throughout the investigated temperature interval was observed in the case of neat biofuel (Fig.3).

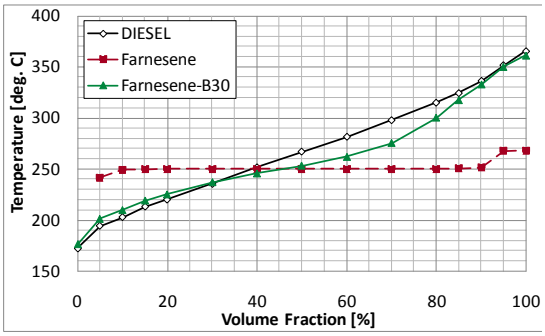

Fig.2: Distillation characteristics of neat diesel, neat Farnesane and Farnesane-B30

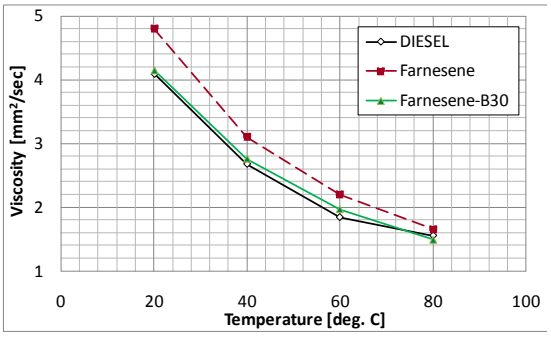

Fig.3: Viscosity vs. temperature for neat diesel, neat Farnesane and Farnesane-B30

Table 1: Main properties of test fuels

Properties	**DIESEL (ULSD)**	**Farnesane**	**Farnesane-B30**
Carbon content C, [w%]	86.2	84.2	85.2
Hydrogen content H, [w%]	13.5	14.9	13.8
Oxygen content O, [w%]	0	0	0
Total Aromatics, [w%]	25.7	-	18.4
Sulphur content S, [mg/kg]	12.9	<3	6.1
Stoichiometric ratio $(A/F)_{st}$	14.5	14.9	14.6
Net heating value, LHV [MJ/kg]	42.84	44.06	43.09
Cetane Number (ISO 5165-98)	51.2	56.7	53.1
Density at 15°C [kg/m^3]	837.5	773.6	818.7
Viscosity at 40°C [mm^2/s]	2.68	3.10	2.76
$LHV/(A/F)_{st}$ [MJ/kg]	2.95	2.96	2.95
Surface Tension at 20°C, [mN/m]	30.4	26.2	29.3

2.2 Experimental Setup and Procedure

The engine tests were carried out at ICE Advanced Laboratory of Politecnico di Torino on a test rig equipped with an eddy current dynamometer connected to the engine under test (Fig. 4), the main characteristics of which are listed in Table 2. Fuel consumption was measured by means of an AVL 733S gravimetric fuel meter, while engine-out emissions were evaluated by analyzing the exhaust gases (sampled between turbine outlet and DOC inlet) by means of an AVL AMA I60 gas analyzer (for gaseous emissions) and of an AVL 415S smoke-meter (for

particulate emissions). The engine is a modern automotive Euro 5 small displacement turbocharged Common Rail DI diesel engine, one of the smallest engines on the market if considering the unit displacement, featuring a closed-loop combustion control capable of maintaining the angular position corresponding to the 50% of burned fuel mass (MFB50) at its optimum position under part load operating conditions [30], [31] by changing the timing of the main injection, while keeping all the other characteristics of the injection pattern (e.g dwell time between pilot and main, pilot quantity, etc.) unchanged.

During the tests, all the engine control parameters were controlled by a PC that was directly connected to the engine ECU. Piezoresistive pressure transducers integrated in the glow plugs used for the closed loop combustion control were also used for the measurement of the in-cylinder pressure. The output from these transducers were firstly filtered by a low-pass filter to reduce high frequency noise and to prevent aliasing errors and signal distortion and then finally sampled by means of a 14 bit high-speed multichannel data acquisition board, coupled to a high resolution crank-angle encoder to ensure proper timing of the sampled data. At each operating condition 100 consecutive engine cycles were recorded to obtain a wide statistical sample. Data acquisition and post-processing were performed by means of ICE Analyzer, a suitable developed program for internal combustion engine indicating analysis [32].

Tests at full load were performed without any modifications to the ECU injection strategy, in order to assess the impact of fuel blends on engine performance with a “standard calibration”, i.e. without any specific adaptation to biofuel blend.

The effects of biodiesel blends on engine emissions and fuel consumption were then evaluated at 7 different part load operating points, listed in Table 3. Operating points were selected after a preliminary numerical simulation as representative of the New European
Driving Cycle (Fig.5).

Table 2: Engine specifications

Parameter	**Specification**
Engine type	Euro 5 Diesel
Cylinders	4 cylinder (in line)
Bore [mm], Stroke[mm] and Displacement [cm^3]	69.6, 82 and 1248
Compression ratio	16.8:1
Rated power [kW × rpm] and Rated torque [Nm × rpm]	72 × 3500 and 230 × 2250
Air management system	Variable Geometry Turbocharger (VGT); Cooled High Pressure EGR
Fuel injection system	Common Rail
Camshaft and Valves	Double Overhead Camshaft (DOHC) and 4 valves per cylinder

Since the change in fuel from diesel to biofuel B30 blends may lead to a reduction in the torque output due to the lower energy content of the injected fuel blend, the same brake mean effective pressure (BMEP) target was obtained by means of an adjustment of the energizing time of the main injection while keeping unchanged the pedal position, and thus the operating point position on the engine calibration map. It should be pointed out that in this way all the main engine control parameters (e.g. injection pressure and timing, EGR rate, etc.) are not changed from the standard calibration, and therefore the biofuel potentialities in terms of emissions reductions may not be fully exploited.

Finally, further experimental investigations were carried out to fully exploit the benefits that could be obtained for instance by adjusting the EGR rates in order to take into account the different biofuel blends Soot-BSNO_x and BSCO- BSNO_x trade-offs: these effects were therefore evaluated for each operating point by varying the EGR rate from 0% to the maximum achievable value corresponding to the fully open EGR valve position.

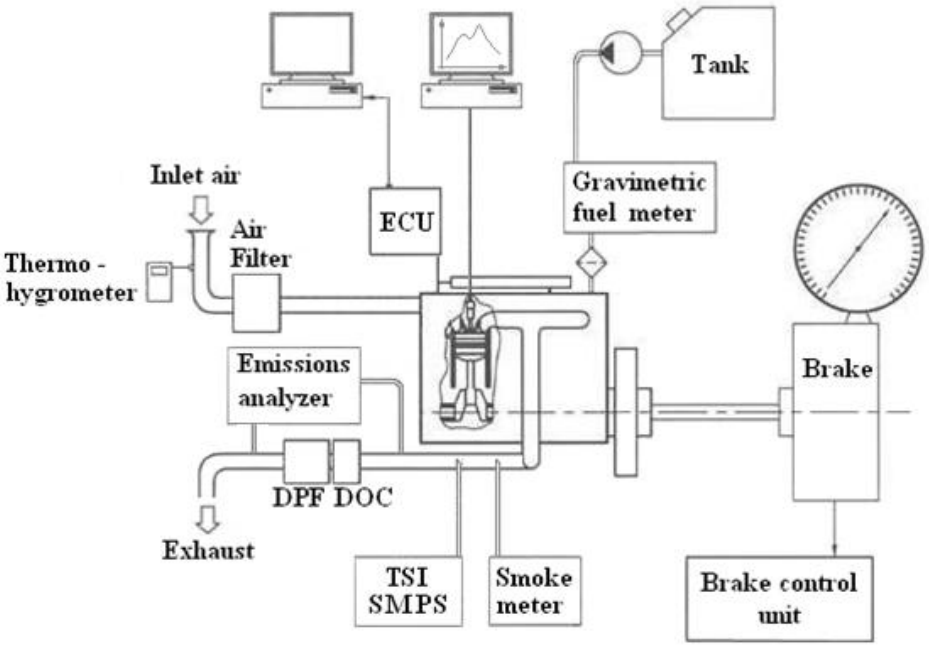

Fig.4: The engine test bench

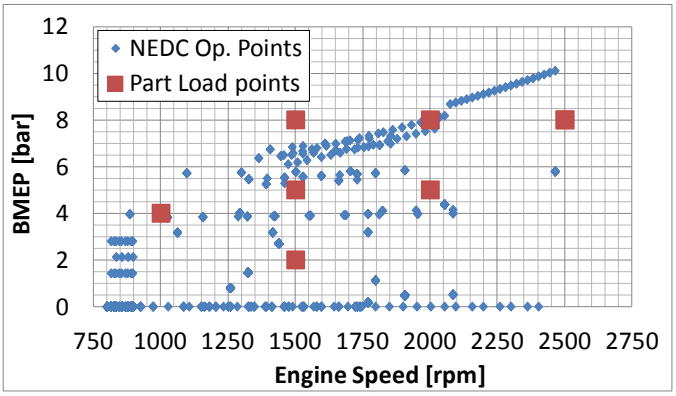

Fig.5: Engine operating points along NEDC cycle and part load points

Table 3: Part load operating points

Operating points	Speed [rpm]	BMEP [bar]
1	1000	4
2	1500	2
3	1500	5
4	1500	8
5	2000	5
6	2000	8
7	2500	8

3. Results and Discussion

3.1. Full Load Tests

Fig.6 shows the comparison of full load engine performance for the evaluated fuels without any modification in ECU calibration. A slight decrease of engine torque output with respect to the reference diesel (about 2% on average) could be observed over almost the entire speed range when biofuel blend was used. Biofuel behavior could be attributed to blend higher LHV which mitigates the negative effect of its lower density. Similar levels of fuel conversion efficiency were registered for Farnesane-B30 and diesel over investigated engine speed range (Fig.7).

Moreover, if the $LHV/(A/F)_{st}$ ratio is considered (since the maximum BMEP which can be achieved at a given λ is proportional to the $LHV/(A/F)_{st}$ ratio), both fuels show identical values, thus suggesting the potential for recovering engine performance at full load with the biofuel blend by means of a proper ECU re-calibration.

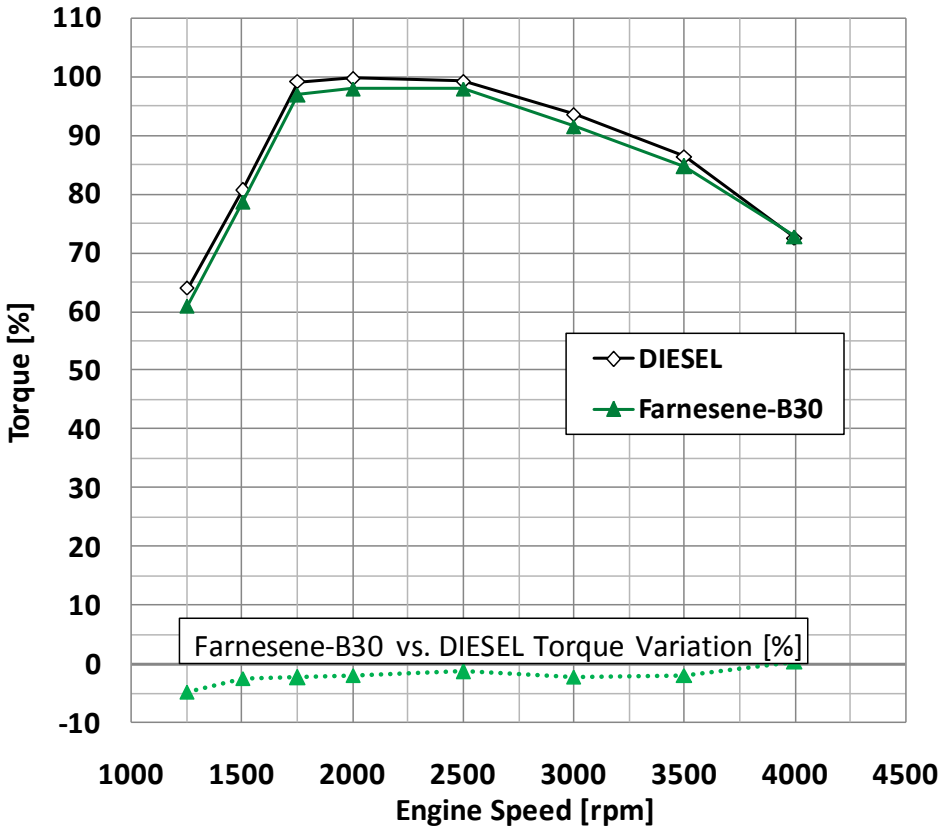

Fig.6: Torque vs.revolution speed at full load with standard calibration

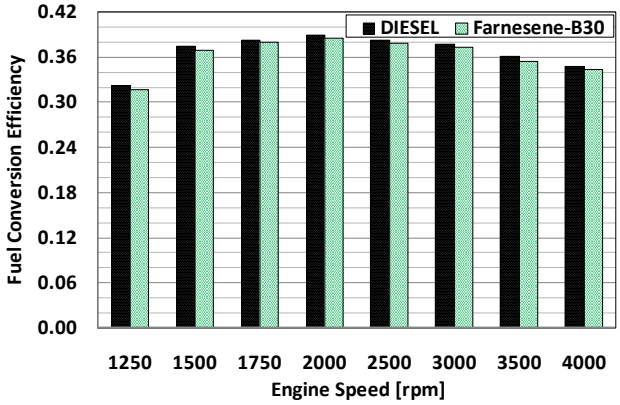

Fig.7: Fuel conversion efficiency at full load for all fuels (Std. Calibration)

3.2.Part Load Tests

The experimental results obtained under part load operating conditions with both engine calibrations (standard and specific) are shown in Figs.8-15, reporting respectively brake specific fuel consumption, engine fuel conversion efficiency, brake specific carbon dioxide (CO_2), CO, HC and NO_x emissions and smoke emissions.

No appreciable variations of brake specific fuel consumption (BSFC), and therefore of fuel conversion efficiency, were found with biofuel blend for both calibrations, in good agreement with the LHV data (Figs.8 and 9).

As far as CO_2 emissions are concerned, differences between Farnesane-B30 blend and the reference diesel fuel are almost negligible for both calibrations being the BSFC and carbon content of the biofuel blend almost identical to the diesel one (Fig.10).

CO and HC specific emissions, for both calibrations, (Figs. 11 and 12) appear to be reduced with biofuel blend at low and medium loads (2 and 5 bars of BMEP), while only modest or even insignificant variations were registered at higher loads (8 bars of BMEP). In more detail, as far as CO is concerned, the more relevant differences were found at the lower load level (2 bar BMEP), and are therefore likely to be attributed to the better ignition quality of Farnesane. This behavior could therefore be emphasized when considering engine cold conditions (i.e. the conditions at the start of the relevant homologation testing procedures).

NO_x specific emissions for both calibrations are reported in Fig. 13. An increase in NO_x emissions was observed when the engine was fuelled with Farnesane and operated with the standard calibration at medium-high loads (5 and 8 bars of BMEP). The rationale for this noticeable increase in NO_x emissions comes from the shift of the engineoperating point on the calibration maps that causes significant variations in engine operating parameters, such as for instance injection pressure and EGR rate. On the other hand, the modified ECU calibration allows to obtain comparable to diesel engine-out NO_x emissions especially at medium-high loads. This modest effect of fuel composition on NO_x with the adjusted calibration could be expected, since the engine will be operated in these conditions with the same calibration parameters (such as EGR rate, injection pressure, etc.) with closely comparable relative air/fuel ratios λ (and so with roughly the same oxygen availability and combustion temperatures).

As far as smoke emissions are concerned (Fig. 14), a noteworthy reduction can generally be observed for medium and high load operating conditions (5 and 8 bar BMEP), with only modest reductions at low loads (2 bar BMEP) when engine was fuelled with Farnesane blend and operated with both calibrations. In more detail, a maximum reduction of smoke emissions of about 0.8 FSN was observed at medium-high loads with standard calibration. These significant smoke reductions could be expected, due to the absence of soot promoters as aromatic hydrocarbons in the biofuel molecule.

Further experimental investigations were also carried out to fully exploit the benefits that could be obtained for instance by adjusting the EGR rates in order to take into account the different biofuel blend Soot-BS NO_x and BSCO-$BSNO_x$ trade-offs. Although the analysis was carried out for all the 7 selected part load operating points, only the results obtained at low engine speed (1500 rpm) and three different engine load levels (2, 5 and 8 bars of BMEP) are hereafter presented for sake of brevity.

At low load biofuel blend does not shows significant advantages in comparison with the reference diesel fuel when Soot-$BSNO_x$ trade-off is taken into account (Fig. 15 on the left). A quite different situation was found instead for the BSCO-$BSNO_x$ trade-off, which is shown in Fig. 15 on the right: in this case significantly lower CO emissions were found for Farnesane-B30, thanks to its better ignition quality. An increase of engine load first to 5 bars and then to

8 bars of BMEP leads to similar Soot-$BSNO_x$ and BSCO-$BSNO_x$ trade-offs for all fuels (see Figs. 16 and 17).

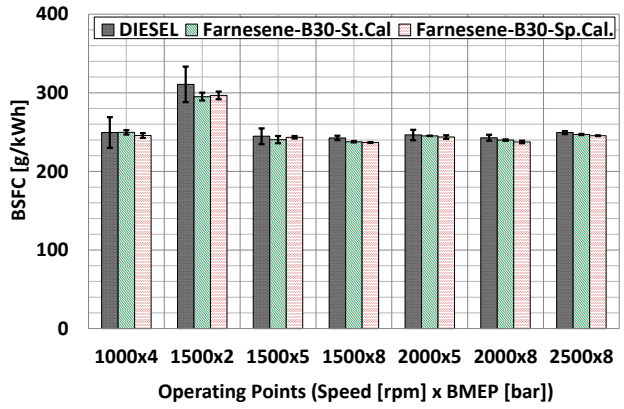

Fig.8: BSFC at part load operating points

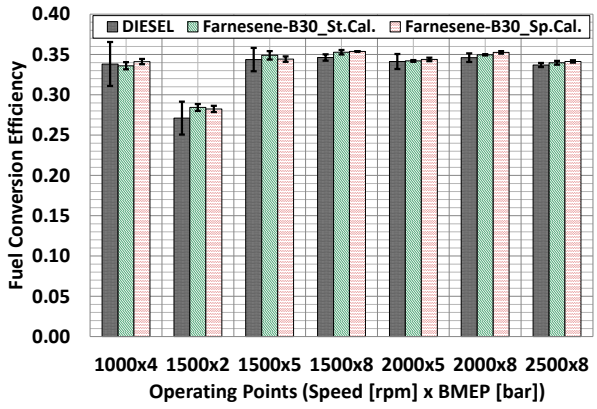

Fig.9: Fuel conversion efficiency at part load operating points

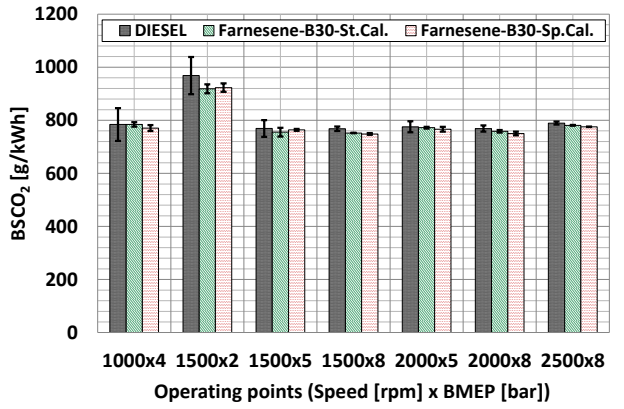

Fig.10: $BSCO_2$ at part load operating points

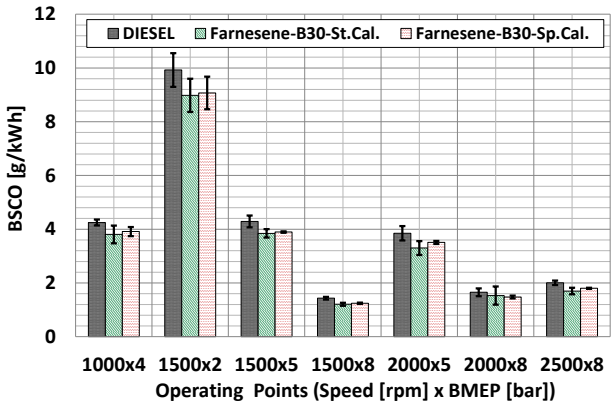

Fig. 11: BSCO at part load operating points

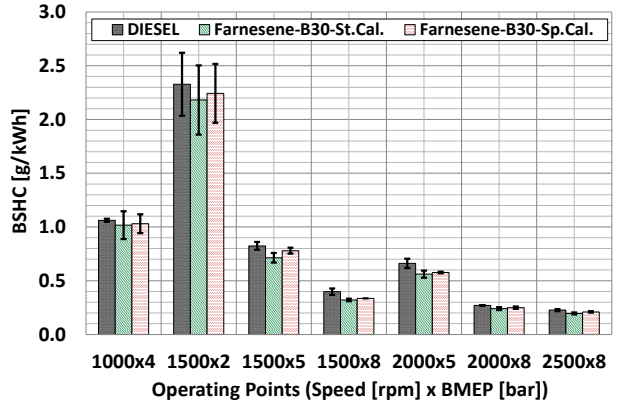

Fig. 12: BSHC at part load operating points

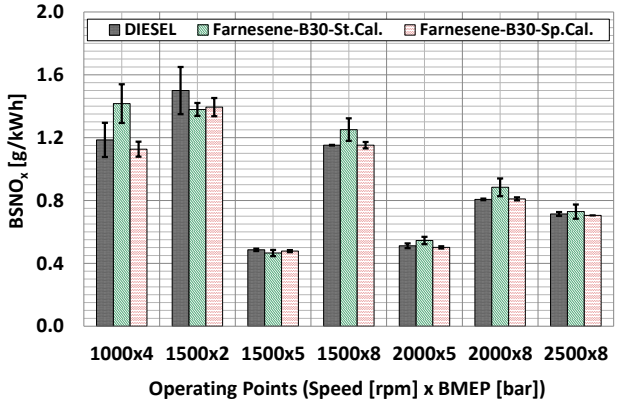

Fig. 13: $BSNO_x$ at part load operating points

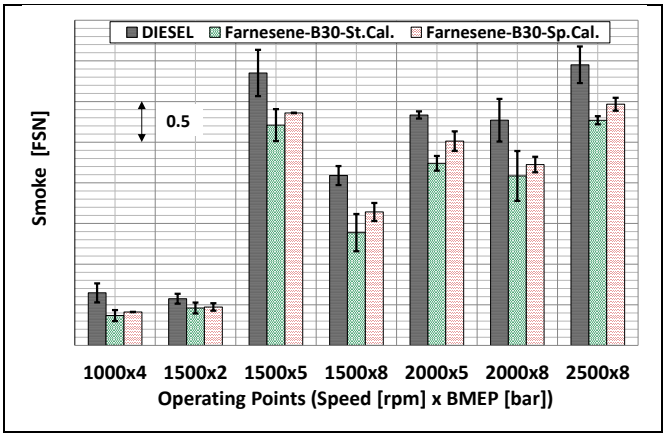

Fig. 14: Smoke at part load operating points

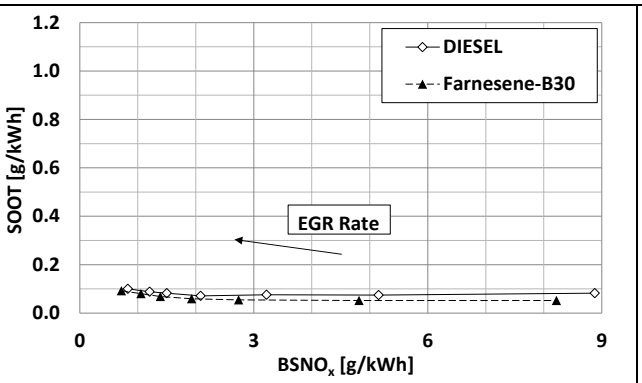

(a) Soot-$BSNO_x$

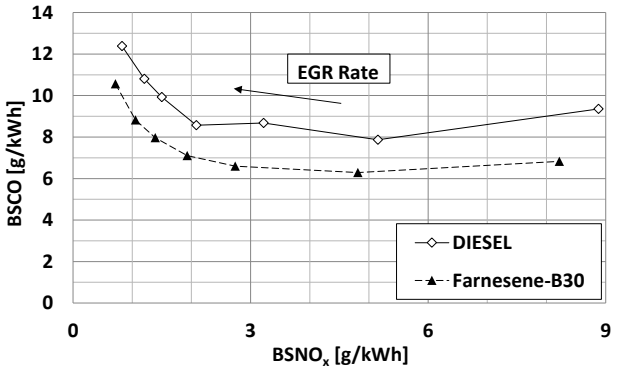

(b) BSCO-$BSNO_x$

Fig. 15: Trade-off results at 1500 rpm, 2 bar BMEP

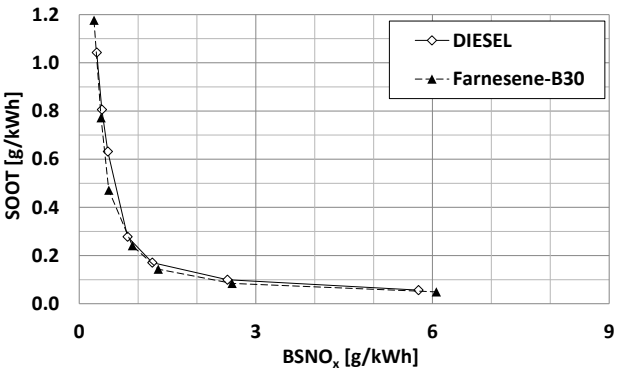

(a) Soot-$BSNO_x$

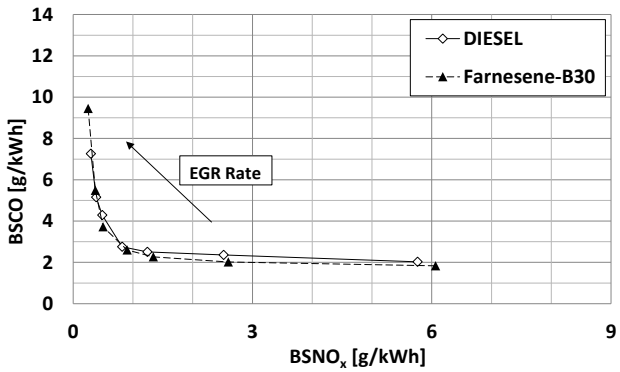

(b) BSCO-$BSNO_x$

Fig. 16: Trade-off results at 1500 rpm, 5 bar BMEP

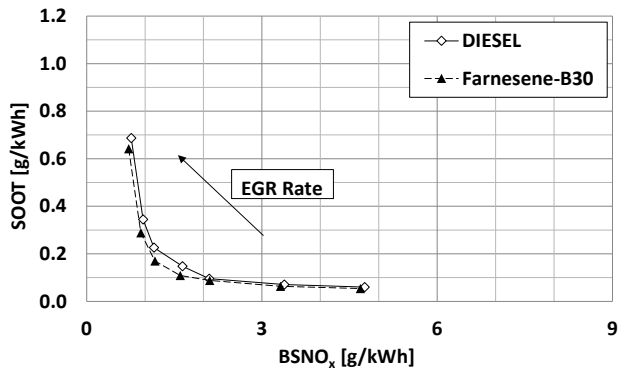

(a) Soot-$BSNO_x$

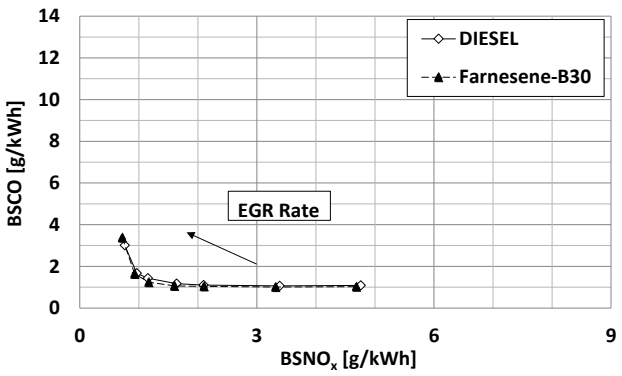

(b) BSCO-$BSNO_x$

Fig. 17: Trade-off results at 1500 rpm, 8 bar BMEP

Conclusions

The effects of using blended Farnesane (30% vol.) in a Euro 5 small displacement passenger car diesel engine have been evaluated in this paper.

At full load operating conditions, without any modifications to the ECU calibration, when fuelling the engine with biofuel blend a slight decrease (~2 % on average) in the torque output could be observed over almost the entire speed range due to the slightly higher LHV of the biofuel which mitigates the negative effect of fuel lower density.

At part load operating conditions, representative of the New European Driving Cycle, no significant variations were found for BSFC and fuel conversion efficiency, as well as for CO2 emissions, when engine was fuelled with biofuel blend.

CO and HC specific emissions were significantly reduced with Farnesane-B30 at low and medium loads, while only modest or even insignificant variations were registered at higher loads. This behaviour could be likely due to the better ignition quality of biofuel, and could therefore be emphasized when considering engine cold conditions (i.e. the conditions at the start of the relevant homologation testing procedures).

NO_x emissions with biofuel blend were generally comparable with those of the reference diesel fuel when ECU was properly re-calibrated, while a noteworthy reduction of smoke levels could generally be observed for medium and high load operating conditions.

Finally, Soot-NO_x and BSCO-$BSNO_x$ trade-off obtained by means of EGR sweeps highlighted the potential for gathering some further emissions benefits through a better exploitation of the biofuel made possible through a more extensive ECU recalibration especially at low engine loads.

References

[1] Lang X, Dalai AK, Bakhashi N, Reaney M, Hertz P. Preparation and characterization of biodiesels from various bio-oils.Bioresource Technology 2001;80:53–62.

[2] Freedman B, Butterfield R, Pryde EH. Transesterification kinetics of soybean oil.Journal of the American Oil Chemists' Society1986;63:1375–80.

[3] Pramanik K. Properties and use of Jatropha curcas oil and diesel fuel blends in compression ignition engine.Renewable Energy2003;28:239–48.

[4] Meher L, Kulkarni M, Dalai A, Naik S. Transesterification of karanja (Pongamiapinnata) oil by solid catalysts.European Journal of Lipid Science and Technology2006;108:389–97.

[5] de Oliveira JS, Leite PM, de Souza LB, Mello VM, Silva EC, Rubim JC, Meneghetti SMP, Suarez PAZ. Characteristics and composition of Jathrophagossypiifolia and Jathrophacurcas L. oils and application for biodiesel production.Biomass and Bioenergy2009;33:449–53.

[6] Demirbas A. Biodiesel from waste cooking oil via base-catalytic and supercritical methanol transesterification.Energy Conversion and Management2009;50:923–27.

[7] Issariyakul T, Kulkarni MG, Meher LC, Dalai AK, Bakhshi NN. Biodiesel production from mixtures of canola oil and used cooking oil.Chemical Engineering Journal 2008;140:77–85.

[8] Saraf S, Thomas B. Influence of feedstock and process chemistry on biodiesel quality.Process Safety and Environmental Protection2007;85:360–4.

[9] Shin H-Y, Lee S-H, Ryu J-H, Bae S-Y. Biodiesel production from waste lard using supercritical methanol.The Journal of Supercritical Fluids2012;61:134–8.

[10] Buyukkaya E. Effects of biodiesel on a DI diesel engine performance, emission and combustion characteristics. Fuel 2010;89:3099–105.

[11] Pillary AE, Fok SC, Elkadi M, Stephen S, Manuel J, Khan MZ, Unnithan S.Engine emissions and performances with alternative biodiesels: a review. Journal of Sustainable Development 2012;5:59-73.

[12] Agarwal AK, Das LM. Biodiesel development and characterization for use as a fuel in compression ignition engines.ASME Journal of Engineering for Gas Turbines and Power2001;123:440–7.

[13] A Comprehensive Analysis of Biodiesel Impacts on Exhaust Emissions. U.S. Environmental Protection Agency, EPA420-P-02-001, October 2002.

[14] Caroca JC, Millo F, Vezza D, Vlachos T, De Filippo A, Bensaid S, Russo N, Fino D. Detailed investigation on soot particle size distribution during DPF regeneration, using standard and bio-diesel fuels. Industrial & Engineering Chemistry Research2011;50:2650–8.

[15] Sharp C, Howell S,Jobe J. The effect of biodiesel fuels on transient emissions from modern diesel engines. SAE Paper 2000-01-1967, 2000.

[16] Fontaras G, Karavalakis G, Kousoulidou M,Tzamkiozis T, Ntziachristos L, Bakeas E, Stournasb S, Samaras Z. Effects of biodiesel on passenger car fuel consumption, regulated and non-regulated pollutant emissions over legislated and realworld driving cycles. Fuel 2009;88:1608–17.

[17] Postrioti L, Battistoni M, Grimaldi CN,Millo F. Injection strategies tuning for the use of bio-derived fuels in a common rail HSDI diesel engine. SAE Paper 2003-01-0768, 2003.

[18] Guido C, Beatrice C, Di Iorio S, Fraioli V, Di Blasio G, Vassallo A,Ciaravino C. Alternative diesel fuels effects on combustion and emissions of an Euro5 automotive diesel engine. SAE Paper 2010-01-0472, 2010.

[19] Beatrice C, Guido C, Di Iorio S, Napolitano P, Del Giacomo N. Impact of RME and GTL fuel on combustion and emissions of a‘Torque-Controlled’diesel automotive engines. SAE Paper 2010-01-1477, 2010.

[20] Westfal PJ, Gardner TS. Industrial fermentation of renewable diesel fuels.Current Opinion in Biotechnology2011;22:344–50.

[21] Knothe G, Sharp CA, Ryan TW. Exhaust emissions of biodiesel, petrodiesel, neat methyl esters, and alkanes in a new technology enginery. Energy & Fuels 2006; 20:403-8.

[22] Stumborg M, Wong A, Hogan E. Hydro-processed vegetable oils for diesel fuel improvement.Bioresource Technology1996;56:13-8.

[23] Kralisch D, Staffel C, Ott D, Bensaid S, Saracco G, Bellantoni P, Loeb P. Process design accompanying life cycle management and risk analysis as a decision support tool for sustainable biodiesel production, Green Chemistry 2013;15:463-77.

[24]Amyris Biotechnologies Inc.(http://www.amyrisbiotech.com/); Accessed on March 8, 2014: 13.42 CET.

[25] Laluce C, Schenberg ACG, Gallardo JCM. Advances and developments in strategies to improve strains of Saccharomyces cerevisiae and processes to obtain the lignocellulosic ethanol – a review. Applied Biochemistry and Biotechnology 2012;166:18–35.

[26] Renninger NS, McPhee DJ. Fuel compositions comprising Farnesane and farnesane derivatives and method of making and using same.Amyris Biotechnologies, Inc., Patent N° US 7,399,323 B2, July 15, 2008.

[27] Conconi CC, Crnkovic PM. Thermal behavior of renewable diesel from sugar cane, biodiesel, fossil diesel and their blends. Fuel Processing Technology 2013;114:6–11.

[28] Hellier P, Al-Haj L, Talibi M, Purton S, Ladommatos N. Combustion and emissions characterization of terpenes with a view to their biological production in cyanobacteria. Fuel 2013;111:670–88.

[29] Jansma H, Fino D, Huitz R, Makkee M. Influence of diesel fuel characteristics on soot oxidation properties, Industrial & Engineering Chemistry Research2012;517559–64.

[30] Millo F, Mallamo F, Vlachos T, Ciaravino C, Postrioti L, Buitoni G. Experimental investigation on the effects on performance and emissions of an automotive Euro 5 diesel engine fuelled with B30 from RME and HVO. SAE Paper: 2013-01-1679, 2013.

[31] Beatrice C, Guido C, Napolitano P, Iorio SD, Giacomo ND. Assessment of biodiesel blending detection capability of the on-board diagnostic of the last generation automotive diesel engines. Fuel 2011;90:2039-44.

[32] Badami M, Mallamo F, Millo F, Testa D. ICE analyzer: a data acquisition system for internal combustion engines. National Instruments Automotive Users' Conference, Turin, Italy, June 2001 (in Italian).

Chapter IV Nanolubricants for diesel engines: Related emissions and compatibility with the after-treatment catalysts

Abstract

The effect of the lubricant oil additivated with MoS_2 nanopowders was assessed through a set of full-scale tests on a real Diesel engine: several engine points and cooling water temperatures were investigated for both a reference oil and a MoS_2-additivated one. The emission abetment efficiency of the DOC and DPF reduces the gas and solid pollutants obtained with the MoS_2-additivated oil to levels equivalent to the ones reached with the reference oil. An endurance test of 100 h (equivalent to 10,000 km) proved the stability of the catalytic system and the suitability of commercial after-treatment catalysts to cope with the emission modifications induced by the inclusion of nano-additives in the oil matrix.

1. Introduction

Fluid lubricants are used in almost every field of human technological activity and their purpose is multi-fold: they reduce frictional resistance, protect the contacting surfaces of engines against wear, remove wear debris, reduce heat and contribute to cooling, improve fuel economy and reduce emissions.

Advanced nanomaterials have shown some promise because of their contribution to reducing friction and enhancing protection against wear [1-3]. When incorporated in full lubricant formulations in a stable way, and if their performance benefits can be sustained under those circumstances, they offer the possibility of some performance breakthroughs which have not witnessed since the development of the now ubiquitous anti-wear additives, Zinc Dialkyl Dithiophosphate (ZDDP) and Molybdenum DiThioCarbamate (MoDTC). It has been demonstrated that ZDDP and MoDTC used together improve the friction and anti-wear performances by the formation of a molybdenum disulphide layer on the rubbing surfaces [4-6]. The developments brought by nanomaterials can contribute to a substantial energy saving, reduce equipment maintenance and lengthen the life of the machines. In the case of engine oil (crankcase) applications, these nanomaterials can help increase the durability and performance of exhaust-treatments and reduce harmful emissions: in fact, exhaust catalysts tend to become poisoned by the sulphur and phosphorous that are present in conventional lubricant additives.

Nanostructured transition metal dichalcogenides, with the generic formula MX_2 (M = W, Mo; X = S, Se), whose synthesis was first demonstrated at the Weizmann institute by Tenne and co-workers [7-9], seem to be very promising materials to be dispersed as nanoparticles in the

oil matrix. They involve a reaction between MO_3 and H_2S, in reducing atmosphere at high temperatures, and the corresponding sulfide (WS_2 or MoS_2) is obtained. Many other synthetic routes have also been followed to obtain these kinds of nano-structured materials [10-12].

The specific lubrication mechanism ascribed to these metal sulphides, often called inorganic fullerenes due to their peculiar structure of spherical concentric layers, is currently debated; however, several studies clearly indicate that an exfoliation process of these layers, and the consequent liberation of nanosheets directly inside the surface contact area, is the prevalent lubricating mechanism for these systems [13,14]. This is very interesting because the lubrication additive is brought directly in the contact area without any prior chemical reaction, avoiding the transient period characteristic of the current additives. It was also hypothesized that these nanoparticles behave as nano-ball bearings, due to their spherical shape, ultra-hardness and nano-size, at least temporarily until they gradually deform and start to exfoliate giving rise to the observed low friction coefficients: investigations involving direct visualization of the nanoparticle behaviour in the contact area, over a broad pressure range, were attempted by combining Transmission Electron Microscope (TEM) and Atomic Force Microscopy (AFM) [15].

The present study focuses on MoS_2 nanoparticles which have to be incorporated in engine lubricant oils. A wet synthesis technique has been devised within our group [16], which is based on the preparation of an aqueous solution of citric acid and ammonium molybdate to form a complex of molybdenum(IV) with citric acid, to which a suitable amount of ammonium sulfide was added to obtain MoS_2. This technique resorts to a simple and scalable process, and involves low-cost reagents, instead of other more complex reaction methods. An example of the MoS_2 particles obtained with this technique is depicted in Figure 1. Moreover, this synthesis route is extremely versatile since it can be adapted for continuous MoS_2 particle production, in specific devices that allow to control the particle diameter and obtain reproducible results in terms of particle size distribution [17,18]**.**

As previously mentioned, a progressive poisoning of after-treatment catalysts occurs due to the presence of species that were originally present in the lubricant oil as additives, and which are then released into the flue gases after in-cylinder combustion. One major requirement for the application of these nanoparticles as lubricant oil additives, in substitution to the currently adopted ones, is their complete compatibility with the catalytic substrates present in the after-treatment line, whose lifetime operation should not be affected to any great extent. This analysis is crucial for the introduction of such nano-sized additives for lubricant oils on the

market, and in this work was applied to EURO 5 compliant catalysts for DOC, DPF and SCR systems.

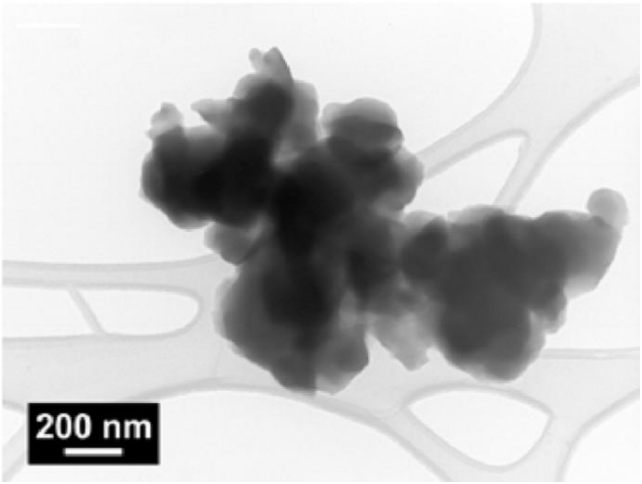

Figure 1. TEM micrograph of MoS_2 nanoparticles.

2. Experimental

One important requirement for the application of these nanoparticles as lubricant oil additives is their compatibility with the catalytic substrates present in the after-treatment line: therefore, an assessment was carried out about a possible interaction between the MoS_2 nanopowders and some commercial catalysts, representative of EURO 5-compliant catalytic converters present in the after-treatment line of light-duty diesel engine vehicles, for which a diesel engine bench (OPEL 1900cm^3 JTD common Rail) connected to a dynamometer (AVL Alpha 240KW) with a maximum rpm/torque of 10000rpm/600Nm, was used (schematically depicted in Figure 2).

The experimental campaign was carried out in different steps: initially, the engine was conditioned with a commercial synthetic oil (multi-grade SAE 5W30), through a standardized procedure for internal oil circulation before the test was started. Then, five different engine points were tested in order to reproduce the different operation conditions of the car (engine frequency in rpm and bpme in bar: 1500x1, 2000x2, 2500x3, 3000x4 and 3500x5, all with 0% EGR), and for each engine point four different cooling water temperatures of the engine were fixed (40, 60, 80 and 95°C). The exhaust gas recirculation was fixed to zero in all operating conditions. This settings were operated through a dedicated AVL PUMA program, by monitoring all engine conditions with INCA software connected to the Electronic Control Unit (ECU) integrated with ETAS and BOSCH instrumentation: the temperature of the cooling water, of the engine outlet exhaust gases and of the lubricant oil were measured with K-type thermocouples.

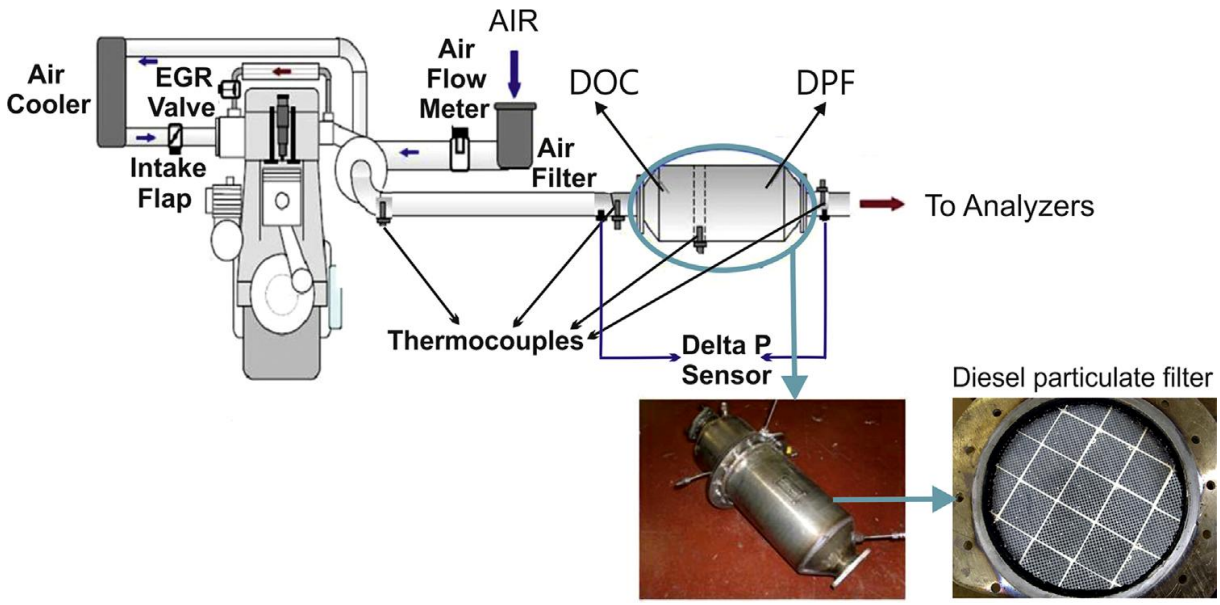

Figure 2. Schematic of the Diesel engine bench.

The same procedure was adopted for the MoS_2 nanoparticle-additivated oil, whose concentration was 0.5wt%.

The tests consisted in monitoring and measuring the gas composition, particle size distribution, the temperature and pressure, at each engine point and in each cooling water temperature in the engine on steady state. In particular, the gas composition was continuously monitored before and after both the Diesel Oxidation Catalyst converter (DOC) and the Diesel Particulate Filter (DPF), with an ABB gas analyzer, equipped with two Uras26 analyzers for N_2O, NO, CO_2, CO and SO_2, and a Magnos206 analyzer to measure O_2. The HCs were measured with a Multifid14 analyzer Hartmann&Braun. The smoke number was measured with Variable Sampling Smoke Meter AVL 415S G002. The soot particle size distribution was recorded using Scanning Mobility Particle Sizer 3080 (SMPS), which consists of an impactor (type 0,0508 cm), a neutralizer, a differential mobility analyzer, and a condensation particle counter, with the sheath and aerosol flows set to 6 and 0.6 l/min, respectively, this system covered the 9,6-422 nm particle diameter range, each scan lasted 75 s (scanning time of 60 s plus retrace of time 15 s). The engine exhaust was sampled using a heated pipe (1m long, 6mm diameter, T~150°C), followed by two ejector pump diluters in series (Dekati Ltd.): each stage provided a dilution factor of ~8, resulting a 64 fold overall dilution, which was calibrated measuring the carbon dioxide concentrations in the exhaust and in the sample flow, and then the exiting gas was transported to the SMPS system through a 4m long tube (OD=6 mm) [19].

Table 1. Physical properties of the base lubricant oil prior MoS_2 additivation.

Physical property	Unit	Value
Viscosity class	-	5W-30
Kinetic viscosity (80°C)	$mm^2 \cdot s^{-1}$	61.5
Kinetic viscosity (100°C)	$mm^2 \cdot s^{-1}$	10.1
Viscosity index	-	155
CCS viscosity (-30°C)	mPa·s	6100
HTHSV (150°C)	mPa·s	3.1

Finally, a long term endurance test was performed, in which the oil additivated with MoS_2 nanoparticles was subjected to 100 hours of engine operation at 2000x2 (with a cooling water temperature of 95°C and an EGR opening of 22% to accelerate soot accumulation in the DPF), corresponding to a total distance of 10,000 km at a constant speed of around 100 km/hr, with start-stop intervals and regeneration periods necessary to clean the DPF each time the pressure drop across the filter attained 80 mbar, which roughly indicated that a 6 g/l soot loading was reached. The regeneration was carried at 2750x7.5. The start-stop intervals were important to expose the oil to repeated temperature changes, which simulate the continuous start-stop of the car. Similarly, the regeneration is one of the most intensive conditions occurring in engine operation, during which the oil containing nanoparticles is exposed to several over-injections of diesel in the combustion chamber, to reach suitable temperatures in the DPF for soot catalytic oxidation [20]. This long term test was meant to see if any ash accumulation or catalyst deactivation was observed due to, among others, the possible emissions of sulfates ascribable to the MoS_2 content in the engine oil. It has to be pointed out that higher ash loadings have to be investigated to be fully representative of the exposure of a DPF to ash-containing soot emissions: therefore, increased travel distances have to be foreseen in the future, such as around 150,000 km which would correspond to the entire lifetime of a DPF, and that the present test is a preliminary assessment of the NP-additivated lubricant oil tendency to produce MoS_2-related ashes.

However, an attempt to quantify the impact of MoS_2 in the ash composition has been indeed performed: the chemical analysis of the soot collected in the DPF filter by employing base oil and NP-additivated oil, respectively, was performed by an Agilent 7500ce ICP/MS. A sample of 100 mg was dissolved in a solution prepared with 3 ml of deionized water, 2ml of hydrogen

peroxide and 5 ml of nitric acid (65% concentrated). The so-obtained solution was treated in a microwave oven (CEM, mod. Mars 250/40) for 1 , at a maximum temperature of 180 °C. The mineralized solution was diluted with deionized water to a final volume of 50 ml and subsequently analyzed.

3. Results and discussion

Figures from 3 to 7 report the particulate emissions measured with the SMPS, at five couples of rpm and bpme (1500x1, 2000x2, 2500x3, 3000x4 and 3500x5), which were tested in order to characterize the various operating conditions of the engine. In each figure, four water cooling temperatures were tested (40°C, 60°C, 80°C, 95°C), and particulate emissions were sampled at the engine outlet (i.e. the DOC inlet), at the DOC outlet (i.e. DPF inlet), and at the DPF outlet.

The comparison between the emissions generated with the base oil, and the ones with the additivated one with MoS_2 nanoparticles, shows the effect of nano-lubricant inclusion in the oil matrix on the particulate in the exhaust gases. The global information based on mass particle concentration are presented in Tables 2 and 3, for the base oil and the NP-additivated ones, respectively.

Starting from Figure 3 at rpm/bpme of 1500x1, which is a low load for the engine, one can notice that the particle size distribution at the DOC inlet follows a Gaussian curve, as described by Kittelson et al. [21], at all cooling water temperature conditions. Similar trends are found in the DOC inlet emissions obtained with the base oil and the NP-additivated one, especially at 40°C, 60°C and 95°C; however, an evident increase of the ultrafine particle concentration belonging to the nuclei mode (<50 nm) is observed for the oil containing MoS_2. The nuclei mode usually includes, besides soot particles, also volatile organic (also called SOF) and sulphur compounds that may form during exhaust gases' dilution and cooling [22]; the latter fraction could represent 1-20% of the total mass concentration. The slight increase of the nuclei mode for the nano-lubricant case is presumably caused by the presence of such volatile organic and sulphuric compounds, which are precursors of the nucleation of the soot particles. The effect of NP-additivation is also evident in terms of total mass concentration (Table 2 and 3), where the engine out emissions are greater with respect to the base oil, at all investigated cooling temperatures.

Table 2. Measured soot particle mass concentration (μg/m^3) before the DOC, before the DPF and after the DPF, for the base oil.

40°C	**Engine Points**	**in DOC**	**in DPF**	**out DPF**
	1500x1	6,677	2,403	0
	2000x2	18,474	5,062	0
	2500x3	21,205	7,936	17
	3000x4	18,517	7,264	1
	3500x5	20,202	6,374	15
60°C	**Engine Points**	**in DOC**	**in DPF**	**out DPF**
	1500x1	15,850	2,483	4
	2000x2	11,221	2,246	0
	2500x3	12,181	5,459	6
	3000x4	19,904	6,912	3
	3500x5	19,882	6,496	33
80°C	**Engine Points**	**in DOC**	**in DPF**	**out DPF**
	1500x1	3,050	2,362	4
	2000x2	5,734	3,085	2
	2500x3	7,637	4,413	3
	3000x4	12,202	5,088	2
	3500x5	13,461	5,434	21
95°C	**Engine Points**	**in DOC**	**in DPF**	**out DPF**
	1500x1	6,054	3,722	22
	2000x2	9,322	3,219	9
	2500x3	7,850	4,518	13
	3000x4	11,946	5,030	4
	3500x5	14,698	4,976	25

If one focuses on the DOC outlet (i.e. DPF inlet) emissions of Figure 3, a significant change in the particle size distribution can be noticed across the DOC itself, for all tested temperatures: the nuclei mode is mostly affected (<50nm), while the accumulation mode (>50 nm) remains quite constant due to the fact that the carbonaceous soot, which belongs to the latter class [21], is refractory to oxidation at the normal DOC operating temperatures. As far as the oil is concerned, the particulate emissions with the base oil exhibit almost the same profile at all investigated temperatures, this being quite similar to the ones with the NP-additivated oil at 40°C and 60°C. Whereas, they strongly differ at higher temperatures (80°C and 95°C), where the emissions observed with the nano-lubricant are surprisingly lower than the ones with the base oil. This is also testified by the comparison of the emissions in terms of

mass concentration (Table 2 and 3). A possible explanation will be later attempted in relationship to gaseous emissions.

Table 3. Measured soot particle mass concentration ($\mu g/m^3$) before the DOC, before the DPF and after the DPF, for the NP-additivated oil.

40°C	**Engine Points**	**in DOC**	**in DPF**	**out DPF**
	1500x1	14,122	2,387	434
	2000x2	24,021	5,078	1
	2500x3	19,306	7,456	1
	3000x4	25,813	6,816	2
	3500x5	16,874	7,264	4
60°C	**Engine Points**	**in DOC**	**in DPF**	**out DPF**
	1500x1	16,362	3,254	584
	2000x2	11,904	2,131	0
	2500x3	16,277	3,296	2
	3000x4	20,394	4,256	1
	3500x5	16,021	5,594	11
80°C	**Engine Points**	**in DOC**	**in DPF**	**out DPF**
	1500x1	10,944	1,805	1,750
	2000x2	32,362	2,179	1
	2500x3	11,370	3,270	0
	3000x4	17,770	4,106	2
	3500x5	14,613	5,098	2
95°C	**Engine Points**	**in DOC**	**in DPF**	**out DPF**
	1500x1	7,146	1,968	1,872
	2000x2	24,928	2,342	10
	2500x3	8,800	3,027	1
	3000x4	10,240	4,266	18
	3500x5	12,320	4,666	35

Finally, the particle size distribution at the DPF outlet in Figure 3 shows a significant difference between the two lubricant oils: a much higher concentration of the particles are noticed in the nano-lubricant case for all investigated temperatures, although this concentration is reduced by two orders of magnitude with respect to the engine outlet. This behavior occurs only for this particular rpm/bmep couple, while for all other conditions the base and NP-additivated oils behave in the same way in terms of outlet DPF emissions

(Figures 4-7); it could be caused by the low exhaust gas temperatures at this engine point, and in particular in the coolest part of the after-treatment line (no DPF regeneration was performed during sampling), which may be below the dew point of some heavy hydrocarbons that undergo nuclei condensation.

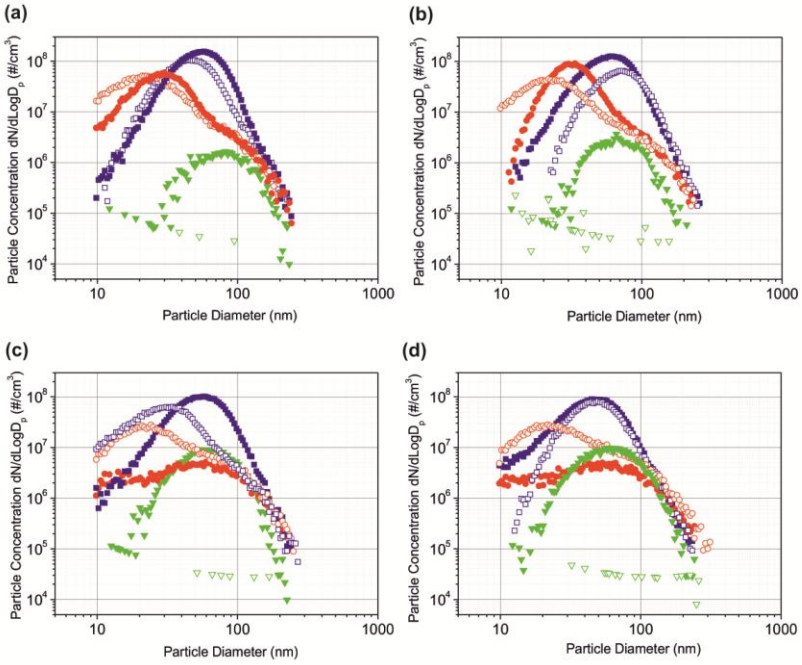

Figure 3. Measured soot particle concentration with respect to the particle diameter before the DOC (blue squares), before the DPF (red circles), after the DPF during loading (green triangles), for the base oil (open symbols) and the NP-additivated oil (closed symbols). Engine point: **1500x1**; cooling water temperature: (a) 40°C, (b) 60°C, (c) 80°C, (d) 95°C.

In the case at 2000x2 (Figure 4), the engine out emissions overlap for the two oils, except for the part of the curve at low particle diameters, whose concentration is higher for the nano-lubricant than for the blank. However, as for the above-mentioned lower engine load, the DOC flatters these profiles, and demonstrates to be more efficient in oxidizing the finest part of the curve obtained with the nano-lubricant, rather than with the base oil. Again, this can be globally observed in terms of mass concentration in Tables 2 and 3. The DPF is almost 100% efficient in soot abatement, irrespective of the tested oil matrix.

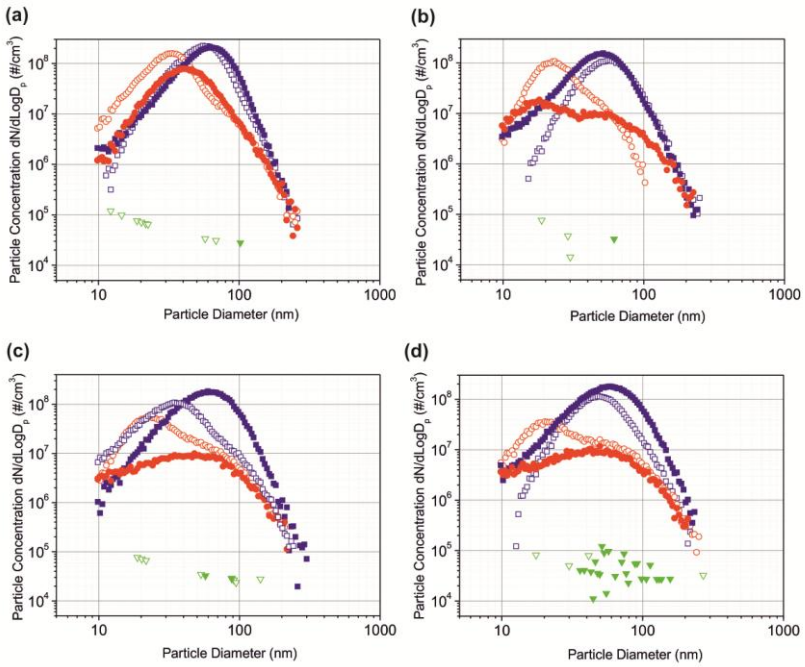

Figure 4. Measured soot particle concentration with respect to the particle diameter before the DOC (blue squares), before the DPF (red circles), after the DPF during loading (green triangles), for the base oil (open symbols) and the NP-additivated oil (closed symbols). Engine point: **2000x2**; cooling water temperature: (a) 40°C, (b) 60°C, (c) 80°C, (d) 95°C.

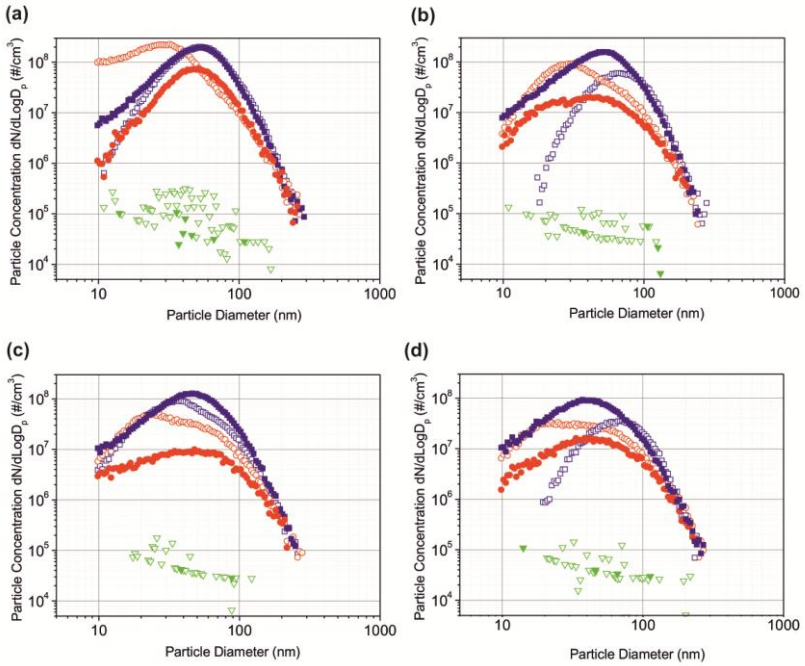

Figure 5. Measured soot particle concentration with respect to the particle diameter before the DOC (blue squares), before the DPF (red circles), after the DPF during loading (green triangles), for the base oil (open symbols) and the NP-additivated oil (closed symbols). Engine point: **2500x3**; cooling water temperature: (a) 40°C, (b) 60°C, (c) 80°C, (d) 95°C.

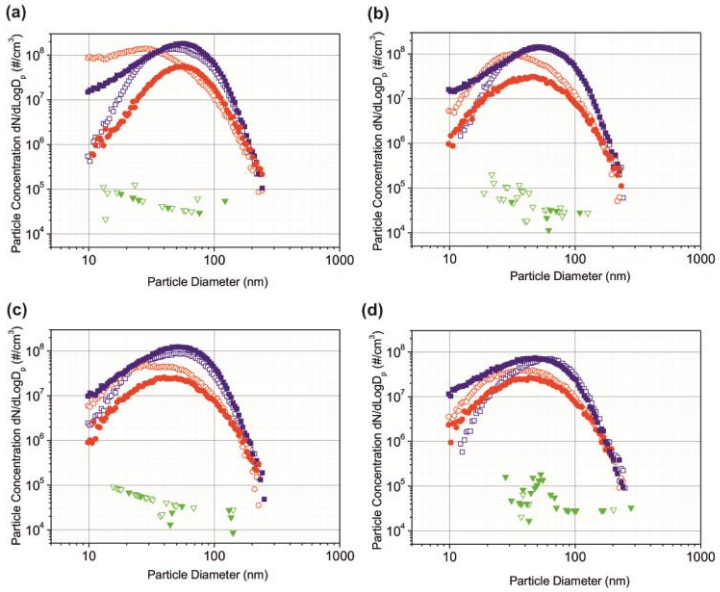

Figure 6. Measured soot particle concentration with respect to the particle diameter before the DOC (blue squares), before the DPF (red circles), after the DPF during loading (green triangles), for the base oil (open symbols) and the NP-additivated oil (closed symbols). Engine point: **3000x4**; cooling water temperature: (a) 40°C, (b) 60°C, (c) 80°C, (d) 95°C.

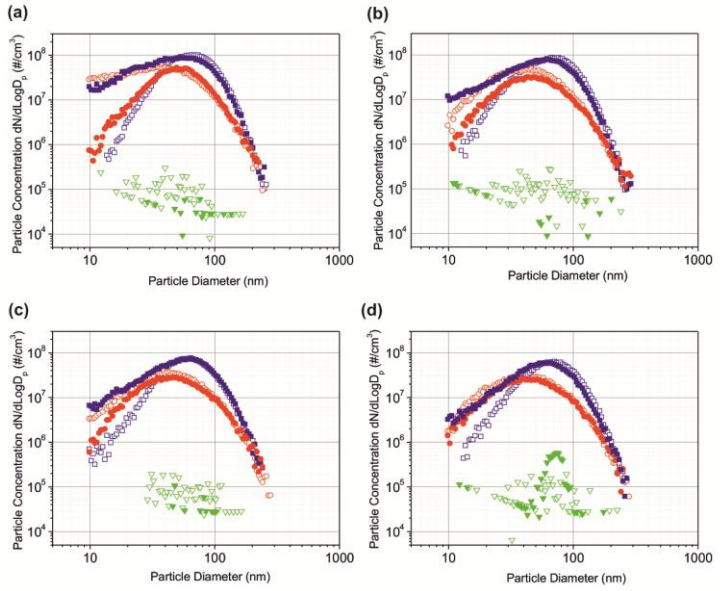

Figure 7. Measured soot particle concentration with respect to the particle diameter before the DOC (blue squares), before the DPF (red circles), after the DPF during loading (green triangles), for the base oil (open symbols) and the NP-additivated oil (closed symbols). Engine point: **3500x5**; cooling water temperature: (a) 40°C, (b) 60°C, (c) 80°C, (d) 95°C.

At increasing load, it can be observed that the differences between the base oil and the NP-additivated oil still remain, but tend to decrease (Figure 5, 6 and 7). The greater engine outlet

emissions of soot ascribable to the original MoS_2 presence in the lubricant oil are limited to the finest particles, while in terms of total mass their concentration equals the one obtained with the base oil in most of the experiments (Tables 2 and 3). An indirect information of this behavior is testified by the similar smoke numbers recorded at the engine outlet (Figure 8-a) for the two oils. The problem of ultrafine particle generation has almost no impact downstream of the DPF.

The effect of the sulphur in MoS_2 is also quite limited in terms of SO_2 emissions, the latter being around 3-4 ppm, while the ones measured with the base oil are below the detection limit (Figure 8-b): in fact, less than 10ppm of S are present in the fuel, therefore the dilution factor introduced by air brings the concentration of SO_2 in the exhausts below 1ppm. As a result, the poisoning effect of the sulphur originated from MoS_2 should therefore be very low, and not relevant throughout the catalysts lifetime, due to very low SO_2 concentration in the exhausts.

Further information of the effect of MoS_2 additivation to a lubricant oil comes from the analysis of the gaseous emissions of HC, CO and NO at the engine outlet (i.e DOC inlet, Figure 9), DOC outlet (i.e. DPF inlet, Figure 10) and DPF outlet (Figure 11).

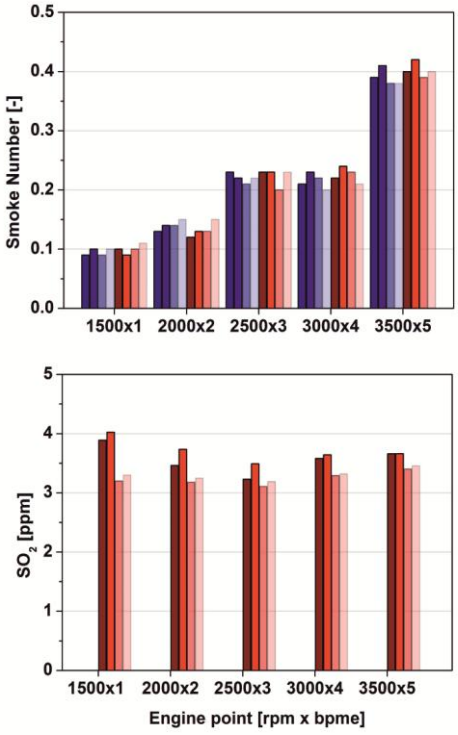

Figure 8. Measured smoke number and SO_2 concentration before the DOC at different engine points for the NP-additivated oil (red) at various cooling water temperatures (40°C, 60°C, 80°C and 95°C, from dark to light); SO_2 concentration for the base oil below the detection limit.

Starting from HC and CO engine outlet emissions (Figure 9), it can be observed their amounts are greater at both low engine points (due to their low efficiency) and high ones (due to the higher fuel consumption, and therefore higher emissions), while they are lower at intermediate ones (due to a better compromise of efficiency and reduced slip of species from incomplete fuel combustion). Moreover, increasing water temperatures tend to reduce the emissions of partially oxidized species like CO. It can be seen that the emissions of HC and CO emitted by the engine are higher in the presence of the nano-lubricant than in its absence, regardless of the engine point.

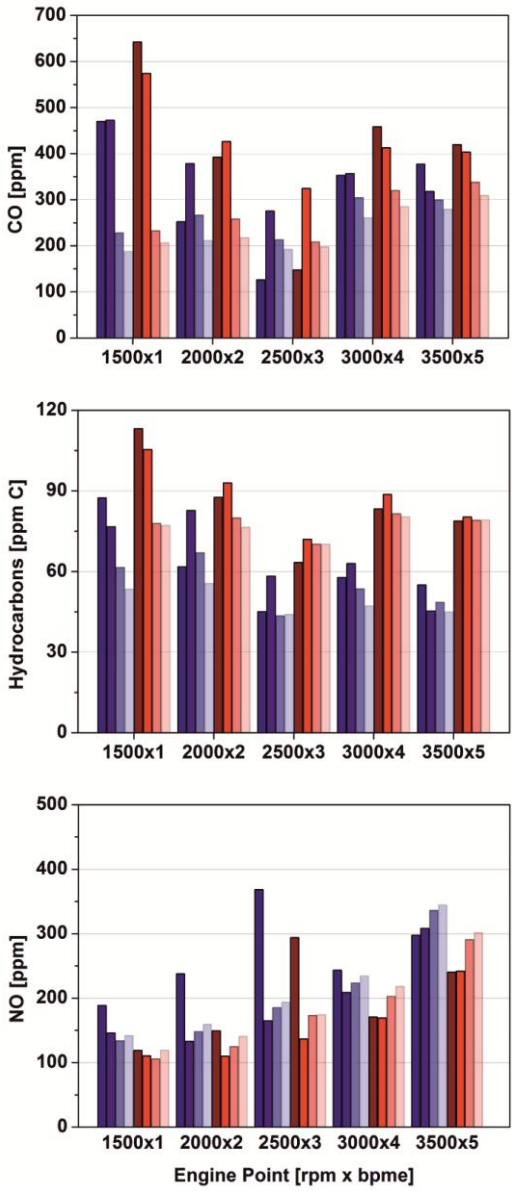

Figure 9. Measured CO, HC and NO concentration before the DOC at different engine points for the base oil (blue) and the NP-additivated oil (red) at various cooling water temperatures (40°C, 60°C, 80°C and 95°C, from dark to light).

This has a strong relationship between HC and soot emissions: hydrocarbons are precursors of soot particle nucleation, and their concentration in the exhaust gases could influence the particle size distribution and mass concentration, thus being responsible for the higher soot emissions observed with the NP-additivated oil. In addition, higher HC concentrations involve that greater amounts of heavy hydrocarbons fractions adsorb inside the porous structure of the particle and on its surface, thus conferring a higher reactivity towards oxidation with respect to the sole carbonaceous structure of soot, which is much refractory.

Figure 10 shows that the DOC tends to reduce the differences between the emissions measured with two oils: the higher temperatures of the exhaust flue gases at high loads cause a consistent reduction of the CO and HC emissions, while the ones of NO remain almost unchanged. The same happens at the DPF outlet (Figure 11), and the slight increase of CO is ascribed to the DPF passive regeneration, although almost negligible in terms of soot combustion rate.

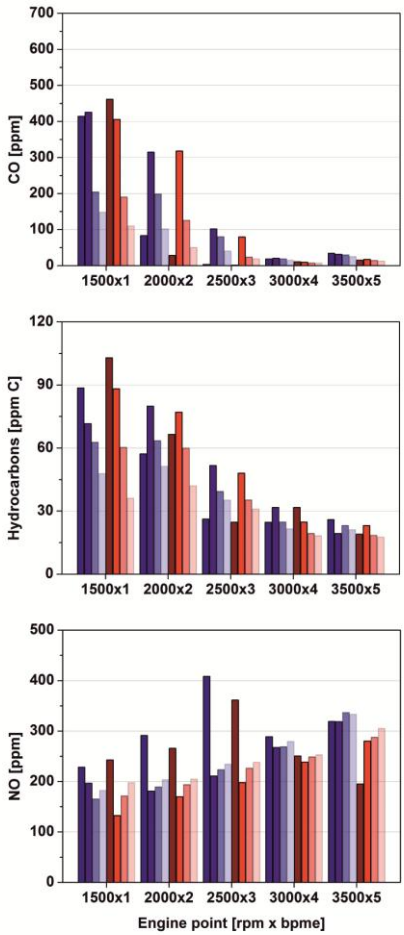

Figure 10. Measured CO, HC and NO concentration before the DPF at different engine points for the base oil (blue) and the NP-additivated oil (red) at various cooling water temperatures (40°C, 60°C, 80°C and 95°C, from dark to light).

It can be concluded that, although the emissions of soot particles are higher in the presence of MoS_2 in the lubricant oil, especially in terms of ultrafine particles, the DOC is able to reduce the mass and number concentration of these particles down to levels comparable (or even lower) than in case of the base oil. This is possible because of the higher hydrocarbon concentration in the gas and, consequently, absorbed in the solid particulates, which confers a greater reactivity to the soot particle itself. Moreover, the DPF emissions are absolutely similar for both oil matrixes, with exception of the engine point at 1500x1 for the above-discussed reasons. In this regard, it can be stated that the MoS_2 as nano-lubricant does not entail neither higher tailpipe emissions, nor any incompatibility with the after-treatment line. In addition, the after-treatment catalysts are able to reduce the HC and CO emissions down to levels quite similar for the base and NP-additivated oil, which indicates a full compatibility of the investigated catalysts towards the MoS_2 nano-lubricant.

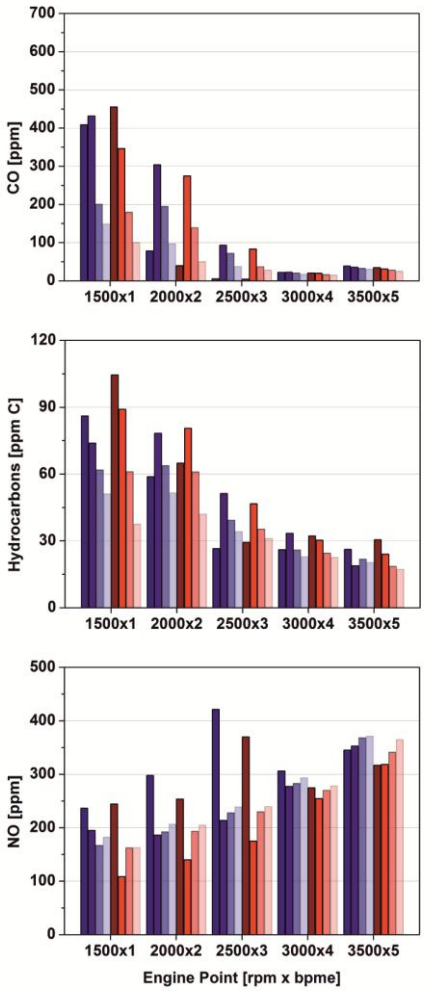

Figure 11. Measured CO, HC and NO concentration after the DPF at different engine points for the base oil (blue) and the NP-additivated oil (red) at various cooling water temperatures (40°C, 60°C, 80°C and 95°C from dark to light).

A challenge which remains undisclosed in the former tests is the long-term performance of the catalysts: for this reason, an endurance test was tailored to monitor the catalyst efficiency throughout a 100 h-lasting test, with intermediate DPF regenerations. The engine point at 2000x2 was selected (at a cooling water temperature of 95°C and an EGR opening of 22%) for the soot loading phase. The regeneration was carried out when 80 mbar were attained at 2000x2, which corresponds to 215-245 mbar at 2750x7.5, depending on the temperature of the exhaust gases during the regeneration itself.

Figure 12 reports the four regenerations (each one lasting 5 min from the time of attainment of 580°C at the DPF inlet) that were performed throughout the tests in terms of DPF pressure drop and of inlet and outlet DPF temperatures, while the loading is not depicted for the clarity of the figure. It can be seen that, at increasing inlet DPF temperature, the pressure drop increases due to the higher gas viscosity; however, at appropriate temperatures for soot ignition, the regeneration starts and the soot consumption is evident in terms of pressure drop decrease and outlet DPF temperature increase above the inlet one [23]. Anyhow, the most important outcome of these four repeated regenerations is that a full recovery of the original pressure drop (50 mbar at 2750x7.5) was attained. This indicates that the same degree of soot removal is obtained in repeated regeneration cycles, without any noticeable ash accumulation. Hence, its occurrence would progressively decrease the clean filter permeability and reduce the filtration area available for soot cake build-up [24].

Moreover, the ash content in the soot emitted by the engine was quantified to further assess the potential of ash accumulation in the DPF. This has been carried out by collecting samples of soot in the DPF, when both the base oil and the NP-additivated oil were employed. The soot samples were analyzed by means of ICP-mass, and the results are reported in Table 4. Elements under or close to the detection limit (0.001 wt%) are not reported. The total amount of ashes was measured to be 10.1 and 7.5 wt% when the base oil and the NP-additivated oil were respectively employed. This demonstrates that the MoS_2 nano-lubricant is able to reduce the content of ashes in soot, whose explanation was attempted through the following analysis of the metal elements in the ashes.

The elements are divided into “wear” metals, meaning elements coming from the abrasion of engine components, mainly constituted by steel, aluminum alloys as well as cast iron, and “additive” metals, meaning elements deriving from compounds employed as additives in the oil. As can be noticed, the tendency for wear metals is their general slight decrease when using the oil additivated with MoS_2 nanoparticles. This is probably ascribed to a reduced abrasion of the engine parts, and consequently a decrease of the friction coefficient.

The same trend can be depicted for the elements coming from additives, except for sodium and zinc, due to a different additive formulation for the oil containing MoS_2 nanoparticles: in fact, their beneficial presence allows to have a reduced content of antiwear additives.
Concerning molybdenum, the quantity measured in the two soot samples is the same, meaning that the presence of MoS_2 nanoparticles in the additivated oil does not in any way affect the final content of Mo in the soot.

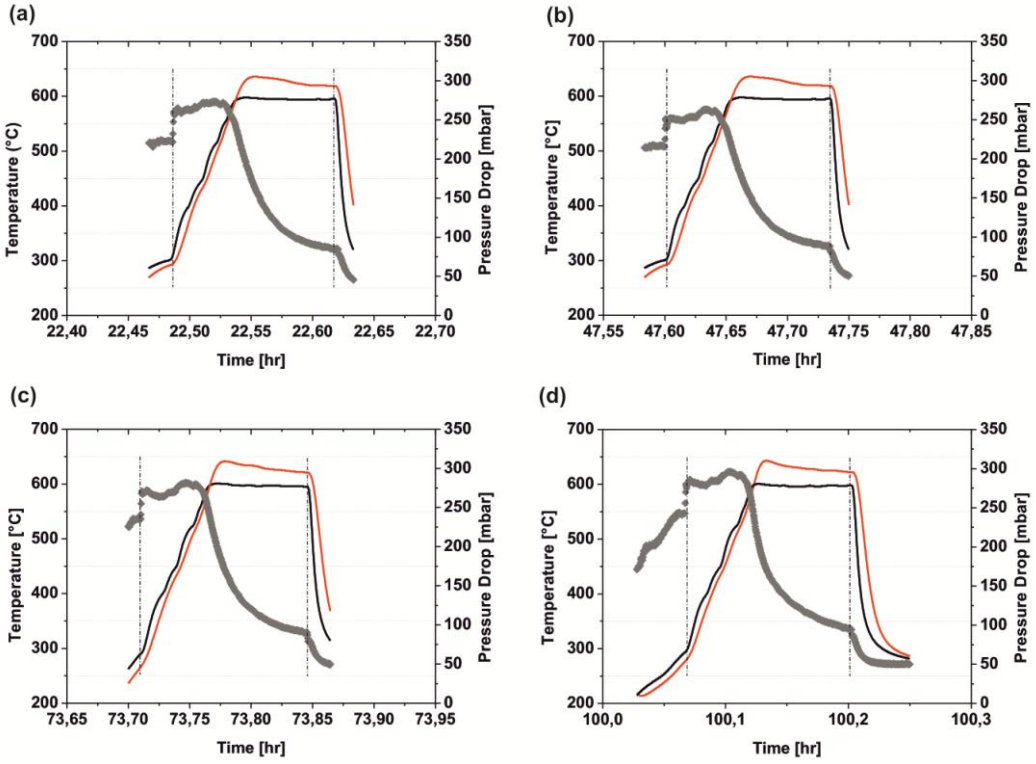

Figure 12. Measured inlet and outlet DPF temperatures (black and red curves, respectively, referred to the left *y* axis) and pressure drop (grey dots, right *y* axis) during successive filter regenerations (from a to d) during the long-term endurance test of 100 h. For the related gaseous emissions, see Table 5.

Finally, no clear deactivation of the soot oxidation catalysts occurs due to the specific soot emissions obtained with the NP-additivated oil, or due to the presence of MoS_2-related SO_2 in the exhaust gases, due to the same degree of regeneration completion after 5 min in all regeneration runs. Table 5 reports the emissions before the four regenerations occurred during the 100 h of tests at 2000x2 with 22% EGR, as well as at the beginning and at the end of the test at 2000x2 with 0% EGR (the letter being the same condition depicted in Figure 4-d for the soot emissions, and Figure 9 for the gaseous ones). It can be seen that no substantial

differences in HC, CO and NO concentration at the engine outlet occur throughout the entire test, which ensures that no specific degradation affects the MoS_2-containing oil after a test corresponding to a travelled distance of 10,000 km.

Table 4. Results of the chemical analysis by ICP-mass on the soot collected in DPF by using base oil and NP-additivated oil.

	Element [wt%]	Base oil	NP-additivated oil
"Wear" metals	Aluminum	0,169	0,115
	Copper	0,235	0,243
	Iron	0,499	0,477
	Manganese	0,122	0,121
	Nickel	0,033	0,027
	Molybdenum	0,757	0,740
Additives	Boron	0,036	0,016
	Calcium	7,081	5,012
	Magnesium	0,251	0,088
	Phosphorus	0,519	0,373
	Potassium	0,078	0,038
	Sodium	0,059	0,083
	Zinc	0,098	0,110

Longer endurance tests might disclose further information on this matter, but 100 h still indicates that the interaction between the emissions from an engine lubricated with MoS_2-formulated oils and state-of-the-art EURO 5 catalysts, does not involve any long-term decrement in emission abatement..

4. Conclusions

A novel wet chemical synthesis method has been developed for the production of molybdenum(IV) sulfide nanopowders, which are used as lubricant additives (0.5wt%) in this work.

The MoS_2-additivated lubricant oil was tested in on real diesel engine: in fact, in the perspective of a practical application on-board the vehicle, one has to carefully address the issues of pollutant emissions possibly related to the new oil, and the emission abatement efficiency of the catalytic converters.

Irrespective of the investigated engine point, the emissions recorded by the SMPS showed an increase of ultra-fine particles associated to the use of the NP additivated oil, which is presumably mainly constituted SOF which form an aerosol, and are absorbed on soot particles or form individual nuclei. This consideration derives from the remarkable abatement efficiency of the DOC towards these particles, both in terms of number and mass concentration, which lowers their emissions down to the same levels encountered in the tests with the reference base oil, or even below. A similar increase of HC and CO emissions is also recorded in the gas phase at the engine outlet, which again suggests that the presence of nanoparticles in the lubricant might induces some little but not negligible modifications of the combustion regime. SO_2 showed a 4 ppm emission in the exhausts, which reasonably excludes any major poisoning effects of the after-treatment catalysts.

In order to check the long-term compatibility of the above mentioned DOC and DPF when exposed to the flue gases produced when the NP additivated oil was used, a 100 h test was performed. The engine gaseous emissions were stable throughout the whole test. The possibility of an anomalous ash production and progressive accumulation inside the diesel particulate filter was excluded: the retention in the filter of the soot incombustible fraction, originated from current fuel and lubricant additives, did not cause any progressive reduction of the available filtration area, which would have increased the bare filter pressure drop at the end of each repeated regeneration. It is worth mentioning that longer accumulation tests should be performed to comprehensively assess the ashing tendency of the NP-additivated oil.

As a result of the present work, the possible advantage arising from the nanoparticle embodiment in the lubricating oil, which is meant to provide friction and wear reduction, was demonstrated not to be offset by any possibly MoS_2-related reduced abatement efficiency or stability loss of the after-treatment catalysts.

References

[1] Rapoport L, Feldman Y, Homyonfer M, Cohen H, Sloan J, Hutchison JL, Tenne R. Inorganic fullerene-like material as additives to lubricants: structure–function relationship. Wear 1999;225-229:975-82.

[2] Rapoport L, Leshchinsky V, Lapsker I, Volovik Y, Nepomnyashchy O, Lvovsky M, Popovitz-Biro R, Feldman Y, Tenne R. Tribological properties of WS_2 nanoparticles under mixed lubrication, Wear 2003;255:785-93.

[3] Wang HD, Xu BS, Liu JJ, Zhuang DM. Characterization and anti-friction on the solid lubrication MoS_2 film prepared by chemical reaction technique. Sci. Tech. Adv. Mat. 2005;6:535-9.

[4] Grossiord C, Varlot K, Martin JM, Le Mogne Th, Esnouf C, Inoue K. MoS_2 single sheet lubrication by molybdenum dithiocarbamate. Tribol. Int. 1998;31:737-743.

[5] Bec S, Tonck A, Georges JM, Roper GW. Synergistic effects of MoDTC and ZDTP on frictional behaviour of tribofilms at the nanometer scale. Tribol. Lett. 2004;17:797-809.

[6] Morina A, Neville A, Priest M, Green JH. ZDDP and MoDTC interactions in boundary lubrication - The effect of temperature and ZDDP/MoDTC ratio. Tribol. Int. 2006; 39:1545-1557.

[7] Tenne R, Margulis L, Genut M, Hodes G. Polyhedral and cylindrical structures of tungsten disulphide. Nature 1992;360:444-6.

[8] Margulis L, Salitra G, Tenne R, Talianker M. Nested fullerene-like structures. Nature 1993;365:113-4.

[9] Hershfinkel M, Gheber LA, Volterra V, Hutchison JL, Margulis L, Tenne R. Nested Polyhedra of MX_2 (M=W, Mo; X=S, Se) Probed by High-Resolution Electron Microscopy and Scanning Tunneling Microscopy. J. Am. Chem. Soc. 1994;116:1914-7.

[10] Yacaman MJ, Lorez H, Santiago P, Galvan DH, Garzon IL, Reyes A. Studies of MoS_2 structures produced by electron irradiation. Appl. Phys. Lett. 1996;69:1065-7.

[11] Parilla PA, Dillon AC, Jones KM, Riker G, Schulz DL, Ginley DS, Heben MJ. The first true inorganic fullerenes? Nature 1999;397:114.

[12] Tian Y, He Y, Zhu YF. Hydrothermal synthesis of fine MoS_2 crystals from Na_2MoO_4 and KSCN. Chem. Lett. 2003;8:768-9.

[13] Cizaire L, Vacher B, Le Mogne T, Martin JM, Rapoport L, Margolin A, Tenne R. Mechanisms of ultra-low friction by hollow inorganic fullerene-like MoS_2 nanoparticles. Surf. Coat. Technol. 2002;160:282-7.

[14] Joly-Pottuz L, Martin JM, Dassenoy F, Belin M, Montagnac R, Reynard B. Pressure-induced exfoliation of inorganic fullerene-like WS_2 particles in a Hertzian contact. J. Appl. Phys., 2006;99:023524-8.

[15] Lahouij I, Dassenoy F, De Knoop L, Martin JM, Vacher B. In-situ TEM observation of the behavior of an individual fullerene-like MoS_2 nanoparticle in a dynamic contact. Tribo. Lett. 2011;42:133-40.

[16] Deorsola FA, Russo N, Blengini GA, Fino D. Synthesis, characterization and environmental assessment of nanosized MoS_2 particles for lubricants applications. Chem. Eng. J. 2012;195-196:1-6.

[17] Santillo G, Deorsola FA, Bensaid S, Russo N, Fino D. MoS_2 nanoparticle precipitation in turbulent micromixers. Chem. Eng. J. 2012;207-208: 322-8.

[18] Bensaid S, Deorsola FA, Marchisio DL, Russo N, Fino D. Flow field simulation and mixing efficiency assessment of the multi-inlet vortex mixer for molybdenum sulfide nanoparticle precipitation. Chem. Eng. J. 2013; doi: http://dx.doi.org/10.1016/j.cej.2013.09.065.

[19] Caroca JC, Millo F, Vezza D, Vlachos T, De Filippo A, Bensaid S, Russo N, Fino D. Detailed Investigation on Soot Particle Size Distribution during DPF Regeneration, using Standard and Bio-Diesel Fuels. Ind. Eng. Chem. Res. 2011;50:2650-8.

[20] Bensaid S. and Russo N. (2011). Low temperature DPF regeneration by delafossite catalysts, Catalysis Today, 176, 417-423.

[21] Kittelson DB. Engines and Nanoparticles: a review. J. Aerosol Sci. 29:5/6 (1998) 575-588.

[22] Abdul-Khalek I, Kittelson DB, Brear F. The influence of dilution conditions on diesel exhaust size distribution measurements. SAE 1999;1999-01-1142:103-11.

[23] Bensaid S, Marchisio DL, Fino D. Numerical simulation of soot filtration and combustion within diesel particulate filters. Chem. Eng Sci. 2010;65:357-63.

[24] Bensaid S, Marchisio DL, Fino D, Saracco G, Specchia V. Modeling of Diesel particulate filtration in wall-flow traps. Chem. Eng. J. 2009;154:211-8.

CHAPTER V Nano-sized additive synthesis for lubricants oils and compatibility tests with after-treatment catalysts (complementary tests)

Abstract

Molybdenum sulfide nanoparticles have been successfully obtained, for lubricant applications, by means of a wet chemical synthesis in an aqueous solution employing ammonium molybdate, citric acid and ammonium sulfide as the reactants.

The compatibility between the obtained MoS_2 nanopowders and some commercial EURO 5 compliant after-treatment catalysts for Diesel vehicle engines was assessed. Diesel oxidation, soot combustion and ammonia-SCR de-NO_x catalysts were considered for this analysis, to evaluate a potential reactivity to the MoS_2 additive, and therefore the possible effects on their catalytic activity. In general, the MoS_2 nano-additive brought in contact with the catalyst nanopowders has demonstrated to slightly decrease the catalytic performance of the commercial catalysts, especially for the Diesel oxidation and SCR ones. The chemical-physical analyses did not detect any chemical interaction between the catalysts and nanoadditives or any decrease in the specific surface areas of the catalysts.

Keywords: lubricants, diesel engine, molybdenum disulphide, nanoparticle, after-treatment catalysts

1. Introduction

Fluid lubricants are used in almost every field of human technological activity and their purpose is multi-fold: they reduce frictional resistance, protect the contacting surfaces of engines against wear, remove wear debris, reduce heat and contribute to cooling, improve fuel economy and reduce emissions.

Advanced nanomaterials have shown some promise because of their contribution to reducing friction and enhancing protection against wear [1-3]. When incorporated in full lubricant formulations in a stable way, and if their performance benefits can be sustained under those circumstances, they offer the possibility of some performance breakthroughs which have not witnessed since the development of the now ubiquitous anti-wear additives, Zinc Dialkyl Dithiophosphates (ZDDP's), about 70 years ago. These developments can contribute to a substantial energy saving, reduce equipment maintenance and lengthen the life of the machines. In the case of engine oil (crankcase) applications, these nanomaterials can help

increase the durability and performance of exhaust-treatments and reduce harmful emissions: in fact, exhaust catalysts tend to become poisoned by the sulphur and phosphorous that are present in conventional lubricant additives.

Transition metal dichalcogenides, with the generic formula MX_2 (M = W, Mo; X = S, Se), whose synthesis was first demonstrated at the Weizmann institute by Tenne and co-workers [4-6], seem to be very promising materials to be dispersed as nanoparticles in the oil matrix. They involve a reaction between MO_3 and H_2S, in reducing atmosphere at high temperatures, and the corresponding sulfide (WS_2 or MoS_2) is obtained. Many other synthetic routes have also been followed to obtain these kinds of nano-structured materials [7-16].

The specific lubrication mechanism ascribed to these metal sulfides, often called inorganic fullerenes due to their peculiar structure of spherical concentric layers, is currently debated; however, several studies clearly indicate that an exfoliation process of these layers, and the consequent liberation of nanosheets directly inside the surface contact area, is the prevalent lubricating mechanism for these systems [17,18]. It was also hypothesized that these nanoparticles behave as nano-ball bearings, due to their spherical shape, ultra-hardness and nano-size, at least temporarily until they gradually deform and start to exfoliate giving rise to the observed low friction coefficients: investigations involving direct visualization of the nanoparticle behaviour in the contact area, over a broad pressure range, were attempted by combining Transmission Electron Microscope (TEM) and Atomic Force Microscopy (AFM) [19].

The present study focuses on MoS_2 nanoparticles which have to be incorporated in engine lubricant oils. A wet synthesis technique has been devised within our group [20], which is based on the preparation of an aqueous solution of citric acid and ammonium molybdate to form a complex of molybdenum(IV) with citric acid, to which a suitable amount of ammonium sulfide was added to obtain MoS_2. This technique resorts to a simple and scalable process, and involves low-cost reagents, instead of other more complex reaction methods. An example of the MoS_2 particles obtained with this technique is depicted in Figure 1 Chapter VI. Moreover, this synthesis route is extremely versatile since it can be adapted for continuous MoS_2 particle production, in specific devices that allow to control the particle diameter and obtain reproducible results in terms of particle size distribution **[**21,22**].**

As previously mentioned, a progressive poisoning of after-treatment catalysts occurs due to the presence of species that were originally present in the lubricant oil as additives, and which are then released into the flue gases after in-cylinder combustion. One major requirement for the application of these nanoparticles as lubricant oil additives, in substitution to the currently

adopted ones, is their complete compatibility with the catalytic substrates present in the after-treatment line, whose lifetime operation should not be affected to any great extent. This analysis is crucial for the introduction of such nano-sized additives for lubricant oils on the market, and in this work was applied to EURO 5 compliant catalysts for DOC, DPF and SCR systems.

2. Experimental

2.1 MoS_2 nanoparticle compatibility tests with after-treatment catalysts in powder form

One important requirement for the application of these nanoparticles as lubricant oil additives is their compatibility with the catalytic substrates present in the after-treatment line: therefore, an assessment was carried out about a possible physical and chemical interaction between the MoS_2 nanopowders and some commercial catalysts, representative of EURO 5-compliant catalytic converters present in the after-treatment line of light-duty diesel engine vehicles. In particular, the analysis regarded a series of commercial catalyst samples:

i) Diesel oxidation catalysts, whose function is to oxidize species like CO and HC, which are frequently present in the flue gases of diesel engines (Figure 1-a);

ii) Soot oxidation catalysts for Diesel particulate traps, which have the aim of reducing the soot combustion temperature during filter regeneration, and therefore leading to a saving in the amount of fuel required to reach the soot ignition temperature (Figure 1-b);

iii) SCR de-NO_x systems, which convert the NO_x present in the exhaust gases by means of a reducing agent, namely ammonia (Figure 1-c);

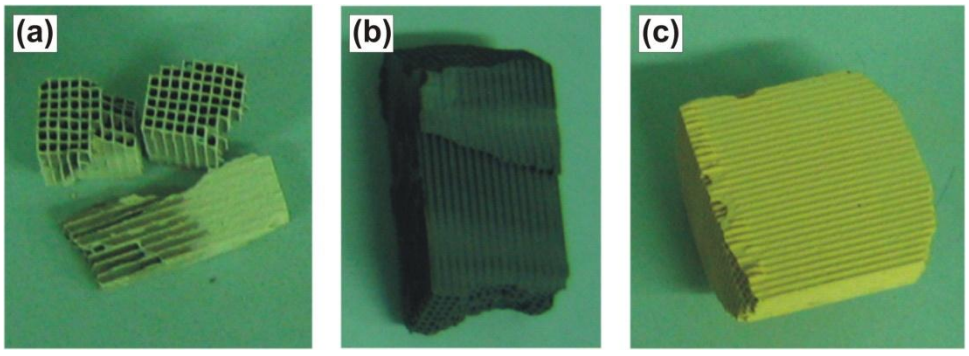

Figure 1. Commercial catalysts used for compatibility tests: diesel oxidation catalyst (a), soot oxidation catalyst (b), ammonia-SCR de-NO_x catalyst (c).

The testing protocol focused on the following aspects:

i) Investigation of the effect of the nanoparticles on the catalyst activity: pollutant conversion was evaluated with and without nanoparticles;

ii) Investigation of the effect of the presence of the nanoparticles via BET and XRD analysis: "loose" rather than "tight" contact conditions were utilized in order to reproduce the degree of contact between the catalysts and the particles that deposit on the surface of the catalyst through the action of the gas flow;

iii) Selection of an ageing procedure which would be representative of a lifetime exposition to MoS_2 nanoparticles: mixtures of the nanoparticles with various after-treatment catalysts were treated in an oven at two different temperatures (600°C and 800°C for 6 h) to promote any possible reactions.

The activity of the three classes of catalysts was analyzed by means of different techniques. The activity of the Diesel oxidation catalysts towards carbon monoxide (CO) and unburned hydrocarbons (HC) was assessed by means of temperature programmed oxidation (TPO) which was carried out in a fixed-bed micro reactor (quartz tube, i.d. 5 mm, placed in an electric oven): the composition of the exhaust flue gases from the diesel engine was simulated (2500 ppm of CO, 800 ppm of C_3H_8, 500 ppm of NO, 10% of O_2 and N_2 as balance), and was fed at a constant rate of 100 Nml·min^{-1} (corresponding to a gas hourly space velocity of 25,000 h^{-1}) to the fixed bed which was constituted by 50 mg of catalyst obtained from ball milling the original monolith (average grain size of less than 1 μm), plus ≈250 mg of inert silica (to act against bed packing, thus minimizing preferential paths and promoting thermal dilution inside the bed itself). The reaction temperature was controlled through a PID-regulated oven and was varied from 200 to 700 °C at a 5 °C·min^{-1} rate. The analysis of the outlet gas was performed via NDIR analyzers (ABB).

The activity of the oxidation catalysts towards soot combustion was analyzed by means of temperature programmed combustion (TPC) which was carried out in the same fixed-bed micro reactor, according to the standard operating procedure described in [23]: a N_2 flow containing 10% O_2 and 500 ppm of NO was fed, at the constant rate of 100 Nml·min^{-1}, to the fixed bed which was constituted by 50 mg of a mixture of carbon and powdered catalyst (1:9 mass basis), diluted with ≈250 mg of inert silica. All the experiments were performed using an amorphous carbon by Cabot Ltd (average particle diameter: 45 nm; BET specific surface area: 200 m^2/g; ashes content after calcination at 800 °C: 0.34%; adsorbed water moisture at room temperature: 12.2%wt; no adsorbed hydrocarbons or sulphates) instead of real diesel soot. This condition can be considered conservative because it is more difficult to burn amorphous

carbon than real diesel soot. The *loose contact* catalyst-carbon mixture was prepared by gently shaking it in a polyethylene vessel for 1 h. As mentioned above, a loose-contact was chosen as it is representative of the real contact conditions that occurs in a catalytic diesel particulate removal trap [24]. As in the former case, the reaction temperature was controlled through a PID-regulated oven and was varied from 200 to 700 °C at a 5 °C·min^{-1} rate. The analysis of the outlet gas was again performed via NDIR analyzers (ABB).

Finally, the activity of the de-NO_x based on ammonia-SCR was measured through Temperature Programmed Reaction (TPRe), which was carried out in the same piece of previously described equipment: a gas mixture containing 800 ppmv NO, 800 ppmv NH_3, 3% O_2, balanced by He, was fed at a constant rate of 300 Nml·min^{-1}; the reactor was loaded with 360 mg of catalyst pelletized from the powder obtained through the ball milling of the monolith, thus a GHSV ≈ 50,000 h^{-1} was reached. The reaction temperature was controlled through a PID-regulated oven, and was varied from 100 to 600 °C with an isotherm step of 25 °C every hour for the lower temperatures and half an hour for the higher temperatures. The analysis of the outlet gas was performed via a Bruker Tensor 27 FT-IR spectrometer.

The above described procedures were carried out on both powders from the original catalysts, and on powders "contaminated" by MoS_2 nanoparticles exposure. In particular, in order to assess the possible negative effect given by the progressive accumulation of MoS_2 nanoparticles on the catalytic surfaces of the converters present in the after-treatment line, MoS_2 nanoparticles were deposited on the active surface of the monolith, i.e. where the catalyst coating resides, in a 4:1 mass ratio between the monolith and MoS_2 weights. This amount is very high, and overestimates by far the real amount that is released by the MoS_2 containing oil, but is required to appreciate any interference of the nanoparticles with the catalytic activity, and constitutes a conservative approach to the problem. After MoS_2 deposition, the whole sample was aged at two different temperatures (600°C and 800°C) for 6 hours, in order to simulate a long exposure of the catalyst to the nanoparticles. After the ageing, the excess MoS_2 nanoparticles were removed, and the catalyst was tested in the same way as for the fresh one. An aged catalyst, but without MoS_2 contamination, was also tested in order to decouple the effects of thermal ageing from those of physical (fouling) or chemical (poisoning of the catalytic active sites) interaction with MoS_2. Therefore, catalytic activity data were collected from three kinds of samples: fresh catalysts, aged catalysts, aged and MoS_2-contaminated catalysts. The following protocol was adopted for all catalytic activity tests: each catalytic activity experiment, including the preparation of the samples, was repeated three times; then the obtained results were averaged. The level of accuracy of each

test was satisfactory, since the maximum discrepancy between the individual run and the average was always lower than 5%.

BET measurements were performed on the same set of catalyst samples to investigate the loss of specific surface area caused by the thermal treatment, and by the addition of MoS_2 (Micromeritics ASAP 2010 analyzer). X-ray diffraction (PW1710 Phillips diffractometer) was also used, in order to assess the purity and crystalline structure of the catalysts before and after the addition of MoS_2: the mixture of MoS_2 and catalyst power was aged, in the above mentioned proportion, and then analyzed. The chemical interaction between the commercial catalysts and the MoS_2 nanoparticles was assessed through XRD analysis, in order to detect the possible appearance of new phases. It should be mentioned that XRD analysis has a resolution which is not able to detect lower mass concentrations than 4%: this required using a high nanoparticle mass ratio; similarly, the formation of phases with a mass weight of less that 4%, but potentially involving the active metals of the washcoat, could not be detected with this technique. Important information that could be extrapolated from this technique concerns particle stability, both in sulfide and oxide form.

2.2 MoS_2-additivated lubricant oil: engine emissions and compatibility with the after-treatment full-scale system

The experimental campaign at full-scale conditions was carried out on a real diesel engine bench, and was presented in the Chapter VI.

3. Results and discussion

3.1 MoS_2 nanoparticle compatibility tests with after-treatment catalysts in powder form

The results of the catalytic activity tests on diesel oxidation catalysts, with and without nanoparticles, and carried out with fresh and aged samples (at 600°C and 800°C), are depicted in Figure 2-a for CO oxidation and Figure 2-b for HC oxidation, both with an ageing temperature of 600°C; the same set of data was produced for catalysts aged at 800°C, and which are shown in Figures 3-a and 3-b, respectively. In Figure 3 it is possible to observe that the fresh catalyst curve (without nanoparticles) shifts to the right when the sample is aged at 600°C (blue and red curves); moreover, the green curve, which represents the sample with MoS_2 nanoparticles, denotes a somewhat masking effect, which is less pronounced for HC oxidation. The ageing effect is much clearer in Figure 3, since 800°C is a very severe

condition, while the effect of the nanoparticles vanishes compared to that due to thermal degradation.

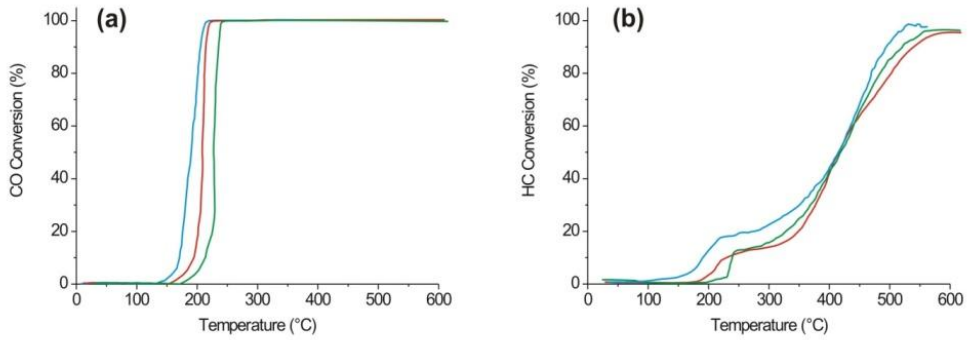

Figure 2. Activity tests on the Diesel oxidation catalyst: CO (a) and HC (b). Blue curve: fresh catalyst; red curve: aged catalyst at 600°C; green curve: aged catalyst at 600°C, in the presence of MoS_2.

The results of the soot oxidation catalytic activity tests (expressed as $\%CO_2$ in the outlet gas), with and without nanoparticles, and carried out with fresh and aged samples, are shown in Figures 4-a for 600°C and 4-b for 800°C. The soot oxidation catalytic activity tests revealed that neither the on-set temperature (the "starting" reaction temperature, corresponding to roughly 5% conversion, representing the intrinsic capability of the catalyst to ignite soot), nor the peak temperature (the maximum reaction rate temperature) are affected to any extent by the presence of the nanoparticles and that their decay is only due to ageing. This consideration is valid for both a 600°C and an 800°C ageing temperature. Only a slight selectivity loss was detected, as a result of the difference between the integral of the CO_2 conversion curves, whose values are proportional to the soot conversion towards CO_2, and 1 s complement to the conversion towards CO.

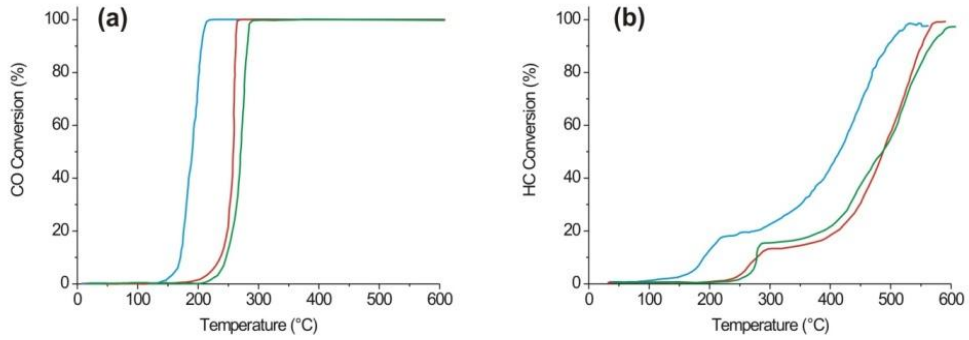

Figure 3. Activity tests on the Diesel oxidation catalyst: CO (a) and HC (b). Blue curve: fresh catalyst; red curve: aged catalyst at 800°C; green curve: aged catalyst at 800°C, in the presence of MoS_2.

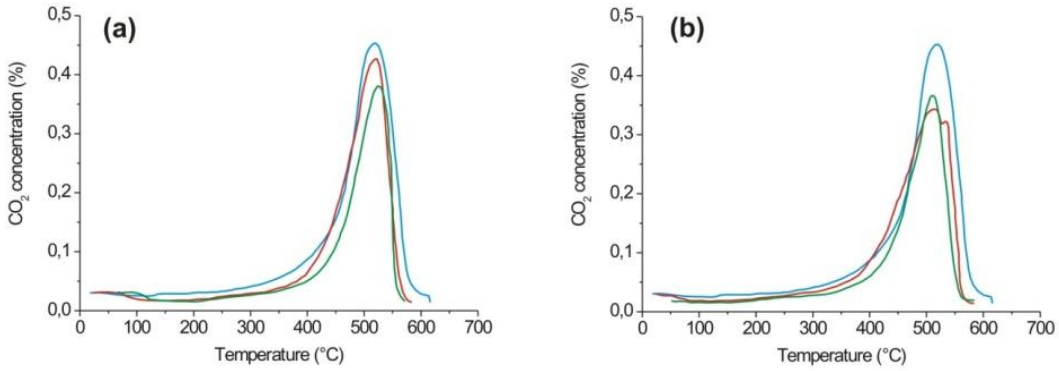

Figure 4. Activity tests on the soot oxidation catalyst: catalyst ageing temperatures of 600°C (a) and 800°C (b). Blue curve: fresh catalyst; red curve: aged catalyst; green curve: aged catalyst in the presence of MoS_2.

The results of the NO conversion via commercial SCR catalysts, with and without nanoparticles, and carried out with fresh and aged samples (at 600°C and 800°C), are shown in Figures 5-a for 600°C and 5-b for 800°C. It is possible to observe a slight decrease in the activity for the samples treated at 600°C compared with the fresh catalyst, while the nanoparticles seem to have an effect at working temperatures above 400°C (Figure 5-a). The same behavior is observed for 800°C, but it is more pronounced. As for diesel oxidation catalysts, high temperatures are usually a condition at which mass transfer is the reaction rate limiting factor, rather than catalysis. In these conditions, masking plays a relevant role which only becomes evident at high temperatures, as observed in Figures 2-a and 5-a (see the difference between the aged catalyst curve and the aged + MoS_2 contaminated one). Conversely, the on-set temperature does not seem to be influenced by the nanoparticles, which would seem to exclude a strong chemical interaction between the nanoparticles and the catalysts.

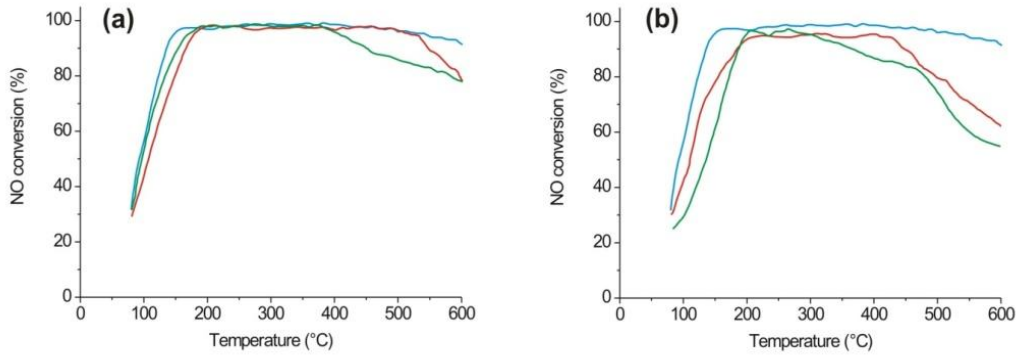

Figure 5. Activity tests on the ammonia-SCR de-NO_x catalyst: catalyst ageing temperatures of 600°C (a) and 800°C (b). Blue curve: fresh catalyst; red curve: aged catalyst; green curve: aged catalyst in the presence of MoS_2.

All the catalyst specific surface areas were assessed in fresh and aged conditions, the latter with the addition of MoS_2 nanoparticles, as mentioned in the section devoted to the experimental procedure. The purpose of this test was to evaluate whether the nanoparticles affected the specific surface area, i.e. if the ageing process caused a collapse in the BET area that could be made worse by the presence of nanoparticles. The results of the BET surface area tests are presented for the Diesel oxidation catalysts, soot combustion catalysts, and SCR de-NO_x catalysts in Table 1. All the samples showed a specific surface area loss that can be imputed to thermal ageing; in particular, the most severe effect was recorded for the SCR de-NO_x catalysts. Nanoparticles appear to artificially increase the BET surface in the case of the Diesel oxidation catalyst, while it is in fact only an effect of their high specific surface, and not of the catalyst surface one (whose BET decreased when aged in the absence of nanoparticles). As far as the BET of both the diesel oxidation and soot oxidation catalysts is concerned, the nanoparticle effect does not seem to be so relevant; whereas, for the SCR de-NO_x catalysts, there might be a synergic effect on the specific surface area loss caused by the presence of nanoparticles, which is also translated in an moderate activity deterioration. Focusing on the nanoparticles, they appear to be poorly stable at a high temperature of 800°C, as compared to the 600°C case. This behavior was confirmed in the XRD analysis.

The XRD spectra, referring to the Diesel oxidation catalysts (**Figure 6**), soot oxidation catalysts (**Figure 7**) and SCR de-NO_x catalysts (**Figure 8**) are presented here. XRD was performed on the fresh commercial catalyst (which includes the structured monolith, the washcoat and the active catalyst) and on the aged one with MoS_2 nanoparticles, at ageings of both 600°C and 800°C. The three XRD in the Figures refer to (from top to bottom): the fresh catalyst, the aged catalyst at 600°C with nanoparticles, and the aged catalyst at 800°C with nanoparticles. A general trend could be extrapolated from all the XRD tests: first, no new phases seem to appear after ageing of the commercial catalysts. The characteristic peaks are preserved in all the samples, and no new ones are detected, which could indicate a chemical interaction between the catalyst and the nanoparticles (given the limit of 4% mass weight of the sample); moreover, MoS_2 turns into its oxide after ageing. However, since MoO_3 has a low thermal stability, it is difficult to detect at 800°C.

All the performed tests had the aim of investigating the possible interaction between commercial catalysts present in the after-treatment line of a diesel engine vehicle and MoS_2 based nanoparticles. Given the high mass amount of the nanoparticles that were used in this analysis in order to be conservative of the whole catalyst lifetime, it can be concluded that a

catalytic activity loss was detected, which is unlikely to be connected to the chemical composition of the nanoparticles, but rather to a masking/fouling effect due to their presence in the catalyst-nanoparticle mixture samples, which have a 4:1 mass ratio.

Table 1 –Specific surface areas (m^2/g) for the Diesel oxidation catalyst (DOC), soot combustion catalyst (DPF), and the ammonia-SCR de-NO_x catalyst (SCR).

	DOC	**DPF**	**SCR**
Fresh	56	12	105
Aged at 600°	48	8	88
Aged at 600°C with MoS	51	7	67
Aged at 800°	40	4	62
Aged at 800°C with MoS	39	4	49

The most critical system appears to be DOC, with a non-negligible activity loss; the SCR de-NO_x catalysts also show a moderate activity loss at high temperatures (> 400°C), compared to the aged catalysts in the absence of MoS_2, which could be connected to the specific surface area reduction measured in the BET performed with MoS_2 nanoparticles. However, these effects do not seem so relevant, and should not hinder the exploitation of MoS_2 nanoparticles as lubricant oil additives.

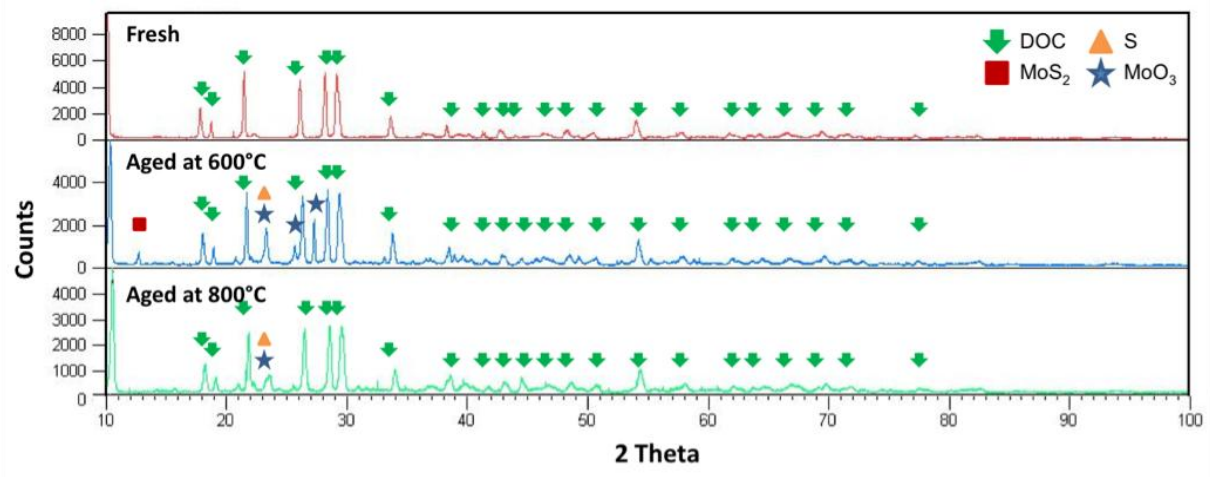

Figure 6 - XRD spectra of the Diesel oxidation catalyst: fresh catalyst (top); aged catalyst at 600°C, in the presence of MoS_2 (centre); aged catalyst at 800°C, in the presence of MoS_2 (bottom).

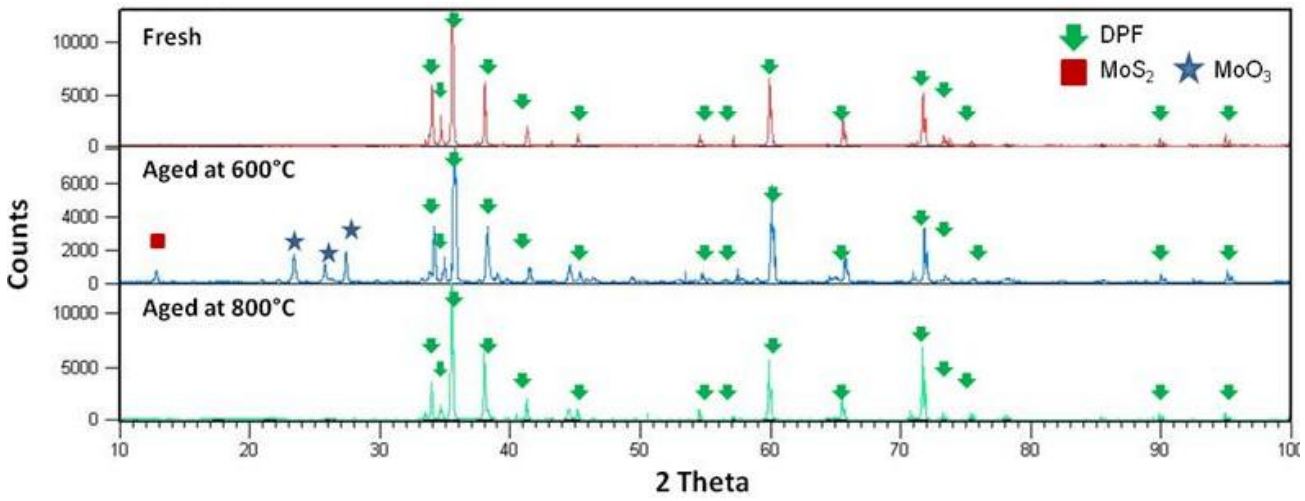

Figure 7 - XRD spectra of the soot oxidation catalyst: fresh catalyst (top); aged catalyst at 600°C, in the presence of MoS_2 (centre); aged catalyst at 800°C, in the presence of MoS_2 (bottom).

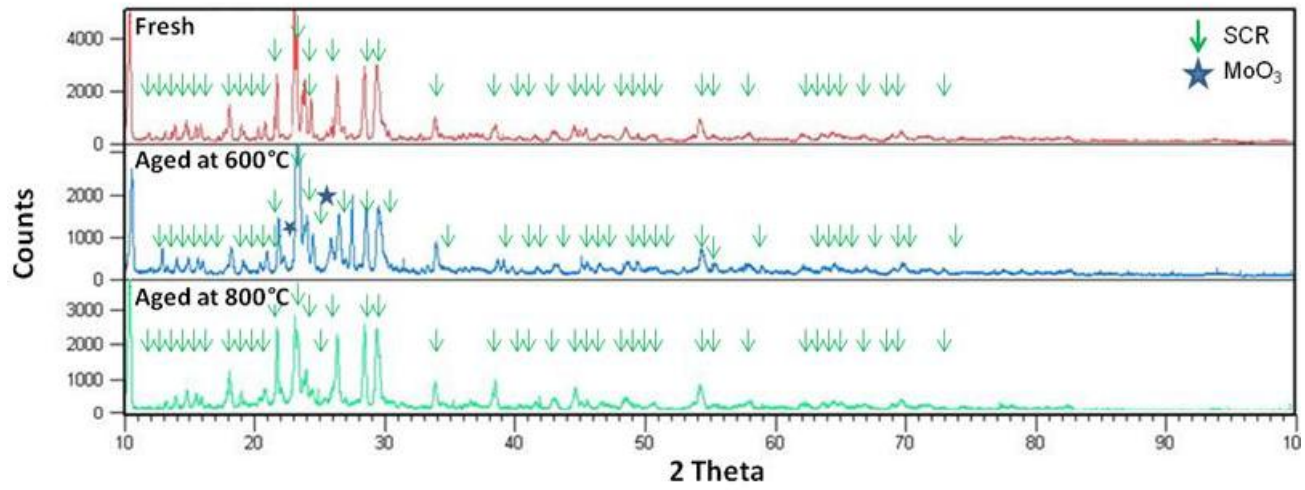

Figure 8 - XRD spectra of the ammonia-SCR de-NO_x catalyst: fresh catalyst (top); aged catalyst at 600°C, in the presence of MoS_2 (centre); aged catalyst at 800°C, in the presence of MoS_2 (bottom).

3.2 MoS_2-additivated lubricant oil: engine emissions and compatibility with the after-treatment full-scale system

The experimental results was presented in detail in in the Chapter VI.

4. Conclusions

A novel wet chemical synthesis method has been developed for the production of molybdenum(IV) sulfide nanopowders, which are used as lubricant additives (0.5wt%) in this work.

The interactions between the MoS_2 nanopowders obtained in this way and some commercial catalysts currently employed in the after-treatment line of a light-duty Diesel vehicle engine were investigated. Diesel oxidation, soot oxidation and Selective Catalytic Reduction (SCR) catalysts were considered. The Diesel oxidation catalyst showed a slight masking effect for the CO and HC oxidation in the MoS_2-contamined catalyst compared to the pure aged one. In the case of soot oxidation catalysts, the tests did not reveal any decay in the catalytic activity apart from that due to the thermal ageing of the pure catalyst. As far as the SCR catalyst is concerned, the presence of MoS_2 nanoparticles affected the catalytic activity for higher temperatures than 400°C, but the on-set temperature remained unchanged. The specific surface areas of the tested catalysts showed a general decrease, due to thermal ageing, and only in the case of the SCR catalyst was a further decay proved in the presence of the nano-additives, which corresponds to the catalytic activity reduction. As a general conclusion, it can be stated that the compatibility between the MoS_2 nanoparticles and the commercial catalysts has been demonstrated to be remarkable and only a masking effect has been shown. Moreover, it is worth noticing that the mass amount of the MoS_2 nanoparticles employed in the powder-scale tests in the mixture with the commercial catalysts was significantly higher than the one that usually occurs in operative conditions.

For this reason, the MoS_2-additivated lubricant oil was tested in on real diesel engine: in fact, in the perspective of a practical application on-board the vehicle, one has to carefully address the issues of pollutant emissions possibly related to the new oil, and the emission abatement efficiency of the catalytic converters. Irrespective of the investigated engine point, the emissions recorded by the SMPS showed an increase of ultra-fine particles associated to the use of the NP additivated oil, which is presumably mainly constituted SOF which form an aerosol, and are absorbed on soot particles or form individual nuclei. This consideration derives from the remarkable abatement efficiency of the DOC towards these particles, both in terms of number and mass concentration, which lowers their emissions down to the same levels encountered in the tests with the reference base oil, or even below. A similar increase of HC and CO emissions is also recorded in the gas phase at the engine outlet, which again suggests that the presence of nanoparticles in the lubricant might induces some little but not negligible modifications of the combustion regime. SO_2 showed a 4 ppm emission in the

exhausts, which reasonably excludes any major poisoning effects of the after-treatment catalysts.

In order to check the long-term compatibility of the above mentioned DOC and DPF when exposed to the flue gases produced when the NP additivated oil was used, a 100 h test was performed. The engine gaseous emissions were stable throughout the whole test. The possibility of an anomalous ash production and progressive accumulation inside the diesel particulate filter was excluded: the retention in the filter of the soot incombustible fraction, originated from current fuel and lubricant additives, did not cause any progressive reduction of the available filtration area, which would have increased the bare filter pressure drop at the end of each repeated regeneration. As a result, any possible advantage arising from the nanoparticle embodiment in the lubricating oil, which is meant to provide friction and wear reduction, was demonstrated not to be offset by any possibly MoS_2-related reduced abatement efficiency or stability loss of the after-treatment catalysts.

References

[1] Rapoport, L., Feldman, Y., Homyonfer, M., Cohen, H., Sloan, J., Hutchison, J.L. and Tenne, R. (1999) Inorganic fullerene-like material as additives to lubricants: structure–function relationship, Wear, 225-229 (2), 975-982.

[2] Rapoport, L., Leshchinsky, V. Lapsker, I., Volovik, Y., Nepomnyashchy, O., Lvovsky, M., Popovitz-Biro, R., Feldman, Y. and Tenne, R. (2003) Tribological properties of WS_2 nanoparticles under mixed lubrication, Wear, 255(7-12), 785-793.

[3] Wang, H.D., Xu, B.S., Liu, J.J. and Zhuang, D.M. (2005) Characterization and anti-friction on the solid lubrication MoS_2 film prepared by chemical reaction technique Sci. Tech. Adv. Mat., Volume 6(5), 535-539.

[4] Tenne, R., Margulis, L., Genut, M. and Hodes, G. (1992) Polyhedral and cylindrical structures of tungsten disulphide", *Nature*, 360, 444-446.

[5] Margulis, L., Salitra, G., Tenne, R. and Talianker, M. (1993) Nested fullerene-like structures, Nature, 365, 113-114.

[6] Hershfinkel, M., Gheber, L.A., Volterra, V., Hutchison, J.L., Margulis, L. and Tenne, R. (1994) Nested Polyhedra of MX2 (M=W, Mo; X=S, Se) Probed by High-Resolution

Electron Microscopy and Scanning Tunneling Microscopy, J. Am. Chem. Soc., 116, 1914-1917.

[7] Yacaman, M.J., Lorez, H., Santiago, P., Galvan, D.H., Garzon, I.L. and Reyes, A. (1996) Studies of MoS_2 structures produced by electron irradiation, Appl. Phys. Lett., 69(8), 1065-1067.

[8] Parilla, P.A. , Dillon, A.C., Jones, K.M., Riker, G., Schulz, D.L., Ginley, D.S. and Heben, M.J. (1999) The first true inorganic fullerenes?, Nature, 397, 114.

[9] Tian, Y. , He, Y. and Zhu, Y.F. (2003) Hydrothermal synthesis of fine MoS_2 crystals from Na_2MoO_4 and KSCN, Chem. Lett., 8, 768-769.

[10] Tian Y., Zhao J., Fu W., Liu Y., Zhu Y., Wang Z. (2005) A facile route to synthesis of MoS_2 nanorods, Mater. Lett., 59, 3452-3455.

[11] Duphil, D., Bastide, S. and Lévy-Clément, C. (2002) Chemical synthesis of molybdenum disulfide nanoparticles in an organic solution, J. Mater. Chem., 12(8), 2430-2432.

[12] Uzcanga, I., Bezverkhyy, I., Afanasiev, P., Scott, C. and Vrinat, (2005) Sonochemical Preparation of MoS_2 in Aqueous Solution: Replication of the Cavitation Bubbles in an Inorganic Material Morphology, M. Chem. Mater. 17 3575-3577.

[13] Chang, L.X., Yang, H.B., Li, J.X., Fu, W.Y., Du, Y.H., Du, K., Yu, Q.Y., Xu, J. and Li, M.H. (2006) Simple synthesis and characteristics of Mo/MoS_2 inorganic fullerene-like and actinomorphic nanospheres with core–shell structure, Nanotechnology, 17, 3827-3831.

[14] Li, X.L., Ge, J.P. and Li, Y.D. (2004) Atmospheric Pressure Chemical Vapor Deposition: An Alternative Route to Large-Scale MoS_2 and WS_2 Inorganic Fullerene-like Nanostructures, Chem. Eur. J., 10(23), 6163-6171.

[15] Etzkorn, J., Therese, A.H., Rocker, F., Zink, N., Kolb, U. and Tremel, W. (2005) Metal–Organic Chemical Vapor Depostion Synthesis of Hollow Inorganic-Fullerene-Type MoS_2 and $MoSe_2$ Nanoparticles, Adv. Mater., 17(19), 2372-2375.

[16] Marchand K.E., Tarret M., Lechaire J.P., Normand L., Kasztelan S., Cseri T. (2003) Investigation of AOT-based microemulsion for the controlled synthesis of MoSx nanoparticles: an electron microscopy study, Colloid Surface A, 214, 239-248.

[17] Cizaire, L., Vacher, B., Le Mogne, T., Martin, J.M., Rapoport, L., Margolin, A., Tenne, R. (2002) Mechanisms of ultra-low friction by hollow inorganic fullerene-like MoS2 nanoparticles, Surf. Coat. Technol. 160, 282-287.

[18] Joly-Pottuz, L., Martin, J.M., Dassenoy, F., Belin, M., Montagnac, R., Reynard, B. (2006) Pressure-induced exfoliation of inorganic fullerene-like WS2 particles in a Hertzian contact. J. Appl. Phys., 99, 023524-023528.

[19] Lahouij, I., Dassenoy, F., De Knoop, L., Martin, J.M., Vacher, B. (2011) In-situ TEM observation of the behavior of an individual fullerene-like MoS2 nanoparticle in a dynamic contact, Tribo. Lett., 42(2), 133-140.

[20] Gavi, E., Marchisio, D.L. and Barresi, A.A. (2008) On the importance of mixing for the production of nano-particles, J. Dispersion Sci. Technol., 29, 548-554.

[21] Zaccone, A., Gaebler, A., Maass, S., Marchisio, D.L. and Kraume, M. (2007) Drop breakage in liquid–liquid stirred dispersions: Modelling of single drop breakage, Chem. Eng. Sci., 62, 6297-6307.

[22] Aridi, T.N. and Al-Daous, M.A. (2009) HDS of 4,6-dimethyldibenzothiophene over MoS_2 catalysts supported on macroporous carbon coated with aluminosilicate nanoparticles, Appl. Catal. A, 359, 180-187.

[23] Russo, N., Fino, D., Saracco, G. and Specchia, V. (2005) Studies on the redox properties of chromite perovskite catalysts for soot combustion, J. Catal., 229 (2005) 459-469.

[24] Van Setten, B.A.A.L., Makkee, M. and Moulijn, J.A. (2001) Science and technology of catalytic diesel particulate filters, Catal. Rev. – Sci. Eng., 43, 489-564.

[25] Samotus, A., Kanas, A. Dudek, M., Grybos, R. and Hodorowicz, E. (1991) 1:1 Molybdenum(VI) citric acid complexes, Trans. Met. Chem., 16, 495-499.

[26] G.C. Stevens and Edmonds, T. (1977) Catalytic activity of the basal and edge planes of molybdenum disulphide, J. Less-Common Metals, 54, 321-330.

[27] Zinggs, D.S., Makovsky, L.E., Tischer, R.E., Brown, F.R., and Hercules, D.M. (1980) A surface spectroscopic study of molybdenum-alumina catalysts using x-ray photoelectron, ion-scattering, and Raman spectroscopies, J. Phys. Chem., 84(22), 2898-2906.

CHAPTER VI Multifunctional catalyst based on BaO/Pt/CeO_2 for NO_2-assisted soot abatement and NO_x storage.

ABSTRACT

In the present work the CeO_2/BaO/Pt system was selected in order to perform an NO_2-assisted soot oxidation. The aim of such catalytic system is to couple the catalytic functionality for soot abatement during DPF regeneration, namely CeO_2, and an embedded Lean NO_x Trap (LNT) functionality given by BaO, for NO_x storage, whose oxidation over Pt to form adsorbed nitrates is facilitated by the presence of CeO_2 itself.

The impact of process parameters, such as the catalyst preparation and the reaction conditions, was analyzed. The activity towards soot oxidation revealed that a physical mixture of CeO_2 and BaO allowed to obtain more performing catalysts than the co-synthesis route, the former reaching a peak temperature of soot oxidation equal to 475 °C, being 25 °C lower than the latter. The Pt addition to the two catalysts reduced their peak temperatures by around 30 °C in both cases.

It is worth noticing that the onset temperature ($T_{5\%}$) was considerably improved in presence of Pt only in the case of the catalyst prepared by co-synthesis (decreasing from 390 to 360 °C), still remaining much higher than the temperature level reached by the ones obtained by physical mixture (280 °C).

As a result, in terms of soot conversion, CeO_2/Pt/BaO catalyst prepared by physical mixture can be considered the catalyst with the best behavior.

Keywords: soot oxidation, NO_x storage, LNT, diesel particulate filter, Ceria, barium oxide

1. Introduction

The health effects caused by particulate matter (PM) and nitrogen oxides (NO_x) from diesel engine exhausts are well known [1], and both are among the most dangerous pollutants for the environment and for human health. In order to satisfy the upcoming regulations, it is necessary to develop more efficient technologies improving the abatement of the pollutants emitted in the flue gases in order to reduce the impact associated to diesel engines equipped vehicles.

Several approaches have been conceived and realized in the two last decades, and the current configuration envisages a diesel oxidation catalyst (DOC) for the oxidation of unburned hydrocarbons (HCs) followed by a diesel particulate filter (DPF) for trapping and oxidizing the soot. Particulate matter adheres to the filter walls and must be periodically removed by increasing the temperature through the addition of small quantities of fuel in combination with the presence of ceria-based catalysts [2,3].

Concerning NO_x, the strategy for the reduction of their concentration passes through the competition between selective catalytic reduction (SCR) and nitrogen storage reduction (NSR), also known as lean NO_x trap (LNT). SCR involves the reduction of NO_x by means of injected NH_3 with an excess of oxygen over several kind of mixed oxide catalysts, whereas in LNT the NO_x are absorbed onto suitable catalysts (mainly alkaline or alkaline/earth metal oxides) during long lean phases and then reduced by H_2, CO and unburned HC during short rich periods [4].

Particularly interesting is the possibility of simultaneously removing NO_x and soot in a single device, at first proposed by Toyota as diesel particulate NO_x reduction (DPNR) [5]. Basing on the approach employed in gasoline engines for the decrease of NO_x through the selective HC reduction method (HC-SCR), NO_x are absorbed on a NSR catalyst coating the DPF walls and subsequently they are reduced to N_2 by soot, which is in turn oxidized to CO_2 by the oxygen

coming from NO_x. The first catalysts developed for DPNR combined typical oxidation catalyst, such as Pt/Al_2O_3, with LNT catalysts, such as K or Ba oxide. Several other catalysts have been developed during the years, such as platinum [6], perovskite-type oxides [7,8] and spinel phases [9,10].

In this work, a multifunctional catalyst, constituted by CeO_2/BaO/Pt is investigated proposed and optimized in terms of the preparation technique, for the exploitation of the oxidizing potential of NO_2 to decrease the temperature of the soot combustion.

The CeO_2 catalyst was selected for this investigation, since its mechanism for the soot combustion is in tight relationship with the soot–catalyst contact nature: the Ce^{4+}/Ce^{3+} redox cycle confers the ability to adsorb gaseous O_2, thus forming active oxygen at the catalyst surface (O_{ads}), which can be transferred to the soot–catalyst interface by superficial diffusion [1,11]. This mechanism coexists with a temporary storage of the adsorbed oxygen as bulk lattice oxygen, which is then delivered as active O_{ads} at the catalyst surface. As a result, the overall activity of the catalyst towards soot oxidation is directly correlated to both the availability of active O_{ads} at the catalyst surface and, especially, the number of soot–catalyst contact points [12].

The BaO/Pt were selected for their important multifunctional role, since a small amount Pt enhances the storage of both NO and NO_2 in the presence of O_2, and it plays a fundamental role in the catalysis of NO oxidation, producing NO_2, which is readily stored on BaO [13,14,**15**]. Recently studies have shown that the NO_x storage capacity could be increased due to the enhancement of NO oxidation conversion and due to the ability of Ce to take part as NO_x storage material [16].

In the present work a screening of catalysts for soot combustion and NO_x abatement was carried out, and CeO_2/BaO/Pt was chosen to optimize the catalytic system in terms of metal loading on the diesel particulate filter. The present study follows on to consider the impact of

process parameters (catalyst preparation and conditions of the synthesis reaction), in conjunction with catalyst composition (weight loadings of BaO and Pt as well as the total weight of the catalyst). Finally, the optimization of the process parameters simultaneously with the optimized catalyst composition allowed to enhance the reactivity and selectivity for a considerable reduction of soot and NO_x emissions.

2. Experimental

2.1 Synthesis

The solution combustion synthesis (SCS) procedure was used for the preparation of the catalysts. This method is widely known and employed to obtain several highly porous pure and mixed metal oxides in a fast and reproducible way. The SCS involves different phenomena and reactions that allow the process to be self-sustaining from an energetic viewpoint [17]. A homogeneous aqueous solution of metal nitrates and urea or glycine is placed into an oven at a constant temperature of between 400 °C and 800 °C; it quickly begins to boil and froth until ignition takes place. The exothermic reaction, due to glycine combustion, provides the heat necessary for the endothermic transformation of nitrates into the desired oxide. The whole process is over in a few minutes and the result is an inorganic foam that can be easily crumbled, with a good specific volume and surface area.

For the synthesis of CeO_2 powders by means of SCS, glycine was added to a 0.08 M $Ce(NO_3)_3 \cdot 6H_2O$ aqueous solution in a 4.5-fold molar ratio with respect to the stoichiometric conditions [17], and a temperature of 650 °C was employed, which ensures the formation of the desired foamy and highly porous morphology.

For the synthesis of pure BaO powders through SCS, glycine was added to a 0.08 M $Ba(NO_3)_2$ aqueous solution in a 4.5-fold molar ratio with respect to the stoichiometric

conditions, and a temperature of 650 °C was employed, which ensures the formation of the desired foamy and porous morphology.

The synthesis of CeO_2/Pt was performed through the wetness impregnation method, by dropping a suitable amount of H_2Cl_6Pt in order to achieve a homogeneous dispersion of platinum of 2 wt% relative to the amount of ceria.

The multifunctional catalysts were obtained by means of two different methods: (1) the co-synthesis method (cs), which involve the simultaneous solution combustion synthesis of CeO_2 and BaO in the same solution with a mass ratio Ce/Ba 2:1, and (2) the physical mixture method (pm), performed by a 15 min ball milling at 280 rpm (IG/W2/E, Giuliani Tecnologie), in order to reach an intimate contact between the catalyst. The second method was used to mix the CeO_2 powders with the BaO ones, both synthesized by the SCS method, in a mass ratio of 2:1. All the catalysts synthesized in this work are summarized in Table 1.

Table 1: Specific surface area (SSA) and soot combustion activity in terms of onset ($T_{5\%}$) and peak temperature (T_p) for the CeO_2/Ba_pm, CeO_2/Pt/Ba_pm, CeO_2/Ba_cs and CeO_2/Pt/Ba_cs catalysts. Reaction conditions: (a) N_2 flow containing 10% of O_2; (b) N_2 flow containing 10% of O_2 and 1000 ppm of NO.

Catalyst	BET (m^2/g)	T_p (°C) [a]	$T_{5\%}$ (°C) [a]	T_p (°C) [b]	$T_{5\%}$ (°C) [b]
CeO_2_SCS	20				
$BaCO_3$_SCS	2				
CeO_2/Pt_SCS	15				
CeO2/Ba_pm	11	476	402	475	284
CeO2/Pt/Ba_pm	9	473	368	444	280
CeO2/Ba_cs	9	502	413	500	390
CeO2/Pt/Ba_cs	25	494	379	473	360

2.2 Characterization

The powder catalysts were characterized by means of X-ray diffraction (Panalytical X'Pert[3] Powder diffractometer equipped with a monochromator, Cu Kα radiation) in order to check the achievement of the desired oxides, field emission scanning electron microscope (FESEM,

Leo 50/50 VP Gemini column) in order to investigate the morphology of the catalysts as well as to correlate it to the activity towards soot oxidation, N_2 adsorption-desorption at 77 K BET analysis (Micromeritics Tristar II analyzer) to evaluate the specific surface area by the Brunauer–Emmett–Teller (BET) equation.

2.3 Catalytic activity

The activity of the oxidation catalysts towards soot combustion was analyzed by means of temperature programmed combustion (TPC), which was carried out in a fixed-bed micro-reactor (a quartz tube, inner diameter of 5 mm, placed in an electric oven), according to the standard operating procedure described in [18]: an N_2 flow containing 10% of O_2 with and without 1000 ppm of NO, was fed at a constant rate of 100 Nml min^{-1}, to the fixed bed which was constituted by 50 mg of a mixture of carbon (Printex U) and powdered catalyst (1:9 on a mass basis), diluted with ≈150 mg of inert silica. The resulting amounts of each species were the following: 45 mg of catalyst, 5 mg of soot, 150 mg of silica.

Only the tight contact condition was investigated. The catalyst–carbon mixture was obtained through a 15 min ball milling at 280 rpm (IG/W2/E, Giuliani Tecnologie), to reach an intimate contact between the catalyst and soot. This technique maximizes the number of contact points, thus better elucidation the intrinsic activity of the catalyst, even if it is less representative of the real contact conditions that occur in a catalytic trap for diesel particulate removal [19].

The reaction temperature was controlled through a PID-regulated oven and varied from 100 to 650 °C at a heating rate of 5 °C/min. The CO/CO_2 concentration in the outlet gas was measured via NDIR analyzers (ABB). Each test was repeated three times to ensure the reproducibility of the obtained results: the maximum deviation from the mean value over the three tests was ±4 °C, therefore being around 1% of the measured temperature.

The peak temperature T_p of the TPC plot of the outlet CO_2 concentration was considered as an index of the catalytic activity. The onset ($T_{5\%}$) combustion temperature, defined as the temperature at which 5% of the initial soot is converted, was also considered in order to better discriminate the intrinsic catalytic activity of the prepared catalysts. In particular, this plays an important role in order to rank the catalyst activity vs its morphology, at low temperatures which could be viable for passive regeneration. In fact, the onset combustion temperature only depends on the catalytic reaction, in a reaction rate limited regime. Whereas, at higher conversion degrees, other phenomena (for instance, mass transfer limitations) could influence the real hierarchy of the catalysts. The inaccuracy of the thermocouple is below 1–2% of the absolute temperature value.

3. Results and discussion

3.1 Characterization of the catalysts

The characterization results regarding all the catalysts prepared are listed in Table 1. BET specific surface area (SSA) values were measured in a range between 2 and 25 m^2/g.

The results of the XRD analysis are illustrated in Fig. 1. For the sake of clarity, only the patterns of the catalysts showing the best performance, on the basis of the results contained in Table 1, are here reported. In all cases, all the expected diffraction peaks were observed (CeO_2 and $BaCO_3$), according to the JPCDS reference cards. No secondary phases were detected by this technique (X-ray diffraction has a ±4% sensitivity). All the samples showed a good level of crystallinity, even if some differences can be drawn. The pattern of the cerium oxide obtained by SCS presented well-defined peaks of the phase, with broadening and intensity compatible with a crystalline material. Sharper peaks with higher intensity characterized the $BaCO_3$ sample. The mixed catalyst, obtained by co-synthesis, showed a significant decrease of the crystallinity, with broader and less intense peaks. This trend was in agreement with the

increase of the SSA values. For the CeO_2 and CeO_2/Ba samples, the addition of Pt by means of wetness impregnation did not affect the structural features of the catalysts.

FESEM images of all the catalyst produced via SCS showed a spongy microstructure (Fig. 2). During solution combustion synthesis, the decomposition/combustion of reacting precursors generates a large amount of gaseous products in a very short period of time, which leads to a foamy catalyst morphology. From the FESEM micrographs, values of the catalyst primary particle size of 100 nm were estimated (Fig. 2). The CeO_2 and $BaCO_3$ particle sizes were in good agreement with the values calculated from the BET specific surface areas when the mere geometrical surface area of the crystals is considered.

Fig. 1 XRD patterns of the catalysts considered: (a) CeO_2_SCS, (b) CeO_2/Pt_SCS, (c) $BaCO_3$_SCS, (d) CeO2/Ba_cs and (e) CeO2/Pt/Ba_cs.

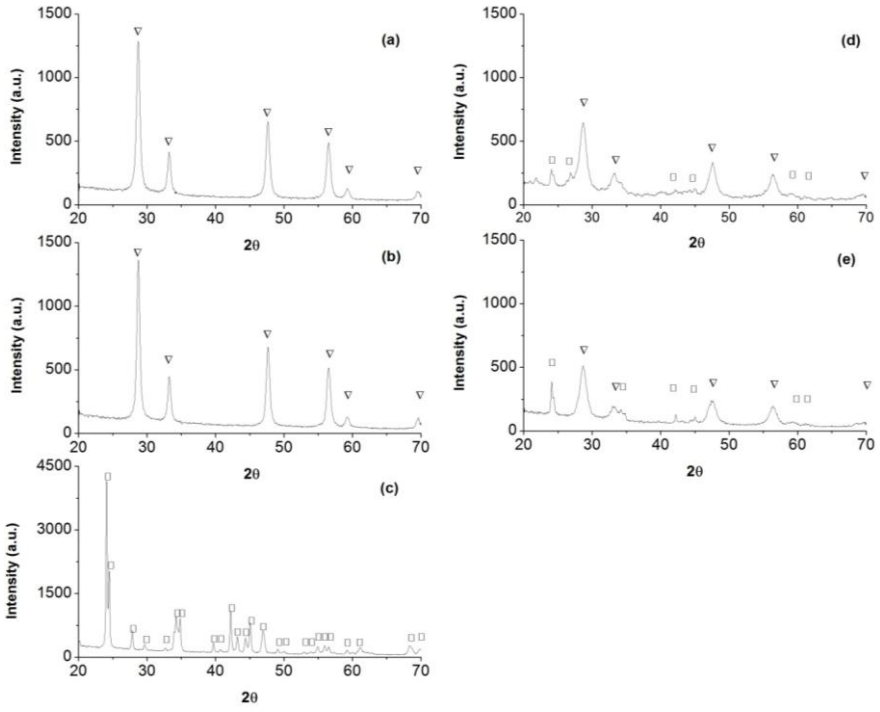

Therefore, the SCS technique allowed obtaining extremely pure crystals having a microstructure characterized by highly corrugated interfaces of the catalyst powder agglomerates. FESEM images of the mixed catalyst obtained by the co-synthesis method (Fig.s 3a and 3b) showed the spongy microstructure morphology of the single CeO_2 and

$BaCO_3$ catalyst synthesized by SCS. On the other hand, as expected, the catalyst obtained by the physical mixture method (pm) (Fig.s 3c and 3d) did not allow an intimate interpenetration between the phases typical of the solid solutions obtained by co-synthesis. This speculation is particularly important in the perspective of depositing this multifunctional catalyst on the channels of the DPF [20], in order to understand if a mixed oxide by co-synthesis or a segregated dual layer, have to be adopted as the best solution.

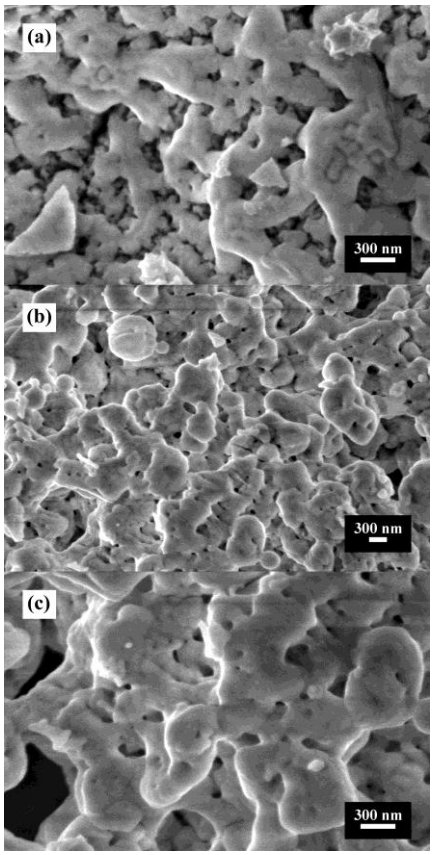

Fig. 2 FESEM pictures of the powders synthesized via SCS: (a) CeO_2_SCS, (b) BaO_SCS, (c) CeO_2/Pt_SCS.

The variation of the CO_2 concentration and the soot conversion as a function of the temperature is shown in Fig. 4. The behavior of carbon dioxide involves several steps. The first one is related to the formation of Ba nitrates by the reaction between the adsorbed NO_x and the Ba-carbonates, as shown in equation (1):

$$BaCO_3 + 2\ NO + 3/2\ O_2 \rightarrow Ba(NO_3)_2 + CO_2 \quad (1)$$

Many studies have reported that only nitrates are formed due to NO adsorption and subsequent reaction with O_2, in a temperature range between 200 and 300 °C [21]. Reaction (1) is responsible for the first CO_2 small peak at about 250 °C, when the formation of Ba nitrates occurred and simultaneously the CO_2 concentration increased. This can be better appreciated in Fig. 5, where the the CO, CO_2 and NO_2 concentrations as a function of the temperature are reported. In the correspondence to the CO_2 peak, a change in the slope of the NO_2 curves can be also noticed.

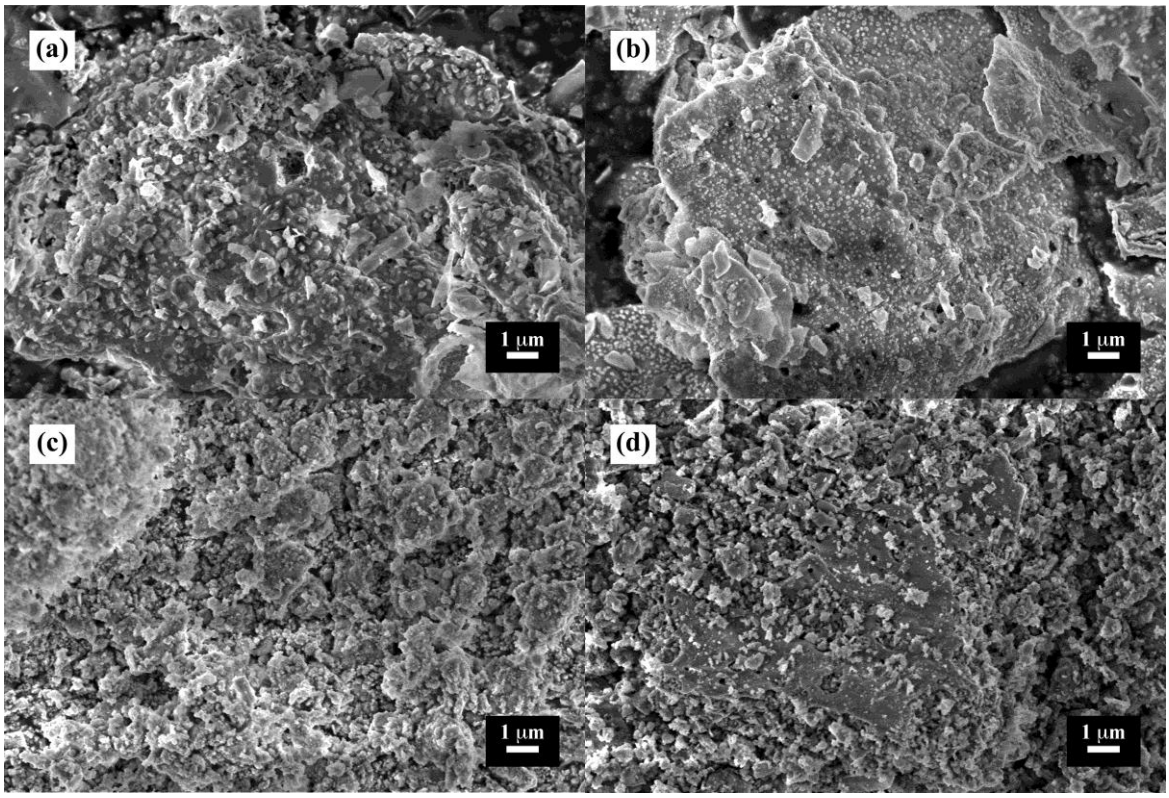

Fig. 3 FESEM images of the catalysts obtained by the co-synthesis (cs) and physical mixture (pm) methods; (a) CeO_2/Ba_cs, (b) CeO_2/Pt/Ba_cs, (c) CeO2/Ba_pm and (d) CeO_2/Pt/Ba_pm.

Then the CO_2 concentration considerably increased above its background level due to soot combustion. In all cases a slight shoulder or peak was observed, suggesting that the nitrates decomposed within the required temperature interval (350–450 °C) and oxygen was available (in the form of NO_2) for reacting with carbon and thus assisting the soot oxidation. These

nitrates may react directly with the adjacent carbon atoms as shown in reaction (2) or can decompose to release NO_2 to react with soot (reactions (3), (4), (5)), accompanied by a production of NO, and producing the first peak of CO shown in Fig. 5.

$$3C + 2Ba(NO_3)_2 \rightarrow 3CO_2 + 4NO + 2BaO \quad (2)$$

$$Ba(NO_3)_2 \rightarrow BaO + 2NO_2 + 1/2O2 \quad (3)$$

$$NO_2 + C \rightarrow CO + NO \quad (4)$$

$$CO + 1/2\ O_2 \rightarrow CO_2 \quad (5)$$

Also NO_2 formation was observed due to the occurrence of the oxidation of NO by O_2 favored by Pt sites, according to the stoichiometry of equation (6).

$$NO + 1/2\ O_2 \rightarrow NO_2 \quad (6)$$

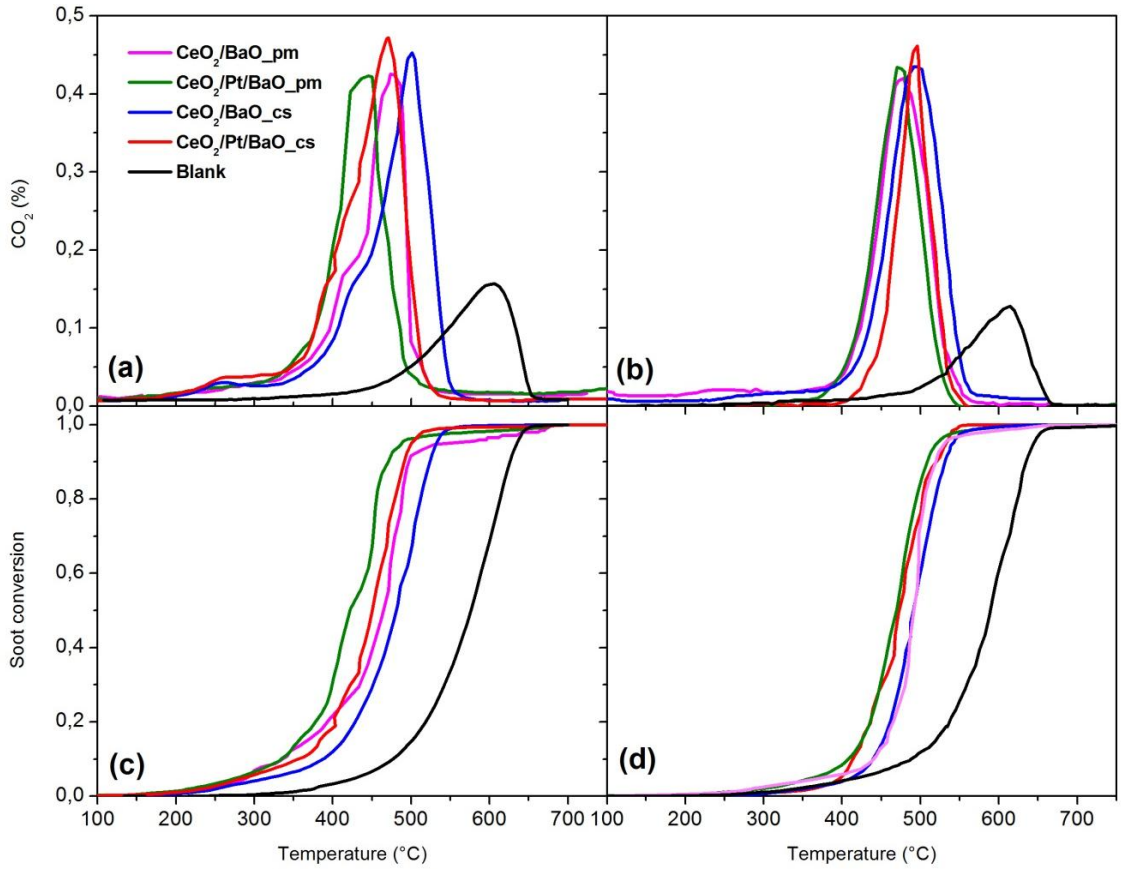

Fig. 4 CO_2 concentration measured during the TPC runs (a,b) and total soot conversion calculated from CO_2 and CO concentrations (c,d). Reaction conditions: (a,c) N_2 flow containing 10% of O_2; (b,d) N_2 flow containing 10% of O_2 and 1000 ppm of NO.

In fact, the CeO_2/Pt/BaO_pm and CeO_2/Pt/BaO_cs catalysts showed a better performance in the soot conversion, with respect to the corresponding catalysts without Pt, as can be observed in Fig.s 4c and 4d.

The characteristic temperatures are summarized in Table 1 for the tests in the absence and presence of NO (temperature columns (a) and (b), respectively).

It is worth noticing that in all cases the reduction of the temperature of soot oxidation was remarkable with respect to the non-catalytic oxidation, that was reduced of about 150-200 °C by employing the described catalysts. More importantly, this reduction was relevant with respect to the TPC experiments without NO: the Pt, which has negligible effect in the absence of NO, fosters soot oxidation reaching a 29 and 21 °C improvement in the peak temperature (for the physical mixture and the co-synthesis, respectively) thanks to the NO_2 formerly produced and then stored on BaO, and an even greater impact on the onset temperatures, thank to the low temperature activity of NO-to-NO_2 oxidation by Pt.

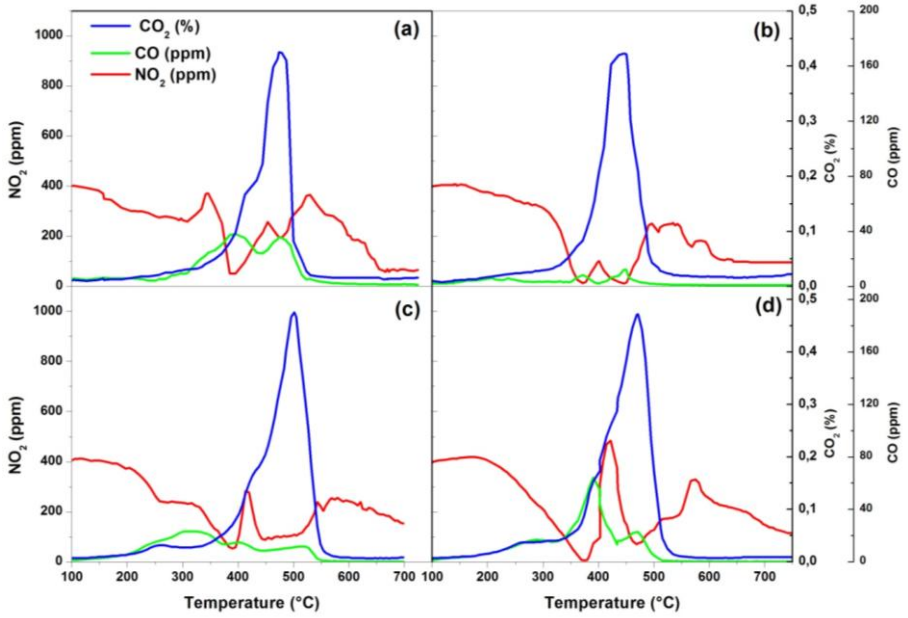

Fig. 5 CO_2, CO and NO_2 concentrations measured during the TPC runs: (a) CeO_2/Ba_pm, (b) CeO_2/Pt/Ba_pm, (c) CeO_2/Ba_cs, and (d) CeO_2/Pt/Ba_cs.). Reaction conditions: N_2 flow containing 10% of O_2 and 1000 ppm of NO.

Comparing the different preparation methods, it can be noticed that, in general, the physical mixture method allowed to achieve more performing catalysts than the co-synthesis route. Considering only the preparation techniques and the tests in the presence of NO, $T_{5\%}$ decreased of nearby 100 °C and T_p of about 30 °C by employing the physical mixture method. The Pt addition slightly affected the $T_{5\%}$ in the catalysts obtained by physical mixture, whereas a significant difference (about 30 °C) was measured for the catalyst prepared by co-synthesis with and without the Pt loading. This difference was flattened considering the peak temperature (T_p), when the difference between catalysts with and without Pt had the value of 30 °C considering both production methods.

In terms of soot conversion, CeO_2/Pt/BaO catalyst prepared by means of physical mixture can be considered the catalyst with the best behavior.

Conclusions

The CeO_2/BaO/Pt catalytic system was investigated for the oxidation of soot, for the after-treatment of the flue gases from diesel engines. This catalyst is multifunctional since it performs an NO_2-assisted combustion of soot, through the oxidation of NO to NO_2 by the Pt, as well as a storage of NO_x. This storage constitutes a "reservoir" of NO_2, which fosters soot combustion when it is released, in addition to the one formed on Pt a immediately available for soot oxidation.

The active oxides, CeO_2 and BaO, the former with oxidative properties and the latter for NO_x storage, were individually prepared and then mixed to form a "physical mixture", or they were simultaneously synthesized to obtain a solid solution through the so-called "co-synthesis" method.

Pt was added in a subsequent step, in order to assess its individual contribution in comparison to the catalysts without it.

After characterization, the effect of the preparation method was assessed: the activity towards soot oxidation revealed that the physical mixture of CeO_2 and BaO allowed to achieve lower soot combustion temperatures, both in terms of onset (corresponding to 5% of total soot conversion) and of peak temperatures. Hence, the onset soot oxidation in the presence of NO was equal to 284 °C for the catalyst without Pt, prepared by physical mixture, which was well below the one measured with the catalyst obtained by co-synthesis (390 °C). This difference slightly decreased in the presence of Pt, being equal to 280 °C and 360 °C, for the physical mixture and the co-synthesis, respectively.

Concerning the peak temperatures, an advantage of around 30 °C was recorded on the favor of the physical mixture procedure, both in the absence and the presence of Pt.

The combined effect of CeO_2/Pt/BaO was investigated: the low temperature activity of Pt to oxidize NO to NO_2 lead to consistent onset temperature reductions, while the availability of NO_2 stored on BaO was functional to the reduction of the peak temperature of soot oxidation.

Finally, CeO_2/Pt/BaO catalyst prepared by physical mixture can be considered the catalyst with the best behavior.

References

[1] A. Bueno-López, K. Krishna, M. Makkee, J.A. Moulijn, Active oxygen from CeO_2 and its role in catalysed soot oxidation. Catalysis Letters, 2005;99 (3-4):203–205.

[2] D. Fino, V. Specchia, Open issues in oxidative catalysis for diesel particulate abatement. Powder Technology 2008; 180: 64-73.

[3] M.V. Twigg, Catalytic control of emissions from cars. Catalysis Today 2011;163:33.

[4] P. Forzatti, L. Lietti, I., Nova, E. Tronconi, Diesel NO_x after-treatment catalytic technologies: Analogies in LNT and SCR catalytic chemistry. Catalysis Today 2010;151:202-211.

[5] J. Sizuki, S. Matsumoto, Development of Catalysts for Diesel Particulate NO_x Reduction. Topics Catal. 2004;28:171-176.

[6] A. Setiabudi, M. Makkee, An optimal NO_x assisted abatement of diesel ssot in advanced catalytic catalytic filter design. J.A. Moulijn, Appl. Cataly. B 2003; 42:35-45.

[7] X. Peng, H. Lin, W. Shangguan, Z. Huang, A highly efficient and porous catalyst for simultaneous removal of NO_x and diesel soot. Catal. Commun.2007; 8:157-161.

[8] D. Fino, P. Fino, G. Saracco, V. Specchia, Studies on kinetics and reactions mechanism of La2-xKxCu1-yVyO4 layered perovskites for the combined removal of diesel particulate and NO_x. Appl. Catal. B 2003;43:243-259.

[9] D. Fino, N. Russo, G. Saracco, V. Specchia, Catalytic removal of NO(x) and diesel soot over nanostructure spinel-type oxides. J. Catal. 2006; 242: 38-47.

[10] W.F. Shangguan, Y. Teraoka, S. Kagawa, Promotion effect of potassium on the catalytic property of $CuFe_2O_4$ for the simultaneous removal of NO_x and diesel soot particulate. Appl. Catal. B 1998;16:149-154.

[11] I. Atribak, A. Bueno-López, A. García-García, Thermally stable ceria–zirconia catalysts for soot oxidation by O_2.Catalysis Communications 2008; 9: 250–255.

[12] S. Bensaid, N. Russo, D. Fino, CeO_2 catalysts with fibrous morphology for soot oxidation: The importance of the soot–catalyst contact conditions. Catalysis Today, 2013; 216:57-63.

[13] K.S. Kabin, P. Khanna, R.L. Muncrief, V. Medhekar, M.P. Harold. Monolith and TAP reactor studies of NO_X storage on $Pt/BaO/Al_2O_3$: Elucidating the mechanistic pathways and roles of Pt Catal. Today 2006; 114 (1): 72–85.

[14] B.M. Weiss, K.B. Caldwell, E. Iglesia, NO_x Interactions with Dispersed BaO: Adsorption Kinetics, Chemisorbed Species, and Effects of Oxidation Catalyst Sites. J. Phys. Chem. C 2011; 115:6561-6570.

[15] S. Morandi, F. Prinetto, G. Ghiotti, L. Castoldi, L. Lietti, P. Forzatti, M. Daturi, V. Blasin-Aubé. The influence of CO2 and H2O on the storage properties of Pt-Ba/Al2O3 LNT catalyst studied by FT-IR spectroscopy and transient microreactor experiments. Catalysis Today, Volume 231, 1 August 2014, Pages 116-124.

[16] Beñat Pereda-Ayo, Unai De La Torre, M. Pilar González-Marcos, Juan R. González-Velasco. Influence of ceria loading on the NO_x storage and reduction performance of model Pt–Ba/Al2O3 NSR catalyst. Catalysis Today, Available online 16 April 2014.

[17] A. Civera, M. Pavese, G. Saracco, V. Specchia. Combustion synthesis of perovskite-type catalysts for natural gas combustion. Catalysis Today 2003; 83:199–211.

[18] P.A. Kumar, M.D. Tanwar, S. Bensaid, N. Russo, D. Fino. Soot combustion improvement in diesel particulate filters catalyzed with ceria nanofibers. Chemical Engineering Journal 2012; 207–208:258–266.

[19] Neeft JPA, Makkee M, Moulijn JA. Catalysts for the oxidation of soot from diesel exhaust gases. I. An exploratory study. Appl Catal B 1996;8:57-78.

[20] Bensaid S., Russo N. Low Temperature DPF regeneration by delafossite catalysts. Cat. Tod. 2011; 176:417-423.

[21] F. Prinetto, G. Ghiotti, I. Nova, L. Castoldi, L. Lietti, E. Tronconi, P. Forzatti., *In situ* FT-IR and reactivity study of NO_x storage over Pt–Ba/Al_2O_3catalysts. Phys. Chem. Chem. Phys. 2003; 5:4428-4434.

CHAPTER VII Overall Conclusions

The more and more restrictive legislation to reduce conventional pollutant emissions from light-duty vehicles (LDVs) have introduced the need of a new challenge in the strategies to improve engine efficiency and reducing pollutant emissions of an Euro6 diesel automotive, Even though the benefits of more stringent standards have been demonstrated and the technologies to achieve those benefits are readily available, there are still large differences in the implementation schedules for increasing emission stringency (Figure B).

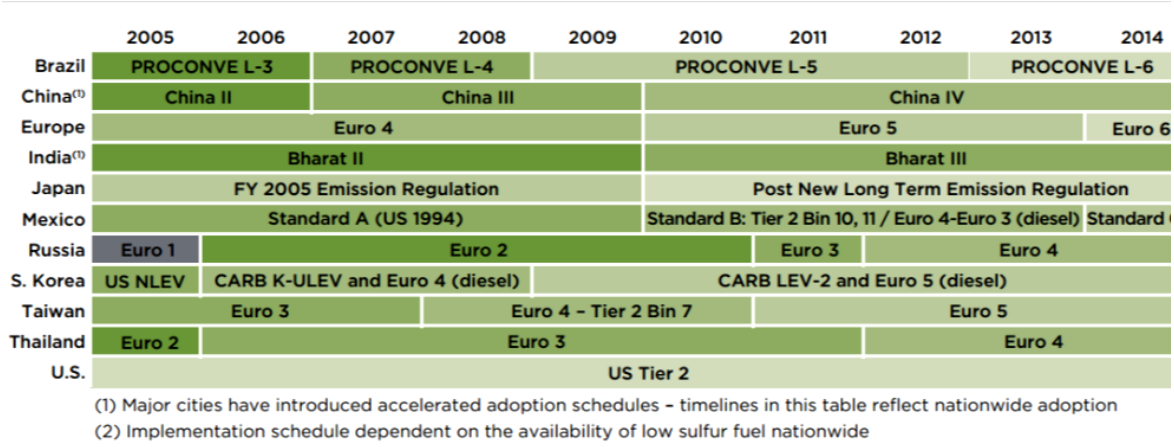

Figure B: Global schedule for implementation of emission regulations in light-duty vehicles

One of the reasons for delaying the implementation of stricter emission levels is the extra cost added to the vehicle for the improved emission control system. In order to satisfy the growing environmental laws this PhD thesis studied three different strategies for a positive impact on air quality and public health which are summarized in this chapter as an overview of the conclusions presented in this thesis.

Biodiesel: Farnesane B30

One of the strategies evaluated in this research was the effect of using blended Farnesane (30% vol.) in a Euro 5 small displacement passenger car diesel engine, for two mainly reasons: the strategic interest in reducing the dependence on oil as an energy source and the aim of reducing CO_2 emissions. In this sense the exploration of Farnesane summarized in this thesis have the potentiality to attract considerable attention by policy makers, researchers and industries as a renewable, biodegradable, and non-toxic fuel.

The exploration of Farnesane B30 volume blend showed almost comparable torque characteristics (-2%, by average) throughout the entire speed range. The equivalent LHV (+1%) of Farnesane-B30 is quite but, paid off the minute drop in viscosity (-2.5%) in fuel

conversion efficiency (-1.2%) as compared to standard diesel run. Nevertheless, a similar $LHV/(A/F)_{st}$ suggests the importance of ECU calibration to recover the minute performance gap.

The standard and specific calibration of Farnesane-B30 run engine provides almost equal levels of CO_2, HC, and CO emission. The recalibrated engine creates lower NO_x emission than the un-calibrated one as well as diesel. Due to the lower aromatic hydrocarbon fraction in the fuel blend, around a 19% and a 14% drop of smoke emissions is produced for the standard and specific calibration respectively with a bigger reduction for standard calibration due to the lower EGR.

The Soot-$BSNO_x$ and BSCO-$BSNO_x$ tradeoff results show that, for the minimum EGR rate the increase in load drops both $BSNO_x$ and BSCO emissions for both the fuels studied. The increase in load reduces air fuel ratio, which squeezes the availability of free oxygen and restricts the formation of thermal NO.

NanoLubricant: MoS2 nanoparticles

The second strategy to improve the engine efficiency is the reduction of the mechanical losses, through the incorporation of molybdenum(IV) sulfide nanopowders, which are used as lubricant additives (0.5wt%) in the lubricant formulation to reduce friction and enhancing protection against wear in a stable way. In the case of engine oil, these nanomaterials help to increase the durability and performance of exhaust treatments and reduce harmful emissions too.

The interactions between the MoS_2 nanopowders and some commercial catalysts currently employed in the after-treatment line of a light-duty Diesel vehicle engine were investigated, since one major requirement for the application of nanomaterials as lubricant oil additives, in substitution to the currently adopted ones, that is their complete compatibility with the catalytic substrates present in the after-treatment line, whose lifetime operation should not be affected to any great extent.

Diesel oxidation, soot oxidation and Selective Catalytic Reduction (SCR) catalysts were evaluated. As a general conclusion, it can be stated that the compatibility between the MoS_2 nanoparticles and the commercial catalysts has been demonstrated to be remarkable and only a masking effect has been shown. Moreover, it is worth noticing that the mass amount of the

MoS_2 nanoparticles employed in the powder-scale tests in the mixture with the commercial catalysts was significantly higher than the one that usually occurs in operative conditions.
For this reason, the MoS_2-additived lubricant oil was tested in on real diesel engine: in fact, in the perspective of a practical on-board application, one has to carefully address the issues of pollutant emissions possibly related to the new oil, and the emission abatement efficiency of the catalytic converters.
Irrespective of the investigated engine point, the results suggests that the presence of nanoparticles in the lubricant might induces some little but not negligible modifications of the combustion regime. SO_2 showed a 4 ppm emission in the exhausts, which reasonably excludes any major poisoning effects of the after-treatment catalysts.
In order to check the long-term compatibility with the DOC and DPF when exposed to the flue gases produced when the NP additived oil was used, a 100 h test was performed. The engine gaseous emissions were stable throughout the whole test. The possibility of an anomalous ash production and progressive accumulation inside the diesel particulate filter was excluded: the retention in the filter of the soot incombustible fraction, originated from current fuel and lubricant additives, did not cause any progressive reduction of the available filtration area, which would have increased the bare filter pressure drop at the end of each repeated regeneration. As a result, any possible advantage arising from the nanoparticle embodiment in the lubricating oil, which is meant to provide friction and wear reduction, was demonstrated not to be offset by any possibly MoS_2-related reduced abatement efficiency or stability loss of the after-treatment catalysts.

LNT catalityc system Ba/CeO

Finally an after-treatment system LNT was developed in order to reduce pollutant emissions. This can be accomplished by mitigating the production of particles matter or the NO_x production and to remove the other contaminants through a post-treatment system.
The CeO_2/BaO/Pt catalytic system was investigated for the oxidation of soot. This catalyst is multifunctional since it performs an NO_2-assited combustion of soot, through the oxidation of NO to NO_2 by the Pt, as well as a storage of NO_x. This storage constitutes a "reservoir" of NO_2, which fosters soot combustion when it is released, in addition to the one formed on Pt a immediately available for soot oxidation.
The active oxides, CeO_2 and BaO, the former with oxidative properties and the latter for NO_x storage, were individually prepared and then mixed to form a "physical mixture", or they were

simultaneously synthesized to obtain a solid solution through the so-called "co-synthesis" method.

Pt was added in a subsequent step, in order to assess its individual contribution in comparison to the catalysts without it.

The activity towards soot oxidation revealed that the physical mixture of CeO_2 and Ba allowed to achieve lower soot combustion temperatures, both in terms of onset (corresponding to 5% of total soot conversion) and of peak temperatures. Hence, the onset soot oxidation in the presence of NO was equal to 284°C for the catalyst without Pt, prepared by physical mixture, which was well below the one measured with the catalyst obtained by co-synthesis (390°C). This difference slightly decreased in the presence of Pt, being equal to 280°C and 360°C, for the physical mixture and the co-synthesis, respectively.

Concerning the peak temperatures, an advantage of around 30°C was recorded on the favor of the physical mixture procedure, both in the absence and the presence of Pt.

The combined effect of CeO_2/Pt/Ba was investigated: the low temperature activity of Pt to oxidize NO to NO_2 lead to consistent onset temperature reductions, while the availability of NO_2 stored on BaO was functional to the reduction of the peak temperature of soot oxidation.

Finally, CeO_2/Pt/Ba catalyst prepared for physical mixture can be considered the catalyst with the best behavior.